Number 2

March-April 1958

ИЗМЕРИТЕЛЬНАЯ
ТЕХНИКА

SOVIET INSTRUMENTATION AND
CONTROL TRANSLATION SERIES

Measurement Techniques

(The Soviet Journal *Izmeritel'naia Tekhnika* in English Translation)

■ This translation of a Soviet journal on instrumentation is published as a service to American science and industry. It is sponsored by the Instrument Society of America under a grant in aid from the National Science Foundation with additional assistance from the National Bureau of Standards.

SOVIET INSTRUMENTATION AND CONTROL TRANSLATION SERIES

■ This translation of the Soviet Journal *Izmeritelnaia Tekhnika* published and distributed at nominal subscription rates under a grant in aid to the Instrument Society of America from the National Science Foundation. This translated journal, and others in the Series (see back cover), will enable American scientists and engineers to be informed of work in the fields of instrumentation, measurement techniques and automatic control reported in the Soviet Union.

The original Russian articles are translated by competent technical personnel. The translations are on a cover-to-cover basis, permitting readers to appraise for themselves the scope, status and importance of the Soviet work.

Publication of *Izmeritelnaia Tekhnika* in English translation started under the present auspices in August 1959 with Russian issue No. 1 of January 1958. The six issues of the 1958 volume year will be published in English translation by December 1959.

All views expressed in the translated material are intended to be those of the original authors, and not those of the translators, nor the Instrument Society of America.

Readers are invited to submit communications on the quality of the translations and the content of the articles to ISA headquarters. Pertinent correspondence will be published in the "Letters" section of the ISA Journal. Space will also be made available in the ISA Journal for such replies as may be received from Russian authors to comments or questions by American readers.

Subscription Prices:

Per year (6 issues) starting with 1958, No. 1

General: United States and Canada	$20.00
Elsewhere	23.00
Libraries of non-profit academic institutions: United States and Canada	$10.00
Elsewhere	13.00
Single issues to everyone, each	$ 6.00

See back cover for combined subscription to entire Series.

Subscriptions should be addressed to:

Instrument Society of America
313 Sixth Avenue, Pittsburgh 22, Penna.

Translated and printed by Consultants Bureau, Inc.

Number 2 – March-April 1958

English Translation Published August 1959

Measurement Techniques

The Soviet Journal Izmeritel'naia Tekhnika in English Translation

Reported circulation of the Russian original 8,000.

Izmeritel'naia Tekhnika is an organ of the Academy of Sciences, USSR

See following page for Table of Contents.

MEASUREMENT TECHNIQUES

1958, Number 2 March – April

CONTENTS

CONTENTS (continued)

UTILIZATION OF THE THEORY OF RANDOM FUNCTIONS IN METROLOGY

N. A. Chekhonadskii

During recent years in various branches of the technical sciences, the theory of random functions which was developed in sufficient detail by V. S. Pugachev [1] is finding more and more applications. However, in metrology this theory has not yet found widespread application.

In the following, one problem in the field of metrology is examined, in the solution of which the methods developed by the theory of random functions can be successfully used.

General Expression for the Resultant Error of a Measuring System

The simplest example of utilization of random functions methods in the solution of problems in the field of metrology is an estimate of the error of a measuring system, which carries out measurements under unvariable external conditions. The problem essentially consists in the following.

At the present time there are very frequently employed in measurement techniques complex electrical telemetering devices which in themselves represent entire measuring systems, consisting of a number of separate links such as a transducer or transmitter, an electrical circuit network, a measuring instrument, etc.

When such a system is used, the physical quantity that is being measured is repeatedly transformed by the links of the system prior to being indicated or recorded by the measuring instrument. Each of the system links, while making the corresponding transformation, carries it out with certain errors. Therefore, the error of the entire measuring system, which arises as a result of the presence of errors in the separate links of the system, may be defined as "the resultant error of the measuring system."

Let us examine in a general way a method for evaluation of the resultant static error of a measuring system.

Let us assume that the system under examination consists of $\underline{n}$ separate links, for which the transformation functions are known (Fig. 1).

Suppose that to the input of the measuring system a certain physical quantity $\underline{y}$ is applied, which is transformed by all the links of the system and then measured by the measuring instruments, whose indications we will denote by the letter $\underline{x}$.

The quantities $\underline{x}$ and $\underline{y}$ are connected by a definite functional relationship, which in the general case can be expressed as follows:

$$x = f(y). \tag{1}$$

However, such a relationship will be valid only in an ideal case, when the system carries out the measurements without any inaccuracies.

Under actual conditions, however, when each of the system links carries out its transformation with a certain inaccuracy, the output from the system $\underline{x}$ must depend also upon the outputs of the separate links of the system.

The outputs of the separate links $y_1, y_2, \ldots y_n$, as well as the original quantity to be measured, $\underline{y}$, are independent variables within certain limits of their variations, and therefore we can write:

$$x = f(y, y_1, y_2, \ldots, y_n). \tag{2}$$

In reality, should the quantity y being measured remain constant, as a result of the variations in the link output $y_1, y_2 \ldots, y_n$, within their individual limits of accuracy, the output of the measuring system x also can have varying values within the limits of the resultant error of the system.

Expression (2) can be utilized for determination of the resultant error of the measuring system. For this purpose let us find the total differential of this expression, assuming the quantity y is remaining constant:

$$dx = \frac{\partial f}{\partial y_1} dy_1 + \frac{\partial f}{\partial y_2} dy_2 + \ldots + \frac{\partial f}{\partial y_n} dy_n. \tag{3}$$

Let us find the relative value of the resultant error. For this purpose we divide (3) by the quantity x.

$$\frac{dx}{x} = \frac{1}{x} \cdot \frac{\partial f}{\partial y_1} dy_1 + \frac{1}{x} \cdot \frac{\partial f}{\partial y_2} dy_2 + \cdots + \frac{1}{x} \cdot \frac{\partial f}{\partial y_n} dy_n. \tag{4}$$

Let us divide and multiply each member of series (4) by the output quantity of the corresponding link:

$$\frac{dx}{x} = \frac{dy_1}{y_1} \cdot \frac{y_1}{x} \cdot \frac{\partial f}{\partial y_1} + \frac{dy_2}{y_2} \cdot \frac{y_2}{x} \cdot \frac{\partial f}{\partial y_2} + \cdots + \frac{dy_n}{y_n} \cdot \frac{y_n}{x} \cdot \frac{\partial f}{\partial y_n}. \tag{5}$$

It is easy to see that a factor of the form $\frac{dyi}{yi}$ represents the error of the i-th link of the measuring system; a factor of the form $\frac{\partial f}{\partial yi}$ represents the sensitivity of the portion of the system including the links from i + 1 to n, which remains when the system is truncated by cutting off the initial links; and the ratios of the form $\frac{x}{yi}$ represent the sensitivity of the same portion of the system in the case when all links of the system are linear.

Thus, the resultant static error of the measuring system (its relative value) can be determined in the following manner:

$$\Delta_p = \sum_{i=1}^{n} \alpha_i \Delta_i, \tag{6}$$

where $\Delta_i = \frac{dy_i}{y_i}$ is the error of the i-th link of the measuring system.

The coefficients α_i are determined by the relationship

$$\alpha_i = \frac{S_{(i+1)n}}{S^*_{(i+1)n}}, \tag{7}$$

where $S_{(i+1)n} = \frac{\partial f}{\partial y_i}$ is the sensitivity of the truncated measuring system with the links from i + 1 to n retained;

and $S^*_{(i+1)n} = \frac{x}{y_i}$ the sensitivity of the same portion of the measuring system in the case when all links in this portion are linear.

The case when the errors of the links are random functions of time.

Let us investigate in a little more detail the error of the i-th link of the measuring system. Let us assume that this link is carrying out the transformation of a certain physical quantity A, which varies with time according to the function A = F(t), into another physical quantity D. Carrying out this transformation in time, the i-th link

introduces a certain error, which also is a function of time of the form of one of the examples shown in Fig. 2.

Assume, that the errors of the i-th link at the moments of time $\Delta_{i1}, \Delta_{i2}, \ldots \Delta_{ik}$ have been ascertained in some way.

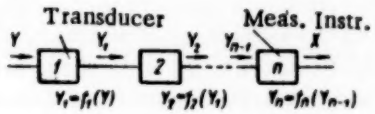

Fig. 1. Block diagram of measuring system.

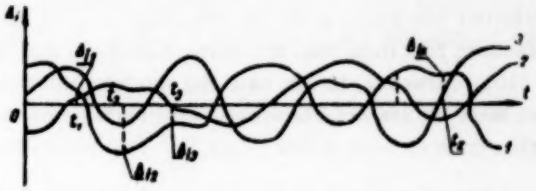

Fig. 2. Errors of the i-th link of a measuring system as functions of time.

Let us assume that the i'th link of the measuring system has carried out numerous transformations of the input quantity in accordance with the formula A = F(t). However, although the input quantity changed every time according to the same law A = F(t), the errors of the i-th link in every case of transformation of the quantity A took place according to different time functions. This is so, because at every one of the time moments $t_1, t_2 \ldots t_k$, the error caused by the i-th link of the measuring system is a random quantity. The experimentally ascertained values of errors at the discrete moments of time $\Delta_{i1}, \Delta_{i2}, \ldots, \Delta_{ik}$ represent only a few possible values of these random quantities.

Because of this, the curves expressing the variation of the error with time for any given link will not be the same for successive transformations (Fig. 2) even though the input quantity A changed everytime in accordance with one and the same function. Thus, at any moment of time the errors in the i-th link of the measuring system occur at random, and the function representing the variation of these errors in time is a random function.

Functions like those described are encountered in various branches of the technical sciences. During the last years V. S. Pugachev has worked out a concise theory dealing with such functions to which has been given the name of theory of random functions, and we shall make use of some of the methods of this theory in the further course of this paper.

The errors of the links of a measuring system are random functions in time. Therefore, to estimate the resultant error of the measuring system as expressed by (6), it is necessary to carry out a summation of random functions representing the errors of the links of the system.

$$\delta(t) = \sum_{i=1}^{n} a_i \delta_i(t), \tag{8}$$

where $\delta_i(t)$ is a random function of time, corresponding to the error of the i-th link, and $\delta(t)$ is a random function of time, corresponding to the resultant error of the measuring system.

To carry out the operations on random functions indicated by (8), we shall use a method developed in the theory of random functions [1]. It is known, that to carry out operations with random functions, it is necessary to know their statistical characteristics, that is, their mathematical expectation and correlation functions.

Let us assume that we know the statistical characteristics of all of the random functions which are members of our summation: all the mathematical expectations $M\delta_i(t)$ and all the correlation functions $K\delta_i(t, t')$.

In that case, it is relatively easy to find the statistical characteristics of the random sum function determined by (8), namely the mathematical expectation of the resultant error of the measuring system:

$$M\delta(t) = \sum_{i=1}^{n} M[a_i \delta_i(t)], \tag{9}$$

and the correlation function for the system:

$$K\delta(t, t') = \sum_{i=1}^{n} K[\alpha_i \delta_i(t, t')], \tag{10}$$

In the general case, when determining the correlation function of a sum of a number of discrete random correlation functions, it is also necessary to take into account the correlation functions of the couplings between the random functions that are being added up, and this will lead to the appearance of additional members in the sum (10). However, in our case the random functions representing the errors in the links of the measuring system in our analysis are not connected with each other, and therefore the correlation functions of their coupling will be equal to zero.

After an analysis of the described conditions, it is possible to come to the conclusion that in applying the methods of random functions theory to an estimation of the resultant error of a measuring system, it is possible to restrict the calculation to such simple operations on the random function as their addition and their multiplication by constant factors. To carry out such operations it is quite sufficient to know only the dispersion of the random functions, without having to go to the computation of the correlation functions. Therefore we set in (10) t = t' and find the dispersion of the random function:

$$D\delta(t) = \sum_{i=1}^{n} \alpha_i^2 D\delta_i(t), \tag{11}$$

where $D\delta(t)$ is the dispersion of the summary random function, corresponding to the resultant error of the measuring system, and $D\delta_i(t)$ is the dispersion of the random time function, corresponding to the error of the i-th link.

Thus, the resultant relative error of a measuring system which is a random function of time is defined by two statistic characteristics: the mathematical expectation and the dispersion, which can be computed by formulas (9) and (11).

When the random functions are stationary, then the formulas can be substantially simplified. In this case the mathematical expectation of the resultant error of the measuring system is determined by the expression:

$$M\delta = \sum_{i=1}^{n} \alpha_i M\delta_i, \tag{12}$$

where $M\delta_i$ is the mathematical expectation of a separate link of the system.

The dispersion in this case is expressed by:

$$D\delta = \sum_{i=1}^{n} \alpha_i^2 D\delta_i, \tag{13}$$

where the $D\delta_i$'s are the dispersions of the random errors of the separate links.

The root mean square error of the measuring system is found by the formula:

$$\sigma = \sqrt{\sum_{i=1}^{n} \alpha_i^2 \sigma_i^2}, \tag{14}$$

where σ_i is the root mean square error of each separate link of the system.

Analysis of the Formulas

It can be proved that the resultant error of a measuring system operating under normal conditions, which has been determined for a given point on the scale, is a stationary random function of time. This makes it possible for us in the analysis of the resultant error of the system operating under normal conditions to use the expressions obtained for stationary random functions.

It is not difficult to convince ourselves, when examining the errors of a measuring system under normal conditions, that a statistical characteristic such as the mathematical expectation of the stationary random function represents the systematic error committed by the system when carrying out a series of measurements with a constant input value.

The second statistical characteristic of the random function , the dispersion, represents the spread of value of the random function around its mathematical expectation, and in our case is a measure of the distribution of the random error values around the center of their grouping.

Thus, the resultant error of the measuring system consists of two parts – a systematic error and a random error. The resultant systematic error is dependent only upon the systematic errors of the separate links of the system and is determined according to formula (12).

The resultant random error of the measuring system is dependent only upon the random errors of the separate links of the system, and is determined according to formulas (13) and (14).

Consequently, when computing the resultant static error of a measuring system, it is necessary to divide the error in every link into a systematic part and a random part, and then add up these parts separately according to the above expressions.

Sometimes the need arises to determine the highest possible error in a measuring system. When the two components of the system's error – the systematic error and the random error – are known, and the latter is expressed in the root mean square form, then the highest possible error can be determined by means of the expression:

$$\delta_m = \delta_0 + \beta\sigma, \tag{15}$$

where β is a coefficient depending upon the specific distribution law of the random errors and for δ_0 and σ absolute values must be taken.

The relationships obtained by us for determination of the resultant error of a measuring system reveal the possibility of decreasing the systematic error of the system. Indeed, the coefficients α_i, in formulas (12) and (14), which determine the resultant systematic and random errors can be either positive or negative. When this coefficient becomes negative for several links of the system, then the resultant systematic error of the entire system will be decreased, and to some extent a mutual compensation of errors will take place. But even when all the coefficients α_i have positive values, there still is the possibility of mutual compensation of the systematic errors in the links of the system. This will take place in the case when some of the systematic errors of the links have negative signs.

It is of interest to note that D. A. Braslavskii, who examined the problem of mutual physical exchangeability of parts of measuring instruments and used in his analysis ordinary methods employed in the theory of accuracy [2], also came to similar conclusions. Such an agreement of results in our opinion proves the possibility of applying the methods developed by the theory of random functions to the solution of some problems in the field of metrology.

It will be expedient to examine next the possibility of utilizing the theory of random functions for solution of problems connected with the analysis of measurements carried out under varying external conditions.

Examples

For measurement of liquid pressures at a distance, in the range of 0 to 15 kg. wt/cm^2, a measuring system is used consisting of two links – a potentiometer transducer and a measuring instrument, both having linear characteristics. It is required to estimate the resultant error of the system when a pressure of a liquid equal to 10 kg. wt/cm^2 is being measured under normal surrounding conditions. For this purpose the statistic characteristics of errors in the links of the system were determined by repeatedly applying to each of the links the proper input values, and as a result it was established that

$$M\delta_1 = -1.3\%;\ \sigma_1 = 0.8\%;\ M\delta_2 = 1.2\%;\ \sigma_2 = 0.8\%.$$

Using (12) and (14), and because the links of this system are linear, putting $\alpha = 1$, we obtain:

$$M\delta = -0.1\%;\ \sigma = 1.1\%.$$

The highest possible error of the measuring system can be estimated by formula (15), and comes out to be

$$\delta_m = -0.1 + 2.5 \cdot 1.1 = 2.9\%.$$

In this case, for the coefficient β the value of 2.5 was assumed, which was found experimentally for similar distributions of errors.

LITERATURE CITED

[1] V. S. Pugachev, Theory of Random Functions and Its Application to Problems of Automatic Control. State Press for Technical and Theoretical Literature, Moscow, 1957.

[2] D. A. Braslavskii, Accuracy and physical interchangeability of sensitive elements, Proceedings of the Moscow Aviation Technology Institute, 1956, v. 27.

LINEAR MEASUREMENTS

ON THE USE OF SLIP GAGES (GAGE BLOCKS)

P. V. Denisov

The methods employed in the use of slip gages are far from being perfect, and the lack of instructions on this question considerably shortens the life of these measuring instruments. One of the causes of such a situation is the incorrect view that the wringing qualities of slip gages are determined only by the cleanliness, hardness and flatness of the surface. The physico-chemical processes taking place on the working surface of slip gages which substantially affect the wringing are completely ignored. For example, the standard specification OST 85,000-39 contains technical regulations on the manufacture of slip gages, and instructions regarding their storage and classification, but gives no information on the conditions in which the working surfaces of slip gages must be kept when they are in use and especially when stacks of different lengths are built up. The underestimation of the role played by the physico-chemical processes causes sticking and results in premature wear of the gages.

In the following we consider one of the most important problems involved in the use of slip gages, the adhesion of their surfaces.

Procedure and results of the investigation. In measuring the adhesive force it was intended to create conditions such that any tangential stresses in the contact plane are either entirely eliminated or correctly measured. With this object in mind a new hydraulic principle of measuring the adhesive forces was developed which ensured a uniform distribution of the normal separating forces over the entire surface of contact, and this was used in designing a hydraulic adhesiometer [1].

The frictional force was determined by means of a sliding friction gage with an error not exceeding 0.5 g.

Semi-finished and finished gage blocks of the "Kalibr" works were used as specimens of surfaces with varying roughness (7th to 13th class of surface finish according to GOST 2789-51) produced by rough and finish grinding and finish lapping; the surfaces were cleaned with activated charcoal powder by Prof. A. S Akhmatov's method.

The paste was applied to the surface by the drip method and the layer thickness h was determined by calculation from the equation

$$h = \frac{i}{vS_a n} \cdot \frac{10^{21}}{10^{14}} \ m\mu .$$

where v is the volume of solvent in which 1 cm^3 of grease is dissolved,

S_a is the actual area of the surface being investigated in cm^2,

i is the number of drops and,

n is the number of drops in 1 cm^3 of the solution.

It should be noted that this thickness of the layer is only obtainable when the surface is perfectly smooth. The general assumption that the layer thickness of actual surfaces is uniform is incorrect.

For use as a thin layer separating the surfaces, the following greases were investigated: a polar grease – myristic acid, a nonpolar grease – medical vaseline oil and, representative of technical greases, a mixture of polar and nonpolar molecules – spindle oil.

The layer was produced during the process of lapping the surfaces with the previously applied grease layer of the required thickness.

Figures 1 and 2 show the experimentally obtained relationships between the adhesive forces and the calculated thickness of the grease layer. The curves show that the adhesive forces (sticking ability) increase with the increasing layer thickness up to a maximum, and then decrease with the further increasing layer thickness; the maximum value of the adhesive force decreases with increasing roughness; this is accompanied by a shift of the interlayer thickness which corresponds to the maximum, in the direction of the increasing grease layer thickness; the value of the adhesive force of steel surfaces bears a strict relationship to the nature of the grease.

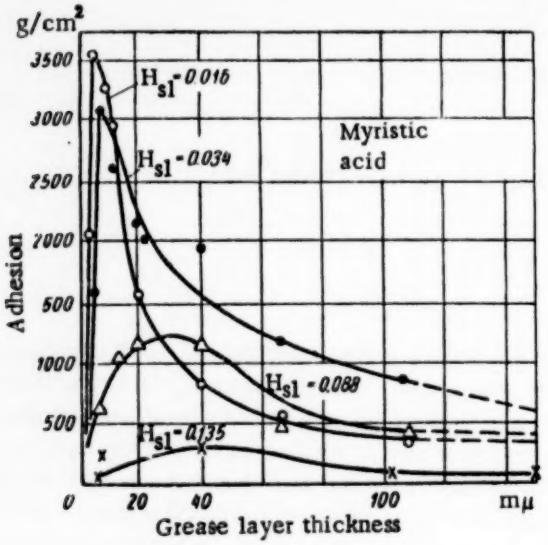

Fig. 1.

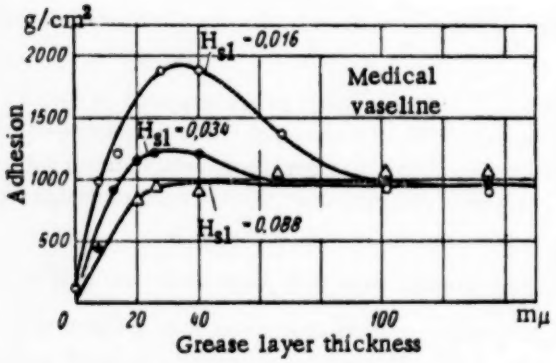

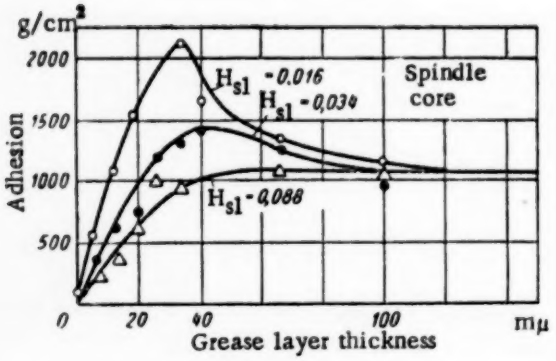

Fig. 2.

It is typical of the adhesion curves of a polar grease (Fig. 1) that, with the increasing thickness of the interlayer, they rise steeply and pass through the maximum at small thicknesses, thus indicating that only up to a certain thickness is the interlayer favorable for the adhesion. A further increase of the layer thickness leads to a weakening of adhesion.

It seems that the grease particles in the space between the gages enter into an interaction with the gage surfaces and with one another, and form "bridges" connecting the metal surfaces. The size of the interaction (adhesion) force of the surfaces depends in such a case on the total area S of the section of such "bridges," as well as on their tensile strength.

It is natural to assume that as the thickness of the grease layer increases the area S_0 is bound to increase too, which leads to the observed increase of the adhesive forces with the thickness in the initial portions of the curves.

With the increased thickness of the interlayer the area S_0 must have a top limit which is equal to the nominal area S obtained when the micro-irregularities of the surface are completely smoothed. It could, therefore, be expected that as the interlayer thickness increases, the increasing adhesive force should asymptotically approach a constant value. In fact, however, the adhesion curve passes through a maximum and falls with the further increase of the thickness of the adhesive layer. Apparently, the adhesion reaches its maximum strength when the area of interaction of the surfaces through the interlayer reaches maximum, and the interlayer itself retains its properties of a quasi-solid body.

It is known [2, 3, 4] that the strength of adhesion of nongreased surfaces increases as their roughness decreases, reaching the maximum in the case of surfaces with the highest obtainable smoothness (slip gages), i.e., in the case of surfaces which have in contact the largest area S_a of actual contact. This viewpoint was supported by our experiments concerned with the investigation of the laws governing dry friction.

As in the case of dry surfaces, the adhesion of greased surfaces is determined, as has already been pointed out, by the area S_0 of the boundary contact. The reduction of the adhesive forces with the increased roughness is explained by the fact that the area S_0 of the boundary contact for a given average thickness of the grease layer, decreases as the roughness increases.

The shifting of the adhesion maximum in the direction of increasing layer thicknesses in similar conditions is of fictitious nature, since in this case the mass of the adhesive is used not for increasing the thickness of the interlayer to the size at which the adhesive forces reach their maximum, but for filling the micro-irregularities. It can be expected that the maxima of all curves of Fig. 1 correspond to almost equal gaps between the metallic surfaces at the points where they are nearest to one another, and which on the whole localize the adhesive forces.

The adhesion curves of the nonpolar grease (Fig. 2) are analogous to the curves of Fig. 1. The difference is that the adhesion maxima are reached at greater grease thicknesses.

If it is assumed that in identical conditions the adhesion is caused by the viscous resistance of the grease, then it could be expected that the adhesion curve will, with increasing layer thickness, asymptotically approach a constant value which is reached at a layer thickness at which the micro-roughness of the surface is completely smoothed out. It follows from Fig. 2 that the adhesion curves of smooth surfaces (H_{sl} = 0.016 and 0.034 microns) pass through a maximum. This maximum is reached at h = 35-40 mμ when the levelling of the surface is not yet complete. This leads to the conclusion that the assumption that the adhesion of surfaces is due to the viscous resistance contradicts the experiment.

The following experimental observation is worth noting. The adhesion curve of surfaces whose roughness H_{sl} > value 0.034 mμ (Fig. 2, a, curve H_{sl} = 0.088) does not pass, with the increasing thickness of the interlayer, through a maximum. Instead it asymptotically approaches a constant value, which is reached at the layer thickness h > 100 mμ, when the strength of sticking is determined mainly by the viscous resistance to separation rather than by adhesion.

The fact that the adhesion curve of smooth surfaces passes through a maximum, while under the same conditions the adhesion curve of rough surfaces (curve H_{sl} = 0.088, Fig. 2,a) reaches no maximum, permits the assumption that in the case of thin grease layers (up to 35-40 mμ) the adhesion is caused by a special condition of the grease at the points S_1, S_2, S_3 . . . (Fig. 3,a) of the boundary contact, rather than by the viscous resistance. This condition is caused by the orientating action of the solid phase field upon the grease particles. Under such conditions the interlayer obtains the properties of a quasi-solid body, which leads to the sticking of the surfaces.

This point of view is confirmed by [5], where it is shown that the surface of a solid body (metal, glass) exerts an orientating effect not only upon the polar, but also upon the nonpolar molecules. The adhesion curves for spindle oil (Fig. 2, b) show that in principle the character of their variation is the same as that of curves taken with vaseline oil. The only difference is that with spindle oil the adhesive forces are greater. This increase can be explained by the presence in such oil of the so-called solvate groups or complexes.

Analysis of the experimental data shows that the thickness and nature of the grease layer have a substantial effect upon the adhesion of steel surfaces.

It is known that even perfectly smooth surfaces have a certain molecular roughness. As far as the virtually perfectly smooth surfaces (slip gages) are concerned, their roughness can be ascertained with a relatively small magnification. It is obvious that when such surfaces touch one another, their molecular interaction occurs only at a few points N_1, N_2, N_3, . . . (Fig. 3, b). The total area of the actual contact (in which the molecular contact takes place) is in such conditions not large, and the strength of cohesion does not exceed 100 g/cm^2.

On the other hand, the contact of surfaces carrying a thin layer of boundary grease results in an interaction of surfaces through the grease medium which in special boundary conditions is located at points S_1, S_2, S_3, . . . (Fig. 3, a), the total area of these points being substantially larger than in the case of dry contact. This fact has a favorable effect upon the wringing properties.

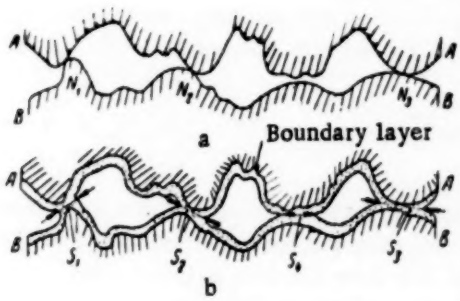

Fig. 3.

Thus, the sticking of surfaces during dry contact can be produced only by a direct interaction of metal surfaces. The sticking of surfaces in the presence of a thin grease layer brought into contact by wringing, is due to the molecular adhesion, partly between both surfaces, partly between each of the surfaces and the grease layer, and, finally, between the molecules of the interlayer.

The fact that the adhesion of surfaces with an interlayer present is very much better than when it is in dry contact, gives reason to assume that the main cause of the adhesion (wringing) of steel surfaces which often reach a considerable size, is the high tensile strength of the interlayer, which is explained by the formation in the boundary conditions of its special structure, which is similar to the structure of a solid body.

In our view the adhesion of greased smooth steel surfaces must thus be considered as the tensile strength of a thin interlayer in special boundary conditions.

This point of view is supported by a number of other researches.

For example, in [6] it was shown for the first time that the boundary layer on a metal (steel) surface is characterized by the same elastic constants as the metal.

Conclusion. As a result of investigations carried out by the author it was established that the wringing properties of slip gages are only possible when two conditions are simultaneously fulfilled:

when the microgeometry of the working surfaces satisfies the requirements specified in OST 85,000-39 and

when the working surfaces are coated with a very thin boundary layer of grease of a specific composition and structure.

If the invisible boundary grease is removed from the working surface by any method (for example with activated charcoal powder) then it is impossible to wring these surfaces together.

It was also found that the tearing away or shifting apart of wrung slip gages is accompanied by an irremediable destruction of the interlayer formed during the wringing process. For this reason a repeated wringing of such slip gages without suitable treatment of their surfaces can lead to a metallic contact between smooth surfaces and, consequently, to the formation of scratches and micro crests, i.e., to damage to their surfaces. The boundary grease on the slip gage working surfaces makes their wringing together possible, and protects their super-fine surfaces against premature wear.

The best wringing properties are obtained when the thin layer of grease consists of surface-active polar molecules. The adhesive value is of greater importance for a grease containing polar molecules (myristic acid) and is less important in the case of nonpolar vaseline oil. With a polar grease a high degree of wringing is achieved by applying thin layers of adhesive (up to 5-10 $m\mu$), and in the case of nonpolar greases, a layer of 40 $m\mu$. This fact should be taken into account in making up the stacks.

Spindle oil as a commercial lubricant containing polar and nonpolar molecules occupies an intermediate position.

In using slip gages the following rules should be adhered to.

1. Before making up a stack the anticorrosion coating should be removed from the entire surface of the slip gage by means of a solvent (gasoline).

2. Before wringing the slip gages together their working surfaces should be thoroughly rubbed with an ordinary cotton cloth or cotton wool, impregnated with a polar substance free of solid particles (metal, glass, etc.)

3. The impregnation of the cloth (wool) with a polar substance can be effected by various methods (for example by wetting with a 1-5% solution of myristic acid in vaseline oil).

4. In order to avoid the application of a thick grease layer which can adversely affect the length of the stack being made up, the slip gages should in such cases be repeatedly cleaned with ordinary cotton cloth. In essence, such rubbing is reduced to the levelling of the micro-profile, i.e., the uniform distribution of the grease over the entire working surface of the gage.

5. On the completion of work, the slip gages should be washed in gasoline (for example, B-70 grade) and given an anticorrosion coating.

If these rules are compiled with, the service life of slip gages is increased several times as compared with the usual way in which they are used. The correctness of this conclusion was proved during our tests. For example, when these instructions were disregarded a new pair of slip gages lost their adhesive properties after being wrung together up to 500 times; when treated in accordance with the instructions, however, they retained these properties after being used up to 2000 times.

LITERATURE CITED

[1] P. V. Denisov and A. S. Akhmatov, "Hydraulic adhesiometer," ITEI, No. PS-55, 422.

[2] V. V. Der'iagin and N. A. Krotova, Adhesion [in Russian] (Izd. AN SSSR, 1949).

[3] B. V. Deriagin, "A new law concerning friction and sliding," DAN, 1934, 3.

[4] I. B. Kratel'skii, "Molecular-mechanical theory of friction," Trudy 2i Vsesoiusnoi Konferentsii po Iznosu, 1949, V. 3.

[5] Zh. Zh. Trillia, UFN, 1931, v. 9, No. 3 and 4.

[6] A. S. Akhmatov, DAN, 1939, 24, No. 9.

MEASUREMENT OF THE WAVINESS OF BEARING RINGS

G. S. Simkin and O. P. Fomina

The device being described which was developed by the authors in cooperation with F. G. Kalmykov, makes it possible to measure the waviness on the working surfaces of the main groove tracks of antifriction bearing rings.

A schematic diagram of the instrument is given in Fig. 1. The ring 1 being tested is placed on spherical supports 2, and pressed against them by means of a flat spring 3, the load produced being about 200 g. The inner (working) surface of the ring is in contact with a steel stylus 4, which is linked with the dial 5, having 0.5 μ divisions. When the ring is rotated the pointer indicates the amount of waviness on the dial. Figure 2 shows the waviness graphs of two rings taken by means of this instrument. The curves show that the pitch of waviness is 30-40 mm on these rings. However, in measuring a number of other rings,a waviness with a pitch of less than 1 mm was found.

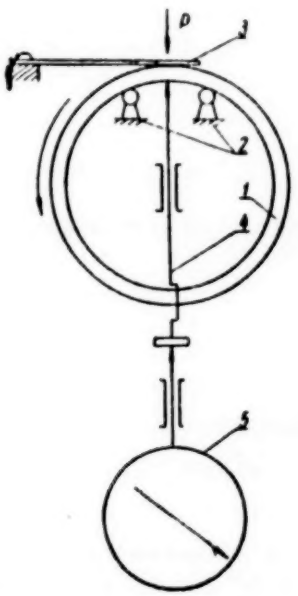

Fig. 1.

In the following we give the main points which must be considered when developing instruments for measuring the waviness of bearing rings.

1. Taking into account the smallest pitch of waviness which can occur, styli should be used with a point radius not exceeding 1/20 of this pitch (in this case 0.03-0.05 mm).

2. The ring being inspected must rest with its working (in this case the inner) surface on spherical supports. The outer surface of the ring should not be used as the base because of differences in the wall thickness of the ring would affect the results of the measurements of the waviness.

3. The distance between the spherical supports should be selected with the effect of ovality of the inner ring surface on the measurements of the waviness taken into account.

When the supports are located on the ring diameter then its ovality will have almost full effect on the waviness readings. For this reason the position of the supports must be selected in such a manner that the effect of ovality on the waviness readings is kept to a minimum.

Figure 3 shows an ellipse (any oval can be replaced with an adequate approximation by an ellipse) and two circles, the diameters of which are equal to the major and minor axes of this ellipse.

The geometrical relations given in Fig. 3 provide the difference $h_1 - h_2 = \delta_1$, which represents the indication error of the device during the measurement of the waviness:

* Ovalness.

$$h_1 = a\left(1-\cos\frac{\varphi_0}{2}\right)=2a\sin^2\frac{\varphi_0}{4},$$
$$h_2=b\left(1-\cos\frac{\varphi_1}{2}\right)=2b\sin^2\frac{\varphi_1}{4}, \quad (1)$$
$$\delta_1=2\left(a\sin^2\frac{\varphi_0}{4}-b\sin^2\frac{\varphi_1}{4}\right).$$

Let us show that $\sin^2\frac{\varphi_0}{2}\simeq\sin^2\frac{\varphi_1}{4}$.

From the relations of an ellipse it follows that $\frac{l_0}{l_1}=\frac{a}{b}$ which can be used to show that also $\frac{\sin\frac{\varphi_0}{2}}{\sin\frac{\varphi_1}{2}}=\frac{a}{b}$ or

$$\frac{\sin^2\frac{\varphi_0}{2}-\sin^2\frac{\varphi_1}{2}}{\sin^2\frac{\varphi_1}{2}}=\frac{a-b}{b}\cdot\frac{a+b}{b}. \quad (2)$$

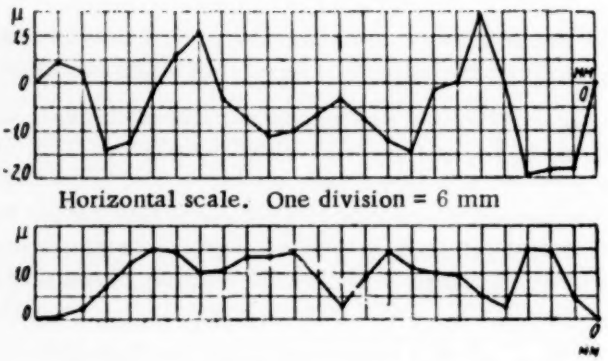

Fig. 2.

According to the specification, the ovality of bearing rings should not exceed 0.01 mm, i.e., $\Delta_0 = 2(a-b) \leq 0.01$ mm. Assuming that the order of b is 5 mm (small bearings) and $(a+b)\simeq 2b$, then (2) it can be written

$$\sin^2\frac{\varphi_0}{2}-\sin^2\frac{\varphi_1}{2}\simeq 0{,}002\sin^2\frac{\varphi_1}{2}. \quad (3)$$

For rings of a larger diameter the coefficients contained in the right-hand side of (3) are even smaller.

For an angle φ_1 of the order of 40-45° the relation (3) can be rewritten as follows

$$\sin^2\frac{\varphi_0}{2}-\sin^2\frac{\varphi_1}{2}\leqslant 0{,}0003,$$
$$\sin^2\frac{\varphi_0}{4}-\sin^2\frac{\varphi_1}{4}\ll 0{,}0003.$$

Thus, it can be assumed with an adequate approximation that $\sin^2\frac{\varphi_0}{4}\simeq\sin^2\frac{\varphi_1}{4}$, and then the equation (1) takes the form

$$\delta_1=2(a-b)\sin^2\frac{\varphi}{4}=\Delta_0\sin^2\frac{\varphi}{4}. \quad (4)$$

If it is assumed that the angular distance φ between the supports is 40 or 30° then, after suitable calculations, we find that

$$\delta_1^{(40^\circ)}=0.029\Delta_0;\ \delta_1^{(30^\circ)}=0.017\Delta_0.$$

Consequently, if the angular distance between the supports is 40°, the error in the measurement of the waviness due to ovality of the ring will not exceed 3% of this ovality. For an angle of 30° this error will not exceed 1.7%, i.e., with a permissible ovality of 0.01 mm this error will be in the region of 0.3-0.2 μ.

The position of the outer ring with a wavy working surface on spherical supports will change according to whether the supports are in contact with the convex or the concave portion of the wave, which in turn is bound to

cause a certain error in the measurement of the waviness.

Different cases of contact between the spherical supports and the ring surface are possible: both spherical supports touch the convex (concave) portion of the wave, or one of the supports is in contact with a convex and the other with a concave part of the wave. The biggest error in the measurement of the waviness occurs in the first case.

Figure 4 shows two positions of the support spheres: when the surface is wavy, and when it is smooth.

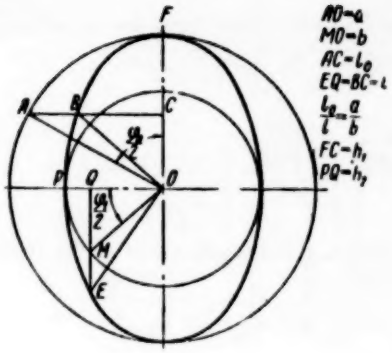

Fig. 3.

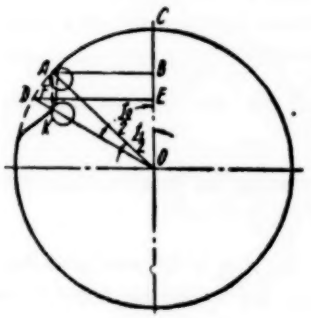

Fig. 4.

The geometrical relations given in Fig. 4 enable the determination of the error $\delta_2 = h_2 - h_1$; to be made with an adequate approximation:

$$\sin\frac{\varphi_0}{2} = \frac{l_0}{R_0}, \quad \sin\frac{\varphi_1}{2} = \frac{l_0 + \Delta_b \sin\frac{\varphi_1}{2}}{R_0}$$

or

$$\sin\frac{\varphi_1}{2} - \sin\frac{\varphi_0}{2} = 2\sin\frac{\varphi_1 - \varphi_0}{4}\cos\frac{\varphi_1 + \varphi_0}{4} = \frac{\Delta_b}{R_0}\sin\frac{\varphi_1}{2},$$

and since $\varphi_1 - \varphi_0 = \Delta\varphi$ is a small quantity then it can be written that

$$2\,\frac{\Delta\varphi}{4}\cos\frac{\varphi}{2} \simeq \frac{\Delta_b}{R_0}\sin\frac{\varphi}{2}.$$

Here Δ_b is the amplitude of the waviness.

Thus,

$$\Delta\varphi = \frac{2\Delta_b}{R_0}\operatorname{tg}\frac{\varphi}{2}. \tag{5}$$

On the other hand

$$h_1 = R_0\left(1 - \cos\frac{\varphi_0}{2}\right).$$

$$h_2 = R_0\left(1 - \cos\frac{\varphi_1}{2}\right)$$

$$\text{и } \delta_2 = h_2 - h_1 = R_0\left(\cos\frac{\varphi_1}{2} - \cos\frac{\varphi_0}{2}\right) = \tag{6}$$

$$= 2R_0 \sin\frac{\varphi_0 - \varphi_1}{4}\sin\frac{\varphi_0 + \varphi_1}{4} = R_0\frac{\Delta\varphi}{2}\sin\frac{\varphi}{2}.$$

By substituting $\Delta\varphi$ from (5) into (6) we obtain

$$\delta_2 = \Delta_b\frac{\sin^2\frac{\varphi}{2}}{\cos\frac{\varphi}{2}}. \tag{7}$$

For angular distances between the supports $\varphi = 40°$ or $\varphi = 30°$, δ_2 is

$$\delta_2^{(40°)} = 0.12\,\Delta_b \quad \text{and} \quad \delta_2^{(30°)} = 0.07\,\Delta_b,$$

respectively.

Consequently, if the amplitude of the waviness is 5 μ, the error due to the effect of the waviness is of the order of 0.6-0.35 μ.

4. The force with which the spring presses the ring against the supports and the measuring force must be selected in such a manner that the deformation of the ring surface remains insignificant at the points of contact between the spherical supports and the stylus.

The size of the deformation produced by the spherical supports can be determined from the relations describing the internal contact of a sphere with another sphere ("Mashinostroenie," v. 2, p. 578) i.e.,

$$\delta_3 = 76 \cdot 10^{-2} \sqrt[3]{P^2 \left(\frac{1}{E_1} + \frac{1}{E_2}\right)^2 \left(\frac{2}{d} - \frac{1}{R}\right)} \text{ cm} \qquad (8)$$

Here P is the force in kg, E_1 and E_2 are the elasticity moduli of spheres, d is the diameter of the inner sphere, and R is the radius of the outer sphere (surface of the ring).

For bearings and spherical supports it can be assumed that $E_1 = E_2 = 2.1 \cdot 10^6$ kg/cm^2, then

$$\delta_3 = 73 \cdot 10^{-6} \sqrt[3]{P^2 \left(\frac{2}{d} - \frac{1}{R}\right)} \text{ cm} \qquad (9)$$

For $\delta_3' \leq 0.2\ \mu$ the diameter of the spherical supports is of the order of 0.5 cm, and the radius of the ring R = 2.5 cm, the calculations show that P is about 150-200 g.

If a steel stylus is used then the equation (9) can also be applied in calculating the deformation of the ring surface due to the measuring force.

Assuming that the radius of the stylus point is 0.05 mm and the radius of the ring is 25 mm, and supposing that the deformations δ_3'' does not exceed 0.2-0.3 μ, it is possible to determine the measuring force P, the order of which in this case is 10-20 g.

It should be noted that the measurements of the waviness are not affected by δ_3' and δ_3'' but by their changes due to the nonhomogeneity of the material of the ring and the presence on its working surface of convexities and concavities. Approximate calculations show that the size of these variations is of the order of 0.1-0.2 μ.

If the errors δ_1, δ_2, and δ_3 are known, and if it is assumed that they are independent quantities and that therefore the total error can be determined by adding their squares, the total error in measuring the waviness with the angle $\varphi = 30°$, is of the order of 0.4-0.6 μ.

DEVICE FOR THE INSPECTION OF THE AXIAL PITCH OF WORMS

V. N. Levitskii

The Leningrad "Vulkan" plant uses a modified KZF machine of the "MIZ" works for the inspection of the axial pitch of worms in the headstock of this machine (see Figure) a special hole is bored to take the small dial gage 1; the spherical stop 2 on the main slide is intended for the slip gages 3,* while mounted on the cross slide are the support 4 for a lever with arm ratio 1 : 1, and the small indicator dial 5.

The axial pitch is measured in the axial section of the worm on a line parallel to the axis. The check is made by comparing the actual distance between the corresponding points of the thread profile with the nominal distance (axial pitch) between the adjacent corresponding points on the thread, or between the corresponding points 3-5 axial pitches apart or (for multi-start worms) a lead apart.

*Gage blocks.

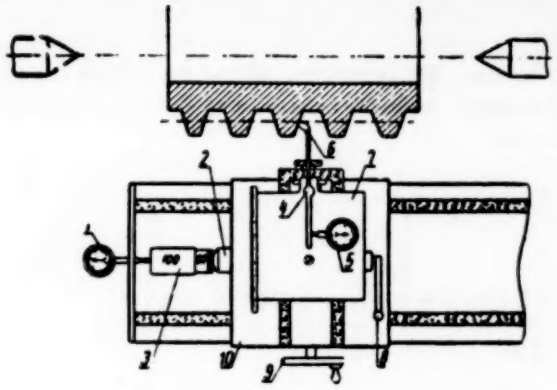

For measuring, the worm is set up between the machine centers, the measuring stylus 6 is brought into contact with the side surface of the thread at a point approximately in the middle of its height, whereupon the reading of the dial 5 is recorded. Then the cross slide 7 is withdrawn from the worm axis in the radial direction by means of the handle 8, and the main slide 10 is moved on the slideway parallel to the worm axis, by the hand wheel 9, through a distance equal to the smallest axial pitch (or 3-5 pitch lengths). Then the cross slide 7 is moved back towards the work axis into its original position.

The difference of the indications of the dial 5, which is connected to the measuring stylus 6 in contact with the thread surface, shows the deviation of the actual pitch from its required value. The displacement of the main slide 10 in the direction parallel to the worm axis is measured by means of the stack 3 of slip gages placed between the stationary stop 2, and the plunger of the dial gage 1 installed on the headstock of the machine. The return of the cross slide into its original radial position relative to the worm axis is ensured by a rigid stop or an additional (third) dial gage mounted on the slide.

DEVICE FOR MEASURING THE THREAD ANGLE OF SCREW THREAD PLUG GAGES

M. I. Malakhov

The device for the inspection of the thread angle developed by the author is used at the Tambov "Komsomolets" Plant directly at the machine tool when no workshop microscope is available.

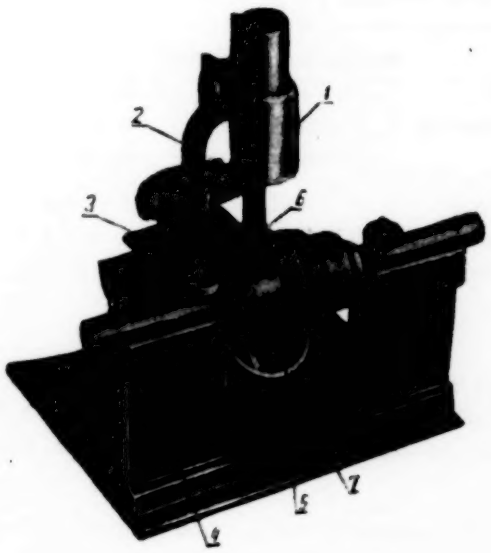

The device (see Figure) consists of the tube 1 which contains the objective and eye piece with a total magnification of 30×; the support 2 with a rack-pinion mechanism for focusing the tube; the table 3 with the angle gage of the "Kalibr" works and the holders 4, with centers for gripping the gage 5 being inspected.

The table 3 is mounted on slides and can be moved in two perpendicular directions by means of micrometer screws.

Master thread insert 6, taken from a screw thread micrometer, is fixed on the movable scale of the angle gage by means of a bracket and screw. The rotating mirror 7 which throws light onto the profile of the gage thread is mounted on the lower slide. All components are mounted on a flat plate which serves as the base of the device.

During the measurement the thread gage is set up between centers, while the standard thread, selected according to the pitch and angle of the profile being

tested, is fixed in the bracket by means of a screw. Thereupon the member with the standard thread is moved into the thread space by means of a micrometer screw, and the light beam from the mirror is directed onto the thread profile.

If the thread angle is correct, there will be no light seen between the generating line of the master thread and the profile of the thread being tested. If the thread angle is larger or smaller than the nominal value, then a gap will be formed whose size can be read on the angle gage scale.

DEVICE FOR THE INSPECTION OF MEASURING INSTRUMENTS WITH SCALE DIVISIONS OF LESS THAN 1μ

S. S. Lipkina

The present method of checking instruments with divisions of less than 1μ by means of slip gages fails to ensure continuity of inspection, does not indicate errors due to the backlash in the instrument mechanisms, and is very labor-consuming.

The device being described incorporates a wedge gage, and makes possible a sufficiently accurate inspection of the above instruments with a relatively high productivity.

The wedge gage 1 (see Figure) is placed into the body 2 of the device secured by means of the screw 3 onto the ribbed table of the vertical optical indicator.

The body 2 carries the screw 4 with a 2-mm pitch thread. The thimble of the screw has 5 divisions engraved on it.

The spring-loaded plunger 6 mounted on the left-hand side of the body ensures a continuous contact between the screw and the wedge gage. With regard to form and surface finish, the wedge gage must meet the same requirements as the class 1 slip gages.

The nominal measurements and the permissible tolerances of the gage are given in the Table.

Divisions of instruments in mm	Taper of the wedge gage	Difference p in dimensions for a 24-mm length, in μ	Permissible deviations		
			of the dimension p in μ	of working surfaces from flatness in μ	from parallelism in transverse cross-section, in μ
0.0002	1:2000	12	±0.1	0.03	±0.1
0.0005	1:1600	15	±0.1	0.03	±0.1
0.001	1:800	30	±0.1	0.03	±0.1

The checking of readings is carried out as follows.

The instrument being inspected is fixed to the stand of the vertical optical indicator, on the table of which the device with the wedge gage is placed. The initial position of the wedge gage is chosen in such a manner that the contact member of the plunger touches the gage at a distance of not less than 3 mm from its edge, and the travel is not less than 15 mm.

By lifting the table of the optical indicator, the pointer of the instrument being tested is set at zero whereupon, after the plunger has been brought into contact three times, the first reading is made on the thimble scale. Then, without altering the zero setting, the thimble is given two turns, thus moving the wedge gage, and again after bringing the instrument plunger three times into contact with the wedge gage, the second reading is taken.

Similar readings are taken with the same wedge gage at two further points. This completes the checking process of the right hand side of the scale.

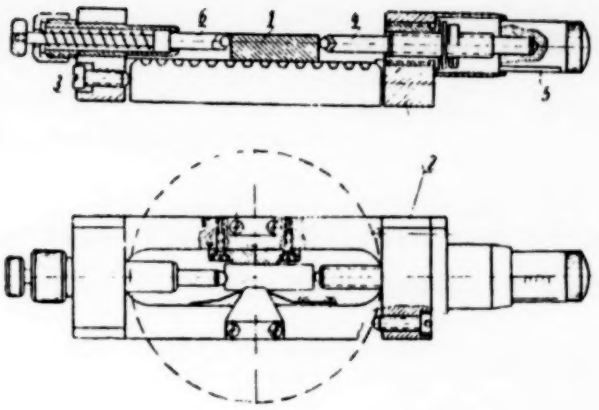

The inspection of the left-hand side of the scale is performed in a similar manner, moving the wedge gage in opposite direction. Here the reading begins at the end position of the wedge gage which was reached when checking the right-hand side of the scale.

If the error of the device at any point of the scale is equal to the maximum permissible error, or is smaller than it by a value not exceeding the variation of indications of the given measuring head, then three more contacts are made with the plunger.

The measuring head is declared satisfactory if the deviations thus obtained do not exceed the permissible values.

The device described was tested with satisfactory results in the testing laboratories of the Bureau of Interchangeability and of the "Kalibr" works in checking PIU-2 interferometers and electric induction instruments with 0.0002 mm dial divisions.

MECHANICAL MEASUREMENTS

ON CERTAIN PRINCIPLES PERTAINING TO THE MELTING OF SUBSTANCES AND THEIR SIGNIFICANCE FOR A HIGH PRESSURE SCALE

M. K. Zhokhovskii

The problem of producing a thermodynamic scale for high pressures is thoroughly discussed in [1]. The phenomenon of melting using phase equilibrium pressures in a single component system at a given temperature, is used as the basis for the scale. A first approximation to the thermodynamic scale was successfully carried out using that principle up to $2 \cdot 10^4$ kg force/cm^2 [2]. The experimental curve for the melting of mercury was used as a base for this scale [3] and was approximated by Simon's empirical equation, using his first form with three constants [4]. The choice of the Simon equation for the approximation was determined largely by the universal character of this equation, which we ascribed to the fact that general laws are apparently hidden in its constants; laws which lie at the base of the melting process. As we shall see this assumption was completely justified.

Together with purely empirical methods for producing a thermodynamic scale, various opinions are stated in [1] as to the desirability of a parallel use of theoretical studies supplemented by experiment. In developing this idea two equations for the melting curve were suggested, both satisfactorily reproducing the experimental data for several substances. Subsequent studies in this direction carried out by the author in the Physics Laboratories for Ultra High Pressures at the Academy of Sciences, USSR, led to a more general solution of the problem and to more valuable results which we shall now discuss.

Let us introduce (as characteristic to the process of melting under pressure) the value for the specific energy which is expended on the melting of a substance, i.e., $\frac{\lambda}{\Delta v}$ where λ is the heat of fusion and Δv is the change in volume. Then from an analysis of experimental data it is easy to discover extremely interesting laws. They were found by comparing the derivatives dp/dT of the Simon equation with the Clapeyron-Clausius equation, written down in terms of the derivative and the initial points on the melting curve. In this paper we present a different method for the solution of the problem.

Let us determine the relationship between the logarithm of the specific energy $\ln \frac{\lambda}{\Delta v}$ and the logarithm of the temperature,* using the numerous experiments of Bridgman [5, 6] up to 12,000 kgf/cm^2. From the corresponding graphs in Fig. 1 and 2 for the large number of substances investigated, it follows directly than $\ln \frac{\lambda}{\Delta v}$ is a linear function of ln T. A certain deviation from linearity is found for calcium. It is probably due to an unusual behavior of the heat of fusion λ along the melting curve which in turn may indicate the presence of experimental errors. For all other substances including those not shown in Fig. 1 and 2, the relation between $\ln \frac{\lambda}{\Delta v}$ and ln T is practically linear with inconsequential deviation of individual points.

The second general law consists in the fact that the angle of the slope of the straight lines in Fig. 1 and 2 for each substance is equal to the constant c of the Simon equation [7].

*In these and in the following calculations the heat of fusion was calculated from experimental data [5] using the Clapeyron-Clausius equation or else it was taken directly from [6, 8].

$$\frac{p+a}{a}=\left(\frac{T}{T_0}\right)^c. \tag{1}$$

in which, as is well known, a and c are constants, determined experimentally for each substance. From the two results given it follows directly that

$$\frac{d\left(\ln\frac{\lambda}{\Delta v}\right)}{d\ (\ln T)}=\text{const}=c, \tag{2}$$

Solution of (2) for the initial condition at atmospheric pressure, i.e., when $T = T_0$, $\frac{\lambda}{\Delta v} = \frac{\lambda}{\Delta v_0}$ gives

$$\frac{\ln\left(\frac{\lambda}{\Delta v}\cdot\frac{\Delta v_0}{\lambda_0}\right)}{\ln\frac{T}{T_0}}=c. \tag{3}$$

The constant character of the values of c, calculated along the melting curve for various substances, as in (3), is evident from Table 1. For the sake of comparison the average values and the actual value of the constant c in the Simon equation are given in the last two columns of Table 1. These were taken directly from [4] or else recalculated. Good agreement for the values of c indicates the validity of (3).

Let us now represent (2) by

$$\frac{d\left(\frac{\lambda}{\Delta v}\right)}{\frac{\lambda}{\Delta v}}=c\frac{dT}{T}$$

and let us substitute $\frac{dT}{T} = \frac{\Delta v}{\lambda}$ from the Clapeyron-Clausius equation.

Then

$$\frac{d\left(\frac{\lambda}{\Delta v}\right)}{dp}=c. \tag{4}$$

It can be seen from (4) that the specific energy $\frac{\lambda}{\Delta v}$ must be a linear function of pressure. The predicted relation is actually confirmed by experimental data for all substances studied and is illustrated by certain curves in Fig. 3. Solution of (4) yields

$$c=\frac{1}{p-p_0}\left[\frac{\lambda}{\Delta v}-\frac{\lambda_0}{\Delta v_0}\right]. \tag{5}$$

where p_0 corresponds to atmospheric pressure, which is taken as the initial point of the melting curve. With high pressures, $p_0 \ll p$, and then

$$c=\frac{1}{p}\left[\frac{\lambda}{\Delta v}-\frac{\lambda_0}{\Delta v_0}\right]. \tag{5a}$$

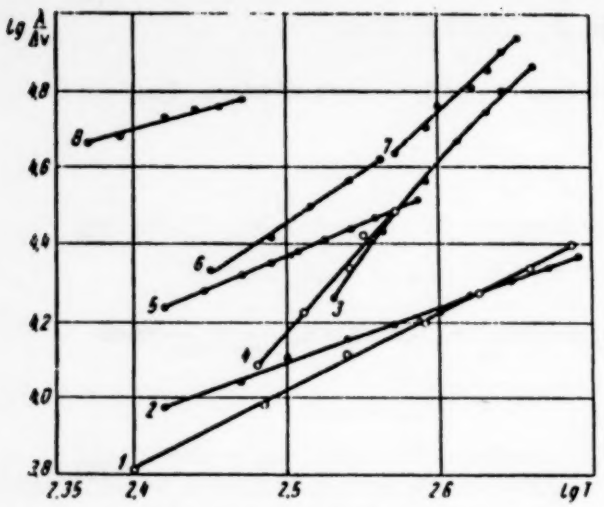

Fig. 1. Logarithm of the specific energy of melting as a function of the logarithm of temperature (pressures 1-12,000 kgf/cm²) for several substances.
1) Carbon tetrachloride; 2) silicon tetrachloride; 3) potassium; 4) cesium; 5) chloroform; 6) carbon dioxide; 7) sodium; 8) mercury.

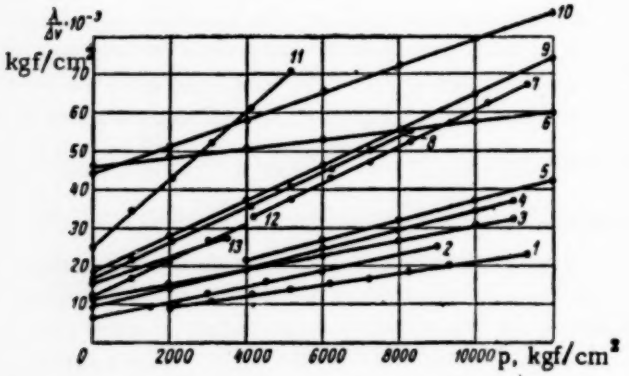

Fig. 3. Specific energy of melting as a function of pressures up to 12,000 kgf/cm² for several substances.
1) Silicon tetrachloride; 2) carbon tetrachloride; 3) bromoform; 4) benzene; 5) carbon dioxide; 6) mercury; 7) acetamide-II; 8) ortho-cresol-I; 9) potassium; 10) sodium; 11) acetamide-I; 12) cesium; 13) rubidium.

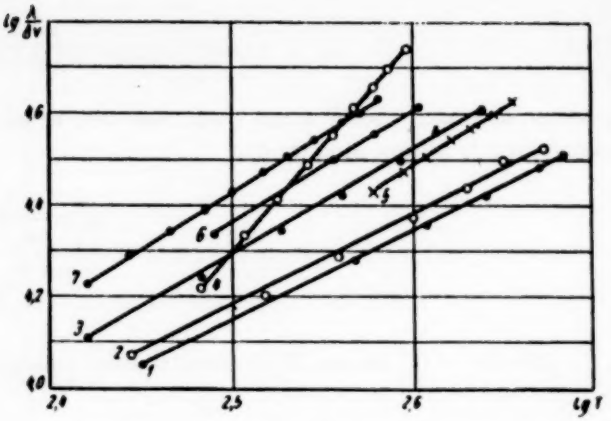

Fig. 2. Logarithm of specific energy of melting as a function of the logarithm of temperature (pressure 1-12,000 kgf/cm²) for several substances.
1) Bromoform; 2) nitrobenzene; 3) aniline; 4) ortho-cresol-I; 5) ortho-cresol-II; 6) bromobenzene; 7) chlorobenzene.

Values of c calculated from (5) are given in Table 2; study of the latter leads us to conclude that the "constant" remains constant along the melting curve and that the calculated and actual value of c for all substances studied are practically the same.

Thus the constant c is analytically expressed by thermodynamic fusion parameters in two ways: by $\frac{\lambda}{\Delta v}$ and T and by $\frac{\lambda}{\Delta v}$ and p. Its physical nature, as a ratio of the increase in specific energy to the increase in pressure, is particularly evident from (4) and (5).

Omitting $\frac{\lambda}{\Delta v}$ from (3) and (5) we obtain the equation for the melting curve

$$\frac{c\,(p-p_0)+\frac{\lambda_0}{\Delta v_0}}{\frac{\lambda_0}{\Delta v_0}}=\left(\frac{T}{T_0}\right)^c \qquad (6)$$

or omitting p_0 as being small in comparison to p

$$\frac{cp+\frac{\lambda_0}{\Delta v_0}}{\frac{\lambda_0}{\Delta v_0}}=\left(\frac{T}{T_0}\right)^c. \qquad (6a)$$

It is readily seen that (6) is a new form of the Simon equation (1) in which the former constant a has taken a definite value and has a definite physical meaning. The new constant $a_0 = \lambda_0/\Delta v_0$ is equal to the specific energy expended on melting at the initial point (at atmospheric pressure). The second constant c has been kept in the new equation and appears on both sides of the equation.

TABLE 1

Substance	Values of the constant c calculated from (3) for temperatures corresponding to pressures in kgf/cm²										Average value of c	Act. value of Simon c constant
	1000	2000	3000	4000	5000	6000	7000	8000	9000	10000	12000		
Sodium		3.49		3.46		3.44		3.45		3.46	3.47	3.46	3.55
Potassium		4.97		4.80		4.72		4.71		4.73	4.70	4.77	4.68
Cesium	4.85	4.64	4.62	4.55								4.67	4.75
Mercury		1.18		1.19		1.20		1.22		1.21	1.19	1.20	1.22
Silicon tetrachloride			1.56	1.53	1.52	1.52	1.51	1.51	1.51	1.50	1.50[4]	1.52	1.50
Carbon dioxide						2.59		2.64		2.74	2.63	2.65	2.64
Carbon tetrachloride		2.04[1]	2.05		2.05[2]	2.06		2.07[3]	2.06			2.06	2.08
Bromoform		1.97		1.95		1.95		1.97		1.97	1.97[4]	1.96	1.94
Chloroform				1.66	1.68	1.68	1.68	1.69	1.69	1.69	1.69	1.68	1.69
Bromobenzene						2.46		2.46		2.47	2.44	2.46	2.42
Chlorobenzene			2.52	2.52	2.51	2.51	2.51	2.51	2.51	2.50	2.50	2.51	2.50
Nitrobenzene		1.71		1.98		1.92		1.99		2.06	1.98[4]	1.94	1.97
Benzene		2.61		2.49		2.34		2.50		2.49	2.49[4]	2.49	2.49
Aniline		2.32		2.32		2.38		2.33		2.43	2.33	2.35	2.33
Ortho-cresol-I	4.61	4.60	4.62	4.64	4.65	4.67	4.68	4.69				4.64	4.69
Para-toluene		2.15		2.04		2.01		2.02				2.05	2.00
Diphenylamine		2.45		2.43		2.44		2.45				2.44	2.44
Benzophenone		2.40		2.35		2.35		2.35				2.36	2.35
Acetamide-I	9.30	8.98	8.78	8.72	8.78							8.91	8.75
Nitrogen	1.64	1.69	1.75	1.76	1.74	1.72						1.72	1.79
Argon	1.51	1.52	1.53	1.56	1.58	1.59						1.55	1.63

Note: 1) When p = 1500 kgf/cm²; 2) when p = 4500 kgf/cm²; 3) when p = 7500 kgf/cm²; 4) when p = 11,000 kgf/cm².

Let us study the results from the points of view of the problem of producing a thermodynamic pressure scale. In principle this problem is completely solved if the laws found remain unchanged over the pressure range of the scale. Actually in this case the equation of the melting curve (6) actually analytically reproduces the scale pressures, as it gives p as a function of T. For a practical application of (6) one needs to determine λ_0 and Δv_0 experimentally and to find the value of the constant c. The latter may be calculated from the initial portion of the melting curve obtained by means of a piston manometer. Also c may be found from (3) and (5) if the specific energy $\frac{\lambda}{\Delta v}$ can be calculated using $\frac{dp}{dT}$ for a known region of the melting curve (from the Clapeyron-Clausius equation) or else if λ and Δv can be determined directly by experiment.

The second method of using (3) is particularly valuable for checking the constance of c at very high pressures, i.e., in the region for which the thermodynamic scale is designed. In this case the method of determining λ and Δv must be such that the manometer which was used in the experiment would be used only as a sensitive equilibrium indicator and that the parameters being studied (λ or Δv) and the temperature could be measured. Then by means of the values found for λ and Δv the constancy of c is established by means of (3) which does not contain any parameter which cannot be accurately measured. This makes it very evident that (3) has great practical value for the construction of a scale.

Let us now consider the question: to what extent can we count on the invariance of the constant c in the region of very high pressures? Let us study, for this purpose, the available experimental material.

In Fig. 4 and 5 and in Table 3 are given data, similar to those previously given, for various organic substances studied by Bridgman [8] in the 10,000-40,000 kgf/cm² range. As can be seen in Figs. 4 and 5, with considerable increased pressure, the linear character of the relations $\ln \frac{\lambda}{\Delta v}$ vs. $\ln T$ and correspondingly $\frac{\lambda}{\Delta v}$ vs. p

TABLE 2

Substance	Value of the constant c calculated from (5) for pressures in kgf/cm²											Average value of c	Actual value of Simon constant c
	1000	2000	3000	4000	5000	6000	7000	8000	9000	10000	12000		
Sodium		3.54		3.55		3.54		3.55		3.55	3.55	3.55	3.55
Potassium		4.69		4.69		4.68		4.69		4.68	4.68	4.68	4.68
Cesium	4.72	4.77	4.76	4.64								4.72	4.75
Mercury		1.24		1.19		1.22		1.23		1.22	1.21	1.22	1.22
Silicon tetrachloride			1.51	1.50	1.50	1.50	1.50	1.50	1.50	1.50	1.50[4]	1.50	1.50
Carbon dioxide						2.64		2.64		2.64	2.64	2.64	2.64
Carbon tetrachloride		2.09[1]	2.09		2.08[2]	2.08		2.08[3]	2.07			2.08	2.08
Bromoform		1.93		1.94		1.94		1.94		1.94	1.94[4]	1.94	1.94
Chloroform				1.68	1.69	1.69	1.69	1.69	1.69	1.69	1.69	1.69	1.69
Bromobenzene						2.42		2.42		2.42	2.42	2.42	2.42
Chlorobenzene			2.50	2.50	2.50	2.50	2.50	2.50	2.50	2.50	2.49	2.50	2.50
Nitrobenzene		1.97		1.97		1.97		1.97		1.97	1.97[4]	1.97	1.97
Benzene		2.46		2.49		2.35		2.49		2.49	2.49[4]	2.46	2.49
Aniline		2.31		2.33		2.33		2.33		2.33	2.33	2.33	2.33
Ortho-cresol-I	4.68	4.69	4.69	4.69	4.69	4.69	4.69	4.69				4.69	4.69
Para-toluene		2.00		2.00		2.00		2.00				2.00	2.00
Diphenylamine		2.44		2.44		2.45		2.45				2.45	2.44
Benzophenone		2.35		2.35		2.35		2.35				2.35	2.35
Acetamide-I	8.75	8.75	8.75	8.75	8.75							8.75	8.75
Nitrogen	1.64	1.70	1.76	1.78	1.75	1.75						1.73	1.79
Argon	1.52	1.52	1.53	1.57	1.60	1.64						1.56	1.63

Note: 1) when p = 1500 kgf/cm²; 2) when p = 4500 kgf/cm²; 3) when p = 7500 kgf/cm²; 4) when p = 11,000 kgf/cm².

TABLE 3

Substance	Equation No.	Value of the constant c for pressures in kgf/cm²							Average value of c	Actual value of the Simon constant c
		10000	15000	20000	25000	30000	35000	40000		
Chloroform	3	1.50	1.46	1.58	1.63				1.54	1.56
	5	1.49	1.53	1.60	1.67				1.57	
Chlorobenzene-II	3		1.80	1.80	1.80				1.80	1.79
	5		1.80	1.81	1.80				1.80	
Carbon bisulfide	3		1.52	1.44	1.43	1.41	1.40		1.44	1.40
	5		1.53	1.45	1.43	1.41	1.40		1.44	
Ethyl alcohol	3			1.81	1.65	1.53	1.48		1.62	1.47
	5			1.76	1.62	1.50	1.44		1.58	
Butyl alcohol	3		2.41	2.54	2.51	2.54	2.60		2.52	2.62
	5		2.42	2.55	2.52	2.55	2.66		2.54	
Ethyl bromide	3			2.55	2.83	2.95			2.78	2.93
	5			2.58	2.86	3.06			2.83	
Propyl bromide	3			1.79	1.83	1.83	1.80	1.79	1.81	1.75
	5			1.77	1.80	1.82	1.80	1.77	1.79	
Methyl chloride	3		1.48	1.47	1.45	1.43			1.46	1.42
	5		1.46	1.46	1.45	1.42			1.45	

are completely retained. The value of c along the melting curve (see Table 3) behaves differently. In a series of substances, such as for example chlorobenzene, propyl bromide and methylene chloride, c is practically constant; in the case of ethyl bromide and chloroform the constant increases slightly with pressure; in the case of ethyl alcohol it decreases and in the case of other substances a change in separate values at the ends of the curve is observed. The average values of the constant for the majority of substances are very close to the real value

and only in the case of the alcohols and the ethyl bromide is the divergence somewhat larger.

The differences in the behavior of the constant c, which were pointed out above, occur in several of the substances studied; the direction of these changes is different and they are not very large in absolute magnitude.

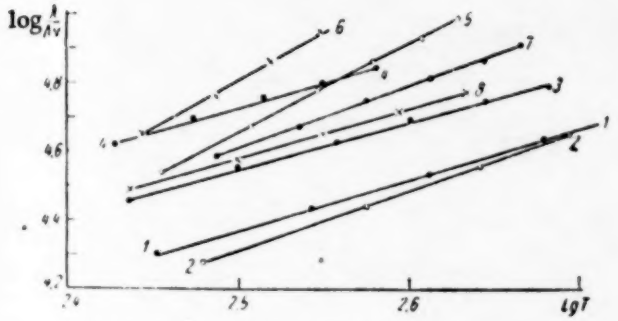

Fig. 4. Logarithm of the specific energy of melting as a function of the logarithm of temperature (pressures 10,000-40,000 kgf/cm²) for various substances. 1) Chloroform; 2) chlorobenzene; 3) carbon bisulfide; 4) ethyl alcohol; 5) butyl alcohol; 6) ethyl bromide; 7) propyl bromide; 8) methyl chloride.

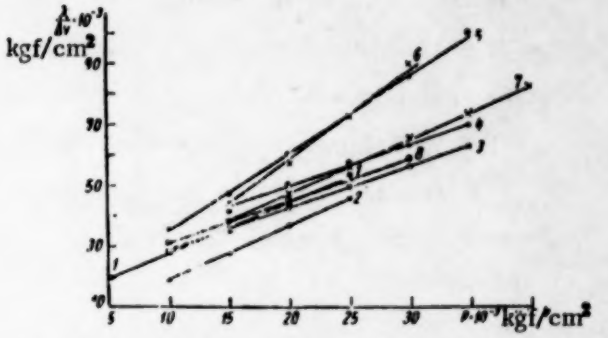

Fig. 5. Specific energy of melting as a function of pressure (5,000-40,000 kgf/cm²) for various substances.
1) Chloroform; 2) chlorobenzene; 3) carbon bisulfide; 4) ethyl alcohol; 5) butyl alcohol; 6) ethyl bromide; 7) propyl bromide; 8) methyl chloride.

We must add that the basic experimental data of Bridgman taken at such high pressures could not be as accurate as the data obtained for 12,000 kgf/cm² according to the author himself. Therefore it seems logical to assume that the somewhat poorer results obtained for the constant c at high pressures are not due to a break down of the laws or underlying principles with an increase in pressure, but are due to experimental errors. All we need to do is refer to the errors in the determination of Δv. The graphs of Δv vs. p shown in [8] are characterized by a considerable spread of points about the smoothed out curve, which is not surprising with such a complicated experiment, which, we might add, so far remains unique.

The effect of experimental errors on the value of c becomes obvious when the data in Tables 1, 2, and 3 are compared for chloroform. One must note that the melting curves for this substance, determined up to 12,000 kgf/cm², [5], and then for 5,000-25,000 kgf/cm², [8], do not correspond and therefore the constant c was considerably different.

All of this makes us assume, with a considerable degree of certitude, that there will be a better constancy of c at such high pressures and then the thermodynamic scale will be based entirely on (6). As has been already indicated, (3) is particularly promising in principle for the checking of the invariance of the constant c along the melting curve. In practice, however, its application may be difficult due to the complexity of the experimental determination of λ.

Whether it will be possible to surmount this difficulty or not, (6) remains a more reliable basis for a scale than the other empiric equations. The constants it contains were physically analyzed and analytically expressed by the parameters of melting. Because of this, new possibilities appeared for the extrapolation of (6).

In conclusion let us note that the principles we have discovered which accompany the process of melting under pressure were true over a wide range of pressures for substances which were not diverse by nature. In the universality of these principles we find considerable physical significance which we were unable to discuss more fully in this paper.

Conclusions. The existence of certain general principles, or laws, accompanying the melting process of substances under pressure has been shown. The physical meaning of the empirical constants of the Simon equation has been revealed and their analytical expression has been given by means of the thermodynamic parameters of melting. A new form of the equation of the melting curve has been obtained. The use of these equations for constructing a thermodynamic scale for high pressures was discussed.

LITERATURE CITED

[1] M. K. Zhokhovskii, Izmeritel'naia Tekhnika No. 2 (1957).

[2] M. K. Zhokhovskii and V. N. Razumikhin, Izmeritel'naia Tekhnika, No. 4 (1957).

[3] M. K. Zhokhovskii, Izmeritel'naia Tekhnika, No. 5 (1955).

[4] F. Simon and G. Glatzel, Z. f. anorg. allgem. Chemie 1928, 178, 309.

[5] P. W. Bridgman, Physics of High Pressure (Russian translation of American text) ONTI (1935).

[6] P. W. Bridgman, Proc. Am. Acad. of Arts Sci. 1935, 70, 1.

[7] F. Simon, Trans. Farad. Soc. 1937, 33, 65.

[8] P. W. Bridgman, Proc. Am. Acad. Arts Sci., 1942, 74, 12.

EFFECT OF MASS ON SPECIMEN OF HARDNESS VALUES DETERMINED BY DYNAMIC METHODS

B. A. Bandyshev

Dynamic methods of measurement are widely employed for determining the hardness of metals, the commonest of these methods being that of indentation by the impact of a ball (impression method) and the elastic recoil method. A characteristic feature of these methods is that when the indenter is impressed into the metal specimen (or component) there is a collision of the latter with the hammer of the instrument. The results of such a collision depend on the inertia forces, which can be made negligible by always using sufficiently massive specimens and by standardizing their sizes [1]. Yet these measures are still inadequate to determine how the mass of the specimen or component affects hardness measurements by dynamic methods and what the minimum mass of the specimen must be so that we can neglect the effect of inertia forces in assessing the results of measurement.

In this connection we examine below how the ratio of the masses involved in the collision affects the results of hardness measurements by dynamic methods.

If we consider the classical mechanical problem of the direct impact of two bodies of mass m and M, where the velocity of the body of mass M before impact is zero, then in the case of the reflected impact in hardness determination by dynamic methods, we have the following expressions for calculating the velocities of the bodies after their collision:

$$v = \frac{V}{k+1}\left[1-k\sqrt{1-\frac{k+1}{k}\frac{A}{E}}\right],$$
$$u = \frac{V}{k+1}\left[1+k\sqrt{1-\frac{k+1}{k}\frac{A}{E}}\right], \qquad (1)$$

where V and v are the velocities of the body of mass m before and after impact respectively, u is the velocity of the body mass M after impact, and A is the work of plastic deformation,

$$E = \frac{mV^2}{2}, \quad k = \frac{M}{m}.$$

In determining hardness by dynamic methods the difference in the hardness values of the test metals affects the value of the coefficient of restitution, which is determined by the ratio

$$c = \frac{u - v}{V}. \tag{2}$$

Assuming that for some fixed energy of the colliding bodies before impact the coefficient of restitution is a constant value, which is independent of the collision velocity or the size of the bodies and depends only on the material of the bodies [1], we can calculate the change in the work of plastic deformation in collision of bodies as a function of the ratio of their masses. For this purpose we replace v and u in (2) by their values from (1). With E = const and with the same metal under test we obtain:

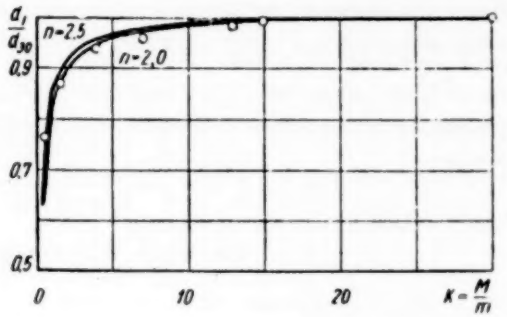

$$c = \sqrt{1 - \frac{k_1 + 1}{k_1} \frac{A_{k_1}}{E}} = \sqrt{1 - \frac{k_2 + 1}{k_2} \frac{A_{k_2}}{E}} = \ldots = \text{const} \tag{3}$$

Hence, with different mass ratios, equal to k_1 and k_2, the ratio of the works of plastic deformation A_{k_1} and A_{k_2} will be:

$$\frac{A_{k_1}}{A_{k_2}} = \frac{k_1 (k_2 + 1)}{(k_1 + 1) k_2}. \tag{4}$$

When $k_2 \to \infty$ (4) has the form:

$$\frac{A_{k_1}}{A_{k\infty}} = \frac{k_1}{k_1 + 1}. \tag{5}$$

Hence we see that with an arbitrary mass ratio k_1, a $\frac{k_1}{k_1 + 1}$ th part of the maximal possible work of plastic deformation $A_{k\,\infty}$ goes towards the work of plastic deformation.

When the identation method is used to measure the hardness of two specimens of the same metal but of different masses, the ratio of the works of plastic deformation may be expressed by the ratio of the mass of each specimen individually to the mass of the instrument hammer, according to (4). This ratio of the works of plastic deformation may be expressed by the metal constants involved in the law relating to impression by a ball, and the diameters of the impressions – by means of the known relations for the work of plastic deformation:

$$\left(\frac{A_{k_1}}{A_{k_2}}\right) = \left(\frac{d_1}{d_2}\right)^{n+2} \tag{6}$$

Equating (4) and (6) we get

$$\frac{d_1}{d_2} = \sqrt[n+2]{\frac{k_1 (k_2 + 1)}{(k_1 + 1) k_2}}. \tag{7}$$

The curves plotted from (7) are depicted on the Figure, on which we have also plotted points from the experimental data contained in the Table.

The experimental data were obtained by the impression of a 10-millimeter ball by the impact of a 3 kg hammer falling from a height of 0.5 m on specimens of the same metal. The figures show the good agreement between the experimental results and the calculations from (7).

Hardness determination by the impression method is made from a calibration curve giving the relating between the diameter of the impression obtained on the test metal by the impact and the value of the static

Mass of specimen in kg	1.35	4.0	11.35	21	39	45	90
Ratio of mass of specimen to mass of hammer	0.45	1.33	3.78	7.0	13.0	15.0	30
Diameter of impression in mm	3.42	3.91	4.25	4.32	4.45	4.50	4.52
Ratio of variable diameter in impression to greatest diameter	0.757	0.865	0.940	0.955	0.985	0.995	1.00

hardness H_B. Hence the relation (7) enables us to answer the questions posed in the present paper. If we use specimens with masses at least 10 times greater than the mass of the hammer, then the effect of inertia forces can be neglected, since in this case the greatest difference between the diameters of the impressions for specimens or components of different mass will lie within the limits of measuring accuracy (0.1 mm). The best value of $\underline{k}$ for the construction of the calibration curve must be taken as 20.

For the elastic recoil method the effect of the mass of the specimen or component on the results of hardness measurement may be established on the basis of the following relation:

$$\frac{h_1}{h_0}=\left(\frac{1-ck}{k+1}\right)^2. \qquad (8)$$

This relation is deduced on the grounds that the height of elastic rebound of a free-falling hammer, which is determined by the hardness, is proportional to the energy of the hammer after impact. This energy comprises some part of the constant energy store of the hammer before impact. The ratio of these energies is determined, on the one hand, by the ratio of the height of rebound of the hammer to the height of its initial fall h_1/h_0, and, on the other, by the ratio of the squares of the speeds of the hammer before and after impact v^2/V^2. Expressing v^2/V^2 by the ratio of the mass of the test metal to the mass of the hammer and by the coefficients of restitution from (1) and (3) we obtain the relation (8) which is in good agreement with the results of the experimental studies of Tritton, and Minkevich [2], who showed that with increase in specimen mass the hardness readings by the elastic recoil method increased.

We should note in assessing the value $\underline{k}$ we must take into account any deviation from direct impact, since indirectness of impact results in a diminution of the mass participating in the collision. The mass reduced to the line of impact from a consideration of the testing conditions may be computed from formulae obtained in the solution of actual problems.

Conclusion. 1. We have obtained relations which enable us to determine the effect of the mass of specimen or component on the results of measuring hardness by dynamic methods.

2. In measuring hardness by the impression made by the impact of a ball on the surface of the specimen, the mass of the specimens must be at least ten times the mass of the hammer. In this case the effect of inertia forces can be neglected.

3. In determining the ratio of the colliding masses we must take into account the indirectness of impact.

LITERATURE CITED

[1] D. B. Gogoberidze, in the book: Hardness of Metals and its Measurement [in Russian] (Mashgiz, Moscow-Leningrad, 1952).

[2] H. O'Neill, in the book: The Hardness of Metals and its Measurement (Russian translation) (Metallurgizdat, Moscow, 1940).

ELIMINATION OF TEMPERATURE ERROR IN WORKING WITH THERMO-COMPENSATED TENSOMETERS

Iu. A. Pykhtin

The theory of the thermo-compensated tensometer has been expounded in [1]. A thermo-compensated tensometer, made of constantan and copper wires connected in series, has been described in [2].

We have developed, tested and employed thermo-compensated tensometers made from unannealed constantan wire of diameter 0.03 mm and nichrome wire of diameter 0.04 mm. These wires are easily welded together, and hence the construction of thermo-compensated tensometers from them presents no difficulties.

Working with thermo-compensated tensometers showed that in the tensometry of components with large temperature gradients there was an error in measurement with these instruments, due to the fact that the wire in the tensometer grid was not uniformly heated.

We will examine this question in more detail.

The figure shows the temperature characteristics of nichrome and constantan tensometers, recorded on a specimen of 40 KhNMA steel.

The ratio of the resistances of the nichrome and constantan portions in the grid of a thermo-compensated tensometer must satisfy the condition

$$\beta_н R_{0н} = \beta_к R_{0к}. \tag{1}$$

Hence from this formula we have

$$R_{0к} = R_{\text{tot}} \frac{\beta_н}{\beta_н + \beta_к}, \tag{2}$$

where

$$R_{\text{tot}} = R_{0к} + R_{0н}.$$

Here $\beta_н = \frac{\Delta R_н}{R_{0н} t}$ is the aggregate temperature coefficient of the nichrome wire (see [2]),

$R_{0н}$ is the resistance of the nichrome wire in the grid of the thermo-compensated tensometer at temperature t_0,

$\beta_к = \frac{\Delta R_к}{R_{0к} t}$ is the aggregate temperature coefficient of the constantan wire.

$R_{0к}$ is the resistance of the constantan wire in the grid of the thermocompensated tensometer at temperature t_0.

Relation (1) is valid if the whole tensometer has the same temperature.

Let us consider a thermo-compensated tensometer with the temperature of the component on which the tensometer is cemented varying linearly across the axis of the tensometer.

For simplicity of argument we will assume that the number of nichrome wires $n_к$ and the number of constantan wires $n_к$ in the tensometer grid are whole numbers.

The total number of wires in the tensometer is

$$n_{\text{tot}} = n_н + n_к. \tag{3}$$

The temperature of each wire of the tensometer will differ from the temperature of each subsequent wire by a value

$$\Delta t = \frac{t_1 - t_2}{n_{tot} - 1}. \tag{4}$$

where t_1 and t_2 are the temperatures of the edge wires of the tensometer.

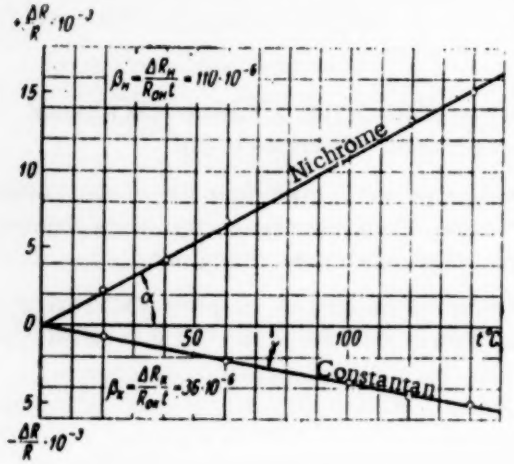

The resistance of one nichrome wire R_N, at initial temperature t_0 is

$$R_{N1} = \frac{R_{0N}}{n_N} \tag{5}$$

and of one constantan wire is

$$R_{K1} = \frac{R_{0K}}{n_K}. \tag{6}$$

The change of resistance of the first nichrome wire on being heated from the initial temperature $t_0 = 0$ to temperature t_1 is

$$\Delta R_{N1} = R_{N1} t_1 \beta_N.$$

The change of resistance of the second nichrome wire is

$$\Delta R_{N2} = R_{N1} (t_1 + \Delta t) \beta_N.$$

The change of the last (n_N th) nichrome wire is

$$\Delta R_{Nn} = R_{N1} [t_1 + (n_N - 1) \Delta t] \beta_N.$$

The aggregate change of resistance of all n_N nichrome wires is

$$\Delta R_{N\Sigma} = \Delta R_{N1} + \Delta R_{N2} + \ldots + \Delta R_{Nn} = n_N R_{N1} \beta_N t_1 - \frac{n_N (n_N - 1)}{2} R_{N1} \beta_N \Delta t = n_N R_{N1} \beta_N \left(t_1 - \frac{n_N - 1}{2} \Delta t\right) = R_{0N} \beta_N t_{m.N}, \tag{7}$$

where $t_{m.N} = \frac{t_1 + t_{nN}}{2}$ is the mean temperature of the nichrome portion of the tensometer.

By a similar argument for the constantan portion of the tensometer, we obtain:

$$\Delta R_K \Sigma = n_K R_{K1} \beta_K \left(t_2 + \frac{n_K - 1}{2} \Delta t\right) = R_{0K} \beta_K t_{m.K}, \tag{8}$$

where $t_m = \frac{t_2 + t_{nK}}{2}$ is the mean temperature of the constantan portion of the tensometer.

The temperature change of resistance of the tensometer is

$$\Delta R_t = \Delta R_{N\Sigma} - \Delta R_{K\Sigma} = R_{0N} \beta_N t_{m.N} - R_{0K} \beta_K t_{m.K}$$

Using (1) we write:

$$\Delta R_t = R_{0K} \beta_K (t_{m.N} - t_{m.K}).$$

Neglecting the difference of temperatures $t_{nN} - t_{nK} = \Delta t$ и and putting $t_{nN} = t_{nK}$, we obtain:

$$\Delta R_t = R_{ok}\beta_k \left(\frac{t_1 + t_{nn}}{2} - \frac{t_2 + t_{nn}}{2} \right) = R_{ok}\beta_k \frac{t_1 - t_2}{2}.$$

Using (2) we obtain:

$$\Delta R_t = R_{tot} \frac{\beta_n \beta_k}{\beta_n + \beta_k} \cdot \frac{t_1 - t_2}{2}. \tag{9}$$

We determine the fictitious relative deformation ϵ corresponding to the resistance change ΔR_t. The sensitivity factor is $k = \frac{\Delta R}{R\epsilon}$. Hence $\epsilon = \frac{\Delta R}{Rk}$ and

$$\epsilon_{fict.} = \frac{\Delta R_t}{R_{tot} k} = \frac{1}{k} \cdot \frac{\beta_n \beta_k}{\beta_n + \beta_k} \cdot \frac{t_1 - t_2}{2}. \tag{10}$$

As we see from (10) the temperature error (fictitious deformation) does not depend on the tensometer resistance.

If, for instance, $\frac{t_1 - t_2}{2} = 2.5°C$, $\beta_n = 110.10^{-6} \frac{1}{°C}$, $\beta_k = 36.10^{-6} \frac{1}{°C}$, $k = 2$, then ϵ fict. $= 33.9 \cdot 10^{-6}$.

In the uniaxially strained state and with a modulus of elasticity $E = 2 \cdot 10^6$ kg/cm^2, this fictitious relative deformation will produce an error in determining the strains:

$$\Delta\sigma_{fict.} = E\epsilon_{fict.} = 67.8 \text{ kg/cm}^2.$$

Conclusion. It is advisable to construct the thermo-compensated tensometer with its nichrome portion situated exactly in the center of the strain-sensitive grid. In this case the temperature error (where the temperature distribution is linear across the tensometer axis) will be zero.

LITERATURE CITED

[1] G. E. Rudashevskii, Izmerital'naia Tekhnika 1 (1956).

[2] G. E. Rudashevskii, Izmeritel'naia Tekhnika 3 (1957).

ACTUATING MECHANISM OF AN AUTOCOMPENSATED MANOMETER

V. I. Bakhtin

A new manometer for accurate measurement of rarefied gases and vapors over a wide range is described in [1, and 2]. The principle of the manometer operation consists in automatic compensation by the ponderomotive forces of a magnetic field of the gas pressure, which strains the elastic envelope.

In the magnetically compensated manometer [1] a moving-coil mechanism provides the force acting on the envelope. For the manometer to be able to cover a gas pressure range up to 100 mm Hg with an effective envelope area of 20 cm^2, the moving coil system must develop an effort of the order of 3 kg –f.* This would require overall dimensions (diameter 235 mm and height 140 mm) and a weight (50 kg) far too large for an instrument which should be essentially portable and light. It is disadvantageous to decrease the envelope area since this greatly decreases sensitivity, which falls proportionately to the 4th power of the envelope diameter.

Having analyzed other actuating mechanisms, most commonly used in industry, we arrived at the conclusion that the best one for our purpose would be an ac electromagnet whose traction force does not depend on the hysteresis of its magnetic circuit and can be made very large with small overall dimensions.

Figure 1 shows the simplest ac electromagnet. Its core consists of E shaped transformer iron laminations; the armature is made in a similar way. The pertinax former with the winding are placed on the middle limb of the core. The winding is connected to an ac voltage source of a fixed frequency $U = U_0 \sin \omega t$, amplitude modulated by the control transducer of small displacements.

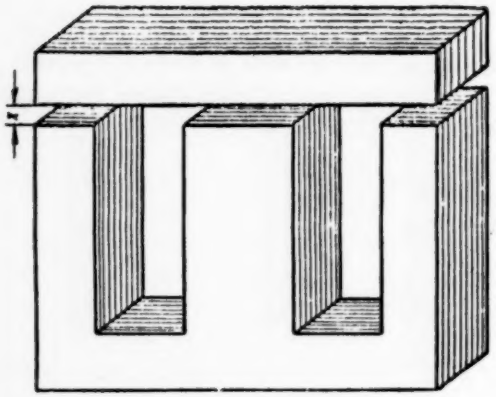

Fig. 1.

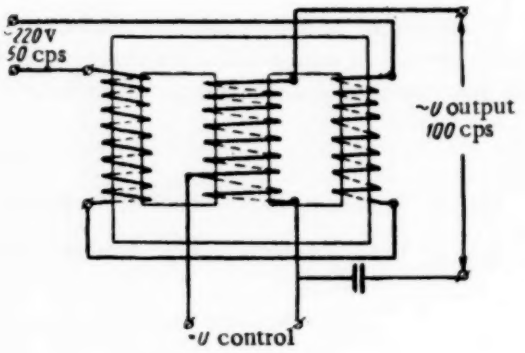

Fig. 2.

The electromagnet traction force is proportional to the rate of change of the system's potential energy

$$P = -\frac{dw}{dx}, \tag{1}$$

where x is the airgap between the magnet poles and the armature.

According to Maxwell

$$\frac{dw}{dx} = \frac{\Phi^2}{8\pi}\frac{dR_M}{dx}, \tag{2}$$

where Φ is the flux and R_M the total reluctance of the magnetic circuit. Assuming that the reluctance is concentrated in the airgap

* Kg · force.

$$R_{\delta} \simeq R_b = \frac{x}{S_b} \tag{3}$$

and transforming the traction force into kilograms we obtain

$$P[\text{kg-f}] = \frac{\Phi^2}{5000^2 S_b} = 4 \cdot 10^{-8} B^2 S_b \tag{4}$$

where Φ is in maxwells, B the flux density in the airgap in gauss and S_b, the airgap cross-sectional area (for small airgaps equal to the area of the middle limb) in cm^2.

For an actual magnet Sh-32 with a core package of 30 mm, n = 1000 turns, x = 0.5 cm and I = 3 amps, we obtain by calculations S_b = 10 cm^2 and B = 3000 gauss.

Hence

$$P = 4 \cdot 10^{-8} \cdot 9 \cdot 10^{-6} \cdot 10 \simeq 4 \text{ kgf.}$$

The traction force is independent of the direction of the current in the winding; the frequency of its pulsations is twice the current frequency

$$\Omega = 2\omega.$$

The amplitude of the forced oscillations of the system "envelope – armature" can be made as small as desired by choosing the appropriate frequency ω. The most general differential equation which represents the oscillatory movement of the system under the action of a force is

$$\ddot{x} + 2\eta\dot{x} + \omega_0^2 x = \frac{1}{m} \sum_{i=1}^{n} P_i \sin(\omega_i t + \nu_i), \tag{5}$$

where 2η is the coefficient of the design force, $\omega_0 = \sqrt{\frac{k}{m}}$ the natural frequency of the system, k the stiffness of the envelope and m the mass of the armature. P_i, ω_i and ν_i are respectively the amplitude, frequency and the phase of the i-th harmonic in the Fourier series of the electromagnet pulsating force.

Dots denote derivatives of x with respect to time t.

In our case it is advisable to examine the oscillations of the system under the effect of the first harmonic of the actuating force (i = 1)

$$\ddot{x} + 2\eta\dot{x} + \omega_0^2 x = \frac{1}{m} P_1 \sin \Omega t. \tag{6}$$

The general solution of this differential equation is

$$x = e^{-\eta t}\left(C_1 e^{i\omega_1 t} + C_2 e^{-i\omega_1 t}\right) + \frac{1}{m} P_1 \frac{e^{i\Omega t}}{\omega_0^2 - \Omega^2 + 2i\Omega\eta} \tag{7}$$

For stable state oscillations

$$x = \frac{1}{m} P_1 \frac{e^{i\Omega t}}{\omega_0^2 - \Omega^2 + 2i\Omega\eta}. \tag{8}$$

The real value of the amplitude

$$x=\frac{P_1}{m}\left[(\omega_0^2-\Omega^2)^2+4\Omega^2\eta^2\right]^{-\frac{1}{2}}. \tag{9}$$

The second term in the square brackets is small and can be neglected, then the final expression becomes:

$$x=\frac{P_1}{m}\left(\frac{1}{\omega_0^2-\Omega^2}\right). \tag{10}$$

In an actual case if K = 0.3 kg · f/mm, m = 0.1 kg, the frequency will be ω_0 = 30 cps. Assuming P_1 = 3 kg · f, $f = \omega/2\pi$ = 150 cps, we shall obtain:

$$x=\frac{3000}{100}\cdot\frac{980}{4\cdot10^4-9\cdot10^2}\simeq7\cdot10^{-3}\text{ cm}.$$

Thus an ac electromagnet of small overall dimensions and weight, working at 150 cps, provides a force sufficient for an autocompensating manometer to cover a range up to 100 mm Hg. The forced armature oscillations in the above condition are small ($7\cdot10^{-2}$ mm) and cannot influence the normal operation of the automatic control circuits, which have a definite frequency characteristic, inertia and selectivity. Such small vibrations can only have a positive effect on the envelope; due to them the effect of preceeding loadings will be anulled a hundred times per second, which will considerably decrease the already small error due to elastic hysteresis.

The requirement of a high voltage supply source is a big drawback of the ac electromagnetic actuating mechanism. For the electromagnet described, neglecting the reluctance of iron, the inductance is

$$L=\frac{0.4\pi n^2 S}{2x\cdot10^8}\simeq0.12\text{ henries}$$

The total resistance of the winding is

$$z\simeq\omega L\simeq120\text{ ohm}$$

Hence, for a current of I = 3 amp a supply voltage of U = 360 v is required, and the reactive power of the winding is W = 1080 w. It would appear that an electronic device for feeding the electromagnet is not suitable. In our manometer model we used a controlled magnetic transformer-type frequency multiplier (Fig. 2). It should be noted that a decreased pulsation of the force can be achieved by splitting the winding into two parts and feeding each half from the same source but with a phase difference between them.

LITERATURE CITED

[1] A. Aleskovskii, V. Andrushkevich and Iu. Solov'ev, Pribory u Tekhnika Eksperimenta, 1 (1957).

[2] V. I. Bakhtin, Priborostroenie, No. 10, 1957.

INSTRUMENT FOR MEASURING TORQUE, AXIAL STRESSES AND FEEDING WHEN DRILLING SMALL HOLES

V. V. Monakov

For measuring torque, axial stresses and feeding when drilling, reaming or threading small holes of 0.2 to 5 mm in diameter the author developed an indicating instrument, based on the principle of elastic strains in steel plates, and shown on the drawing attached.

The work is placed on Table 1 which revolves freely on ball bearings and is centered by a needle bearing. The torque produced by drilling, reaming or threading rotates the table and bends two tempered steel plates 2, which displace the measuring rods of horizontally mounted extensometers 3. The extensometers measure the bending of the plates to 0.01 mm.

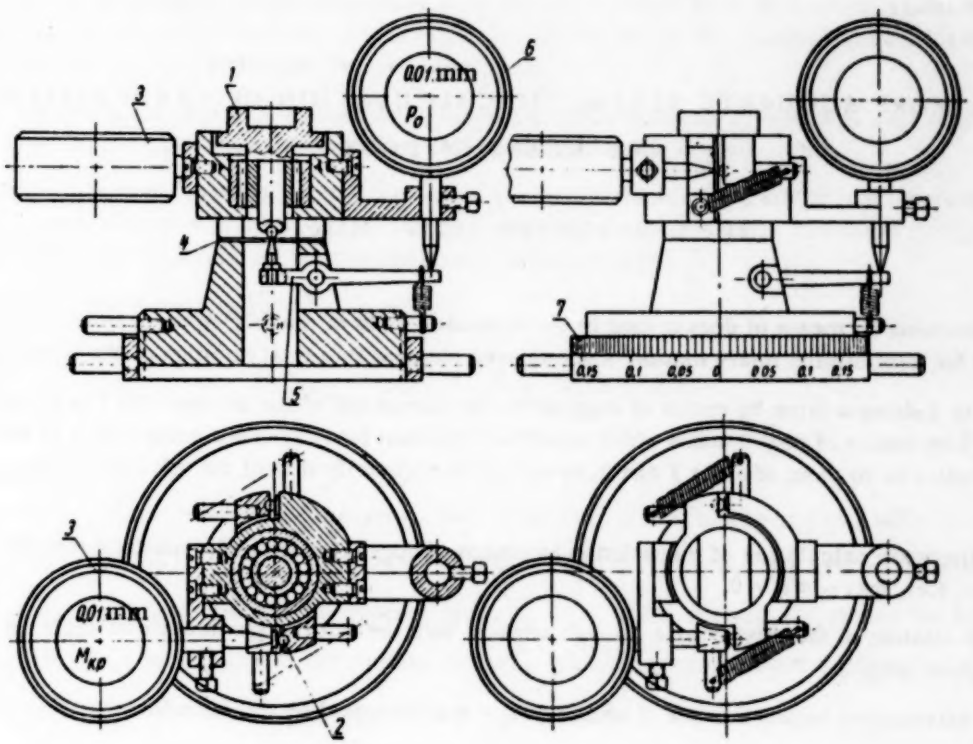

The axial stresses due to the feeding of the drill are measured by means of a horizontal elastic plate 4, which bears the table ball-pivot. Under the stress of the drill-feed the table is pressed down and bends plate 4, displacing lever 5, which is connected to extensometer 6.

For investigating the effect of feeding on axial stresses and torque, the table can be moved in such a way that feeding in the range of 0.005 to 0.2 mm/turn is obtainable. For this purpose a micrometer thread with a 1 mm pitch is provided on the body of the instrument and dial 7 with 0.005 mm calibrations attached to it. The drill is fed by turning the dial while the torque and axial stress are being recorded.

The calibration of the instrument consists in selecting and calibrating the elastic plates.

For axial stress calibration a polished plate finished to 1.25 ± 0.01 mm is inserted horizontally into the body of the instrument. Weights of 0.5, 1, 2, 3, 4, 5, 6, 7, 8, 9, and 10 kg are placed consecutively on the table of the instrument and the bending of the plate is read off the extensometer. From these readings a calibration chart is made up.

For torque calibration the instrument is rotated through 90° and secured in a vise by its base, then two elastic plates (0.5 × 8 × 40 mm) are inserted into it, weights of 2, 3, 4, 5, 6, 7, 8, 9 and 10 kg are consecutively suspended from the plates at the ball rest, extensometer readings recorded and from them a calibration chart made up.

By means of this instrument dynamic relationships were investigated when drilling brass L-62.

The high speed drills used for this test were type PF-1 made by the "Frezer" plant, normally heat treated, either polished electrically or not, 0.25 to 5 mm in diameter, with a pitch angle of 26 to 19°, cutting edge angle of 120° and a lip angle $\alpha = 22°$.

The shape of the drills was selected after extensive testing for durability. Dry machining was used.

As the result of these investigations the effect of the drill size and feeding on the torque and axial stress was found and it was also established that both the torque and axial stress are reduced on an average by 40% when electrically polished drills are used as compared with those not polished electrically.

A MORE ACCURATE KINEMATIC CALCULATION OF TRANSMISSION BY MEANS OF DOGS

Iu. L. Lakin and Iu. V. Miloserdin

Transmission by means of dogs is used in the kinematic links of the driving mechanism of various measuring instruments for transforming rotary motion of the driving element into rotary motion of the driven element.

Figure 1 shows a drive by means of dogs where the movement of the driving axle 1 is transmitted to the driven axle 2 by means of dogs 3 and 4 which consist of cylinders (usually of the same radius r) whose axes are either perpendicular to those of axles 1 and 2, or one of them (usually that of the driving dog) is at an angle $\gamma \neq 90°$.

In kinematic calculation of transmission by means of dogs [1] it is usually assumed that the dogs are straight lines, i.e., that $r_1 = r_2 = 0$.

Let a rotation of the driving axle through angle α turn the driven axle through an angle β, generally not equal to angle α (Fig. 1).

The relationship between α and β when $r_1 = r_2 = 0$ is expressed by the formula

$$\beta = \operatorname{arctg}\left[\frac{b \operatorname{tg} \alpha}{a + \frac{b \operatorname{ctg} \gamma}{\cos \alpha}}\right] \qquad (1)^*$$

or when $\gamma = 90°$

$$\beta = \operatorname{arctg}\left(\frac{b}{a} \operatorname{tg} \alpha\right), \qquad (2)$$

where a and b are distances from crossing point O of the axle axes to the crossing points A and B of the dog axes with those of the corresponding axles.

The ratio of angle increments $\frac{d\beta}{d\alpha}$ is known as the transmission ratio and is the basic parameter characterizing the transmission kinematics.

The formulae for the transmission ratio have the following form

$$K = \frac{d\beta}{d\alpha} = \frac{\frac{a}{b} + \cos \alpha \operatorname{ctg} \gamma}{\cos^2 \alpha \left(\frac{a^2}{b^2} - 1\right) + 2\frac{a}{b} \cos \alpha \operatorname{ctg} \gamma + \operatorname{ctg}^2 \gamma + 1} \qquad (3)$$

*Trans. note: arctg = $\tan^{-1}$; tg = tan; ctg = cot.

and when $\gamma = 90°$

$$K = \frac{d\beta}{d\alpha} = \frac{a}{b\left[1+\left(\frac{a^2}{b^2}-1\right)\cos^2\alpha\right]}. \qquad (4)$$

However, the transmission ratios determined from (3) and (4) differ from their actual values due to the assumption that $r_1 = r_2 = 0$, which does not in fact exist. When the mechanism is manufactured, this assumption makes it necessary to carry out additional "blind" adjustments.

Below we give a technique for a kinematic calculation of transmission by means of dogs, which provides an accurate value for the transmission ratio, taking into consideration the dog diameters.

In order to determine the relationship between angles of rotation of dogs, taking into consideration their diameters, for a case when $\gamma = 90°$, let us make use of equations expressed in terms of straight lines running through the axes of the dogs, and then find the shortest distance between them [2].

The straight line equations have the form:

$$\frac{x-x_1}{X_1} = \frac{y-y_1}{Y_1} = \frac{z-z_1}{Z_1} \;\&\; \frac{x-x_2}{X_2} = \frac{y-y_2}{Y_2} = \frac{z-z_2}{Z_2},$$

where for our case

x_1, y_1 and z_1 are the coordinates of point A, the intersection of the driving dog axis with that of the axle.

x_2, y_2 and z_2 are the coordinates of point B, the intersection of the driven dog axis with that of the axle.

X_1, Y_1 and Z_1 are projections of the guiding vector $\bar{L}_1$ which coincides with the axis of the driving dog.

X_2, Y_2 and Z_2 are projections of the guiding vector $\bar{L}_2$, which coincides with the axis of the driven dog.

and $\underline{x}$, $\underline{y}$ and $\underline{z}$ are the general straight line coordinates.

The coordinates of points A and B (Fig. 2) are:

$$x_1 = a;\ y_1 = 0;\ z_1 = 0;$$
$$x_2 = 0;\ y_2 = b;\ z_2 = 0.$$

By taking one of the guiding vector projections to be equal to unity we find the remaining projections:

$$X_1 = 0;\ Y_1 = 1;\ Z_1 = \operatorname{tg}\alpha;$$
$$X_2 = 1;\ Y_2 = 0;\ Z_2 = \operatorname{tg}\beta.$$

By substituting the values of the coordinates of points A and B and the vector projections into the straight line equations we obtain:

$$\frac{x-a}{0} = \frac{y}{1} = \frac{z}{\operatorname{tg}\alpha};$$
$$\frac{x}{1} = \frac{y-b}{0} = \frac{z}{\operatorname{tg}\beta}.$$

When the transmission by means of dogs is operating, its kinematic circuit is always closed, i.e., the dogs are touching each other. In this case the shortest distance between their axes is $h = r_1 + r_2$ (where r_1 and r_2 are the radii of the dogs).

Making use of the formula for the shortest distance between straight lines we have

$$h=\frac{\begin{vmatrix} x_2-x_1 & y_2-y_1 & z_2-z_1 \\ X_1 & Y_1 & Z_1 \\ X_2 & Y_2 & Z_2 \end{vmatrix}}{\sqrt{\begin{vmatrix} Y_1 Z_1 \\ Y_2 Z_2 \end{vmatrix}^2+\begin{vmatrix} Z_1 X_1 \\ Z_2 X_2 \end{vmatrix}^2+\begin{vmatrix} X_1 Y_1 \\ X_2 Y_2 \end{vmatrix}^2}} \tag{5}$$

or by substituting the values of the point coordinates and vector projections in (5) we obtain:

$$r_1+r_2=\frac{\begin{vmatrix} 0-a & b-0 & 0-0 \\ 0 & 1 & \operatorname{tg}\alpha \\ 1 & 0 & \operatorname{tg}\beta \end{vmatrix}}{\sqrt{\begin{vmatrix} 1 & \operatorname{tg}\alpha \\ 0 & \operatorname{tg}\beta \end{vmatrix}^2+\begin{vmatrix} \operatorname{tg}\alpha & 0 \\ \operatorname{tg}\beta & 1 \end{vmatrix}^2+\begin{vmatrix} 0 & 1 \\ 1 & 0 \end{vmatrix}^2}}$$

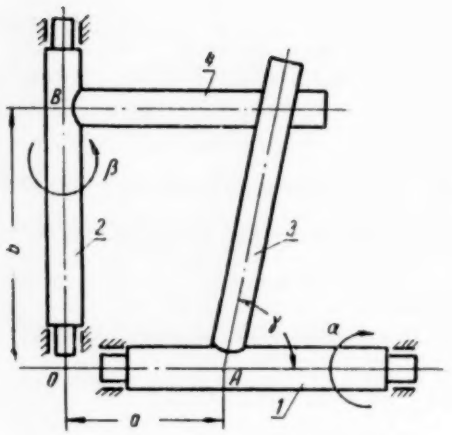

Fig. 1.

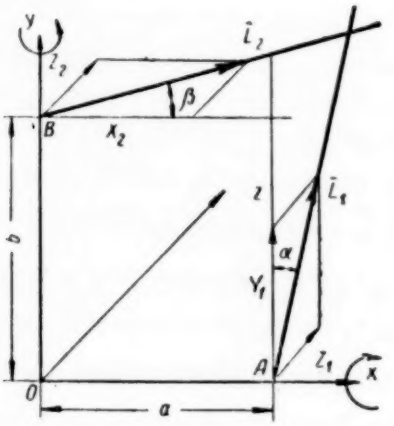

Fig. 2.

Solving the determinants and taking $r_1 = r_2 = r$ we have:

$$2r=\frac{-a\operatorname{tg}\beta+b\operatorname{tg}\alpha}{\sqrt{\operatorname{tg}^2\alpha+\operatorname{tg}^2\beta+1}}. \tag{6}$$

Solving (6) with respect to $\operatorname{tg}\beta$ and substituting $2r$ by $\underline{d}$ we obtain:

$$\operatorname{tg}\beta=\frac{ab\operatorname{tg}\alpha\mp d\sqrt{(a^2-d^2)\sec^2\alpha+b^2\operatorname{tg}^2\alpha}}{a^2-d^2}. \tag{7}$$

In (7) the sign in front of the radical is chosen according to the position of the driving dog with respect to the driven one. For the case shown in Fig. 1 the radical is positive.

From (7) we obtain the value of β:

$$\beta=\operatorname{arctg}\frac{ab\operatorname{tg}\alpha+d\sqrt{(a^2-d^2)\sec^2\alpha+b^2\operatorname{tg}^2\alpha}}{a^2-d^2}.$$

By differentiating this expression we obtain:

$$K=\frac{d\beta}{d\alpha}=\frac{(a^2-d^2)\left[ab+\dfrac{d(a^2+b^2-d^2)\sin\alpha}{\sqrt{a^2-d^2+b^2\sin^2\alpha}}\right]}{(a^2-d^2)^2\cos^2\alpha+\left(ab\sin\alpha+d\sqrt{a^2-d^2+b^2\sin^2\alpha}\right)^2}. \tag{8}$$

By assuming that d = 0 in (8) it is easy to obtain (4).

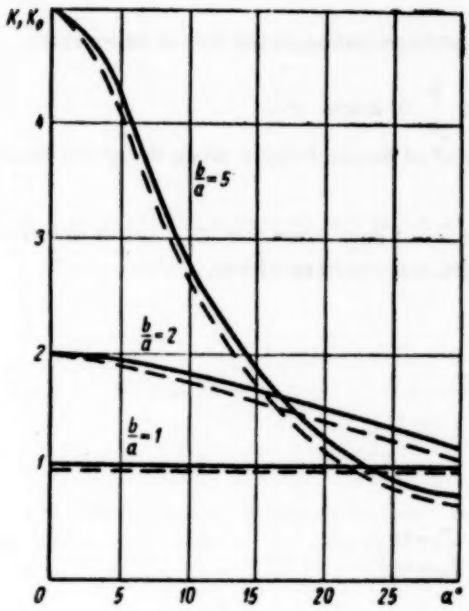

Fig. 3.

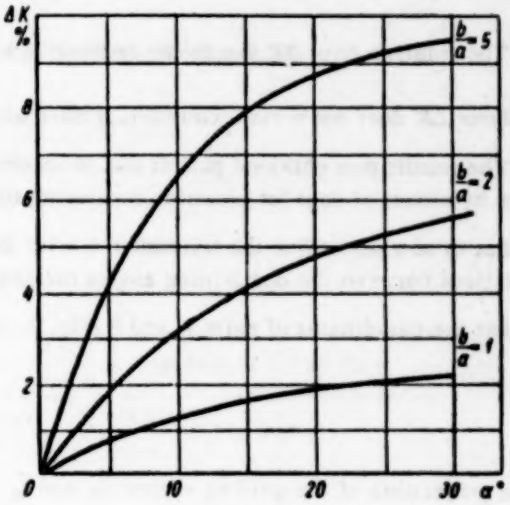

Fig. 4.

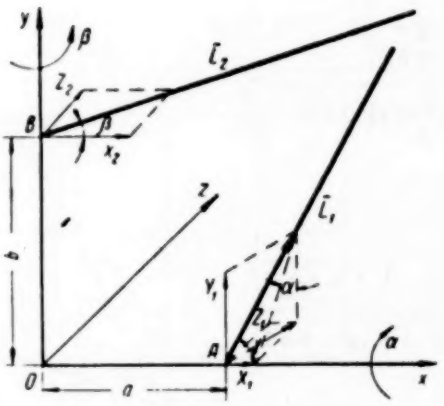

Fig. 5.

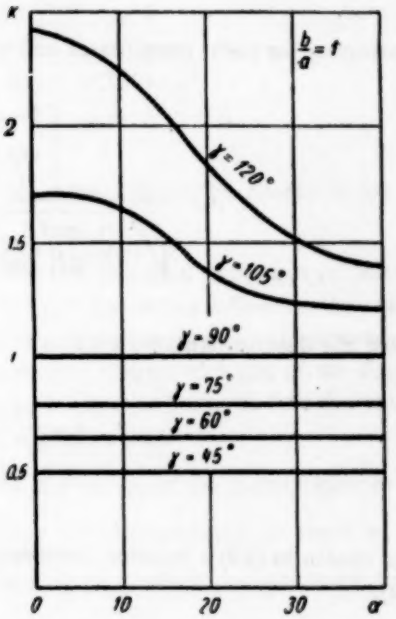

Fig. 6.

Taking into account that the exact value of the transmission ratio found from (8) depends to a great extent on the diameters of the dogs, let us find the relative error ΔK of the approximate method of calculation by (4) and express it in percent:

$$\Delta K=\frac{(K-K_0)\ 100\%}{K}. \tag{9}$$

where K_0 is the value of the transmission ratio when $r_1 = r_2 = 0$.

For the case when the angle of rotation of the driving dog is changed in the limits of 0 to 30°, d = 2 mm and $\frac{b}{a} = 1$, 2 and 5 (b = 20, 40 and 100 mm with a = 20 mm) the value of K_0 (full line) and K (dotted line) and ΔK are given in Figs. 3 and 4.

Inspection of the graphs leads to the following conclusions.

The value of the transmission ratio changes considerably with angle of rotation α and ratio $\frac{b}{a}$.

The relative error ΔK due to the approximate method of calculation increases the transmission ratio.

Error ΔK does not remain constant, it rises with a rise in ratio $\frac{b}{a}$ or angle α.

The results thus obtained permit one to recommend this method of determining K when designing transmission by means of dogs for precision measuring instruments.

Let us now determine the transmission ratio for a drive by means of dogs when $\gamma \neq 90°$. Let us determine the relations between the dog turning angles making use of the technique described above.

Let the coordinates of point A and B (Fig. 5) be:

$$x_1 = a;\ y_1 = 0;\ z_1 = 0;$$
$$x_2 = 0;\ y_2 = b;\ z_2 = 0$$

and the projections of the guiding vectors $\bar{L}_1$ and $\bar{L}_2$ be:

$$X_1 = \operatorname{ctg}\gamma\sqrt{1+\operatorname{tg}^2\alpha};\ Y_1 = 1;\ Z_1 = \operatorname{tg}\alpha;$$
$$X_2 = 1;\qquad\qquad Y_2 = 0;\ Z_2 = \operatorname{tg}\beta.$$

Substituting for point coordinates and vector projections in (5) their values we find:

$$d = \frac{\begin{vmatrix} 0-a & b-0 & 0-0 \\ \operatorname{ctg}\gamma\sqrt{1+\operatorname{tg}^2\alpha} & 1 & \operatorname{tg}\alpha \\ 1 & 0 & \operatorname{tg}\beta \end{vmatrix}}{\sqrt{\begin{vmatrix} 1 & \operatorname{tg}\alpha \\ 0 & \operatorname{tg}\beta \end{vmatrix}^2 + \begin{vmatrix} \operatorname{tg}\alpha & \operatorname{ctg}\gamma\sqrt{1+\operatorname{tg}^2\alpha} \\ \operatorname{tg}\beta & 1 \end{vmatrix}^2 + \begin{vmatrix} \operatorname{ctg}\gamma\sqrt{1+\operatorname{tg}^2\alpha} & 1 \\ 1 & 0 \end{vmatrix}^2}}$$

or by solving the determinants we obtain:

$$d = \frac{-a\operatorname{tg}\beta + b\operatorname{tg}\alpha + b\operatorname{tg}\beta\operatorname{ctg}\gamma\sqrt{1+\operatorname{tg}^2\alpha}}{\sqrt{\operatorname{tg}^2\beta + (\operatorname{tg}\alpha - \operatorname{tg}\beta\operatorname{ctg}\gamma\sqrt{1+\operatorname{tg}^2\alpha})^2 + 1}}. \tag{10}$$

[In order to obtain in (10) a solution satisfying the conditions of the problem, radicals should be taken with a minus sign].

From (10) the relation between angles α and β take the form:

$$A\operatorname{tg}^2\beta + B\operatorname{tg}^2\alpha + C\operatorname{tg}\alpha\operatorname{tg}\beta + D\operatorname{tg}\alpha\operatorname{tg}\beta\sqrt{1+\operatorname{tg}^2\alpha} - E\operatorname{tg}^2\beta\sqrt{1+\operatorname{tg}^2\alpha} + F\operatorname{tg}^2\alpha + d^2 = 0, \tag{11}$$

where

$$A = d^2 - a^2 + d^2\operatorname{ctg}^2\gamma - b^2\operatorname{ctg}^2\gamma,$$

$$B=d^2-b^2,$$
$$C=2ab,$$
$$D=2(d^2+b^2)\operatorname{ctg}\gamma,$$
$$E=2ab\operatorname{ctg}\gamma,$$
$$F=(d^2-b^2)\operatorname{ctg}^2\gamma.$$

When calculating transmission by means of dogs for any given case the values of A, B, C, D, E and F are constant.

The transmission ratio can be found by differentiating the implicit function (11):

$$K=\frac{d\beta}{d\alpha}=-\frac{\partial f(\alpha,\beta)}{\partial\alpha}:\frac{\partial f(\alpha,\beta)}{\partial\beta},$$

where $f(\alpha, \beta)$ is the differentiated function (11).

After certain transformations we obtain:

$$K=\frac{\cos^2\beta}{\cos^2\alpha}\cdot\frac{2B\operatorname{tg}\alpha+C\operatorname{tg}\beta+D\operatorname{tg}^2\alpha\operatorname{tg}\beta\cos\alpha+\dfrac{D\operatorname{tg}\beta}{\cos\alpha}-E\operatorname{tg}^2\beta\sin\alpha+2F\operatorname{tg}^2\beta\operatorname{tg}\alpha}{-2A\operatorname{tg}\beta-C\operatorname{tg}\alpha-D\dfrac{\operatorname{tg}\alpha}{\cos\alpha}+2E\dfrac{\operatorname{tg}\beta}{\cos\alpha}-2F\operatorname{tg}\beta\operatorname{tg}^2\alpha}, \tag{12}$$

For obtaining the transmission ratio from (12) it is necessary first to find the relation between angles α and β by solving (11) with respect to tg β:

$$\operatorname{tg}\beta=-\frac{C\operatorname{tg}\alpha+D\operatorname{tg}\alpha\sec\alpha}{2A-2E\sec\alpha}\pm$$
$$\pm\sqrt{\left(\frac{C\operatorname{tg}\alpha+D\operatorname{tg}\alpha\sec\alpha}{2A-2E\sec\alpha}\right)^2-\frac{B\operatorname{tg}^2\alpha+F\operatorname{tg}^2\alpha+d^2}{A-E\sec\alpha}}. \tag{13}$$

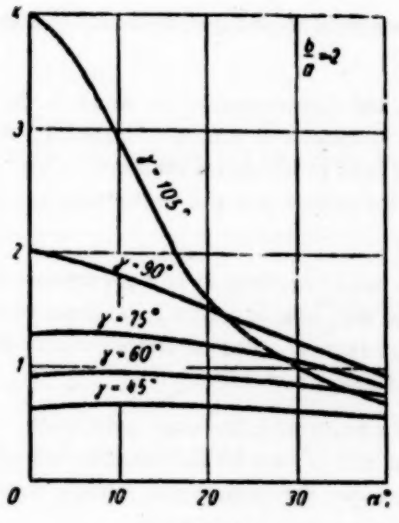

Fig. 7.

In (13) the sign of the radical should be chosen in the same manner as it was done for (10).

It should be noted that the proposed technique of determining K for the case when $\gamma \neq 90°$ and the direct differentiation of expression (13) lead to complicated and labor-consuming calculations. Hence when designing transmission by means of dogs with one of the dogs at an angle $\gamma \neq 90°$ to the axis of the axle, it is better to find the value of K by graphic differentiation of equation (13).

Figures 6 and 7 show the curves of the transmission ratio plotted at $\frac{b}{a}$ = 1 and 2 respectively, for various values of angle γ, against the angle of rotation of the driving dog, which changes from 0 to 40°.

It will be seen from the graph that the characteristic of the transmission ratio depends, in addition to other parameters, also to a considerable extent on the angle of incline γ of the driving dog.

The curves can be divided into two groups with respect to the angle of incline γ, those with $\gamma > 90°$ and with $\gamma < 90°$. The family of curves with $\gamma < 90°$ should be used for designing transmission by means of dogs in instruments with a constant value of K and the family of curves with $\gamma > 90°$ in instruments with a variable K so as to obtain the required scale shape.

From the comparison of the values of K obtained from (3) and (12) it appears that the relative error in the transmission ratio due to the approximate calculation method, i.e., when the diameters of the dogs are not taken into account is considerable. Thus, for instance, with $\frac{b}{a} = 2$; $\gamma = 105°$ and $r_1 = r_2 = 1$ mm, ΔK attains 20% at driving dog turning angle $\alpha = 30°$.

This fact should be taken into account when designing driving mechanisms for instruments.

LITERATURE CITED

[1] S. S. Tikhmenev, Elements of Precision Instruments [in Russian] (Oborongiz, 1956).

[2] N. I. Muskhelishvili, A Course of Analytical Geometry [in Russian] (Gostekhizdat, 1947).

CALIBRATION OF VIBRATION PROBES FOR MEASURING MACHINE VIBRATIONS

A. K. Novikov, A. E. Kolesnikov and B. Sh. Masharskii

Measurements of vibrations of the body or the foundations of working machines are still made in the main by comparative methods which do not require calibrated instruments. It is possible to measure the absolute vibration amplitudes only if the measuring scales (of the vibrometers) are calibrated over the whole frequency range to be measured.

The vibration probes are calibrated by attaching them to the surface of plates oscillating sinusoidally at a known frequency and amplitude. The frequency of their oscillations is determined by the mechanical and electrical oscillator.

The amplitude is measured optically by means of a microscope. At vibration frequencies of the order of 1000 cps and higher, the oscillatory displacements become so small that they cannot be measured by means of a microscope.

Thus the main difficulty in an absolute calibration of vibration probes consists in the complexity of measuring small displacements at frequencies higher than 500-600 cps.

For the purpose of calibrating vibration probes the authors designed and constructed, in the Acad. A. N. Krylov Central Scientific Research Institute, a portable device producing vibrations of a known frequency, whose amplitude is controlled by a special circuit. Such a device can be easily used in industrial laboratories and on the site. It consists of a vibrating plate, a capacity deviation measuring instrument and and audiofrequency oscillator.

As a vibrating plate the authors used (Fig. 1) the flat surface of the body (membrane) of a piezo-electric vibrator 1, placed on a massive base inside a cylinder. In the cylinder lid they placed a small flat horse-shoe shaped electrode 2, insulated from the body and forming with it a certain capacity. The calibrated vibration probe 3 is fixed by means of a holder with its point at the center of the vibrator membrane.

The whole of the surface of the membrane fixed at its sides cannot vibrate with the same amplitude. Hence, only the central part of the membrane with a diameter of about 40 mm is used for calibration purposes. An experimental check in the frequency range of 50 to 1500 cps confirmed that the central part (with a diameter 0.3 to 0.5 of the overall membrane diameter) of the membrane vibrated at a constant amplitude.

The excitation of the piezo-electric vibrator was supplied by an oscillator voltage of a known frequency. In the audio-frequency range the piezo-electric vibrator acts as a displacement transducer, i.e., at a constant amplitude excitation voltage, the central part of its membrane vibrates at an approximately constant amplitude within the frequency range.

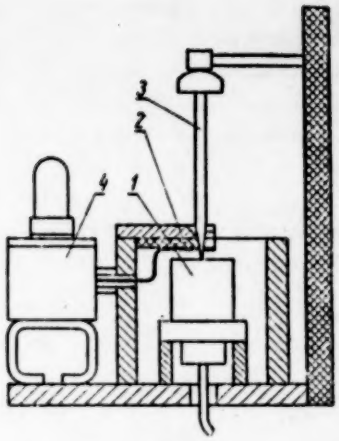

Fig. 1.

For the purpose of keeping the membrane amplitude constant and for accurate control, a capacity vibration measuring device is used, which consists of the capacity between the flat surface of the horse-shoe shaped electrode and the membrane surface acting as a variable capacitor C_0 in the tuned circuit of a high frequency oscillator 4. The capacitor C_0 responds to the vibrator excitation, and frequency modulates the high frequency oscillator signals, which are amplified in a superheterodyne amplifier, voltage limited and fed to a frequency detector (discriminator) from whose load an audio-frequency signal is obtained, which is proportional to the amplitude of the membrane vibrations.

It can be shown that the frequency deviation (Δf) is directly proportional to the oscillator frequency f_0 and the capacity variation ΔC and inversely proportional to the circuit capacity ($C_M + C_0$)

$$\Delta f = \frac{f_0 \Delta C}{2(C_M + C_0)},$$

where C_M is the installation stray capacity and
C_0 the capacity between the electrode and the vibrator surface.

By substituting its value for ΔC we obtain:

$$\Delta f = \frac{f_0\, \Delta d}{2d\left(\frac{C_M}{C_0} + 1\right)},$$

where d is the gap between the electrode and the vibrating plate surface, and
Δd is the variation of the gap due to the oscillation of the vibrator surface.

This expression provides a measure of the channel bandwidth and the possible error of measurement.

Let us note that for a plate vibration amplitude of $\Delta d = 0.5 \cdot 10^{-2}$ mm a gap of d = 0.5 mm, a carrier frequency of f_0 = 50 Mc and with $C_M = 9C_0$, the frequency deviation is equal to 25 kc. With a maximum vibration frequency of F = 20 kc, the modulation ratio will be $\beta = \frac{\Delta f}{F} \simeq 1$ and the bandwidth of the frequency modulated signal $\delta = 2(1 + \beta)F = 80$ kc.

The intermediate frequency amplifier and the discriminator of the capacity vibration measuring set should, therefore, be designed for the above bandwidth.

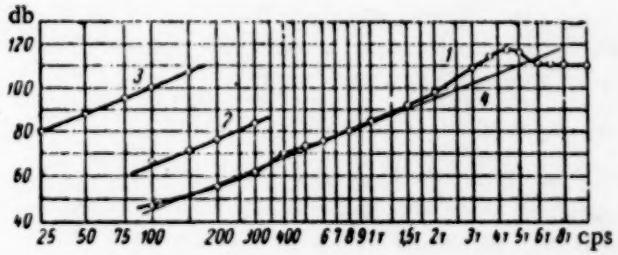

Fig. 2. Noise meter vibration probe calibration curves. Obtained 1) on a piezo-electric plate with a capacity vibration-measuring device; 2) on an electrodynamic plate with a microscope; 3) on an electro-mechanical plate; 4) the level of vibrations set on a piezo-electric plate.

The instrument's design characteristics are as follows: 1) the sensitivity with a gap between the electrode and the vibrating membrane of 0.5 mm is $8.5 \cdot 10^3$ v/cm, 2) the instrument can measure amplitude variations from $2 \cdot 10^{-6}$ to 10^{-2} mm, 3) the frequency range of the measured vibrations is from 50 to 20,000 cps.

The instrument consists constructionally of three units: the vibrating plate, the capacity vibration measuring device and an audio oscillator. The instrument is easily portable and can be periodically calibrated.

The piezo-electric vibrator membrane displacement amplitudes are small even at low audio frequencies and cannot be measured by means of an

optical microscope. In order to determine the absolute value of the vibrator membrane displacement amplitude, calibrations were made with the same vibration measuring channel. Moreover two series of measurements were made: 1) by placing the vibration probe on the membrane of the vibrator here described, when relative values of displacement and acceleration were measured; 2) by placing the vibration probe on the surface of an electrodynamic vibrator, whose displacement amplitudes were large enough to be measured on an optical microscope.

Thus the described set was used as a secondary reference instrument.

An example of a calibration curve for a vibration meter is given in Fig. 2. Acceleration amplitudes are plotted logarithmically along the Y-axis. As a rule, vibration is measured in decibels, $3 \cdot 10^{-2}$ cm/sec^2 being taken for the zero acceleration level.

In Fig. 2, curve 1 corresponds to the calibration of the channel by means of the piezo-electric plate with the capacity vibration measuring device at a constant value of displacements. Curve 2 corresponds to the calibration of the same measuring channel with a electrodynamic vibration meter. The displacement was determined by an optical microscope and maintained at $0.127 \cdot 10^{-3}$ cm. (amplitude value). Curve 3 corresponds to the calibration of the channel on a "Dawe" mechanical type plate at a constant displacement level of $6.35 \cdot 10^{-3}$ cm (amplitude value). The value of curves 1, 2 and 3 were taken from the scale of the vibration measuring channel which is being calibrated (taking into account the reading in the decibel attenuator). In its low frequency portion curve 1 is parallel to curves 2 and 3. The difference of the ordinates of curves 1 and 2 as well as 1 and 3 is explained by the difference in the level of the impressed vibrations. In our case this difference is 19 db between curves 1 and 2 and 53 db between 1 and 3.

For a given value of a displacement amplitude of the electrodynamic plate at any frequency common to curves 1 and 2, the set acceleration is calculated from formula $\ddot{\xi} = \xi (2\pi f)^2$; for $\xi = 0.127 \cdot 10^{-3}$ cm at frequency $f = 100$ cps, $\ddot{\xi} = 50$ cm/sec^2; $20 \log \frac{K}{K_0} = 64.5$ db.

It will be seen from Fig. 2 that the amplitude of the set accelerations for the piezo-electric plate is 19 db lower than that of the electrodynamic plate, i.e., it amounts to (at 100 cps) 45.5 db. We can obtain the level of the accelerations set for the piezo-electric plate by driving through the above point (100 cps, 45.5 db) a straight line increasing at a rate of 12 db per octave (curve 4), which will determine the calibration of the piezo-electric plate at the output of the vibrometer for the corresponding low frequency tension.

The same calibration curve can be obtained with a slightly greater error by using curve 3 for the purpose.

Once the exciting vibrator with the capacity vibrating measuring device has been thus calibrated, i.e., once the level of the actual values of acceleration determined by curve 4 is known, the calibration of vibrometers is reduced to plotting curve 1 and compiling a table of corrections. The combined vibrometer and measuring channel calibration consists in placing the vibrating probe on the vibrator surface oscillating at a known frequency and amplitude. The displacements amplitude is checked by the capacity displacement-measuring instrument.

The instrument readings at the output of the channel are plotted on the same graph as the vibrator calibration curve. The difference between the two curves at any frequency provides corrections for the given channel.

Let us note that it follows from curve 1 (Fig. 2) that the given vibration probe is working as an acceleration transducer up to 5000 cps and as a displacement transducer at higher frequencies. Hence, with the above vibration probe, the measuring channel cannot be used above 5000 cps for acceleration measurements.

The most important component of the instrument is the capacity vibration measuring device.

The measured capacity forms part of the high frequency oscillator tuned circuit connected to one half of a double triode 6N1P and tuned to 50 Mc. The frequency modulated signal, generated in the circuit when the vibrating plate is operated, is fed to the grid of a cathode follower (the second half of the triode) which is connected through a junction coaxial cable to the measuring unit.

The frequency-modulated signal is amplified by means of a superheterodyne amplifier with an intermediate frequency of 6.5 Mc. The amplifier comprises a converter tube (6A7) with a separate oscillator (1/2 of 6N1P) and two amplifying IF stages (6Zh4 and 6P9). The last IF stage serves as a voltage limiter. The constant amplitude signal is fed to the discriminator circuit; on the load of the latter there appears an audio frequency voltage with

an amplitude proportional to that of the vibrator plate displacement. From the detector output the low frequency signal is fed to two cathode follower stages (6N8). The output on one of them is connected to a voltmeter mounted on the front panel of the displacement measuring set; the output of the other is terminated on the front panel for connecting an oscillograph when required.

The instrument also contains a microammeter for checking the intermediate frequency signal fed to the discriminator and another microammeter for checking the tuning of the superheterodyne amplifier. For convenience of tuning, an automatic tuning control system is used which includes half of the double triode 6N1P.

The suggested device and method of calibrating vibration measuring channels may find a wide application in engineering plants.

LITERATURE CITED

[1] S. V. Novakovskii and G. P. Samoilov, Frequency Modulation Technology [in Russian] (Gosenergoizdat, 1952).

[2] Measurement of Mechanical Quantities by Electrical Methods [in Russian] (Mashgiz, 1952).

FREQUENCY METHOD FOR PRECISE MEASUREMENT OF ANGULAR VELOCITY

R. I. Utiamyshev

A circuit of an instrument developed for measuring angular velocities in the range of 500-15,500 rpm with an error of ±0.05% is described below. The operation of the set is based on measuring the difference between the frequency supplied by a generator and that of a reference crystal oscillator.

The instrument (block schematic in Fig. 1) consists of two crystal oscillators, a mixer, a shaping device, frequency dividers and a power amplifier.

Since the generator frequency must be of the same order as that of the crystal oscillator, the former has a higher than normal frequency determined by the equation

$$f_g = 120\frac{n}{60}$$

where n is the number of revolutions to be measured, and 120 is the number of the generator poles.

The difference frequency is measured by means of an induction tachometer with a synchronous motor fed by the difference frequency divided by 8 and amplified, producing a final frequency of 250 to 750 cps.

The whole operating scope of the instrument is divided with the help of 13 crystal resonators, controlled by pushbutton switches, into 15 ranges of 1000 rpm each.

The second crystal oscillator is provided for periodically checking the circuit operation by means of measuring the difference frequency of the two crystal oscillators.

Components which limit the accuracy of the instrument are the checking generator and the frequency meter which measures the difference frequency.

Tests have shown that the instrument's maximum error in the range of 500 to 15,500 rpm amounts to ±0.05%.

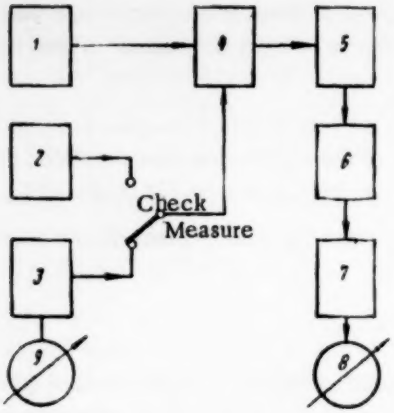

Fig. 1. Block schematic of the instrument. 1) The main crystal oscillator, 2) checking crystal oscillator, 3) synchronous generator, 4) mixer, 5) shaping stages, 6) difference frequency divider, 7) power amplifier, 8) difference frequency measuring device, 9) continuous indicator.

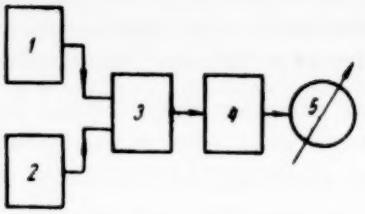

Fig. 2. Block schematic of an instrument using hysteresis (Latour) motors. 1) Crystal oscillator, 2) photoelectric transducer, 3) mixer, 4) power amplifier, 5) difference frequency measuring device.

For measuring the difference frequency other measuring devices can be used (for instance condenser frequency meters). But the best results are obtained with induction tachometers driven by synchronous motors, since they provide a linear scale with a large resolution, and they are independent of the supply voltage within large limits. Thus, in the set in question, the measuring instrument's scale length for each 1000 rpm amounts to 800 mm.

The circuit is considerably simplified if hysteresis (Latour) motors are used instead of the salient pole synchronous motors for driving the induction tachometers.

The application of hysteresis motors eliminates the frequency dividing and shaping stages since these motors work satisfactorily in the range of 20 to 600 cps.

Raising the accuracy of multiple relations in the synchronous generator is important for improving the general precision of the instrument.

In this connection great possibilities are provided by the use of photoelectric transducers. Thus, by using hysteresis motors and photoelectric transducers an instrument (Fig. 2) was produced which measures angular velocities in the range of 110 to 11,100 rpm with an accuracy of 0.25 rpm.

Conclusions. The application of the method of measuring the tachometer generator frequency by means of a heterodyne frequency meter with a reference crystal oscillator and a synchronous-motor induction meter for measuring the difference frequency in a narrow band provides tachometers of great precision (0.03 to 0.05%), with a smooth continuous measuring range, which may find a wide application in the field of measuring technique.

A NEW METHOD OF FASTENING TRANSDUCERS BY MEANS OF MAGNETS

A. N. Chalyi-Prilutskii and B. E. Bolotov

In dynamic and vibration tests of various machines many types of transducers are widely used. There are many ways of fastening the transducers to the objects of measurement. Transducers are supplied with lugs for bolt fixing; they are fixed by means of clamps, braces and other means. The normal means of fastening are labor consuming, usually spoil the surface of the measured object and are not always applicable.

Below a new method of fastening by means of magnets is described. For this purpose either permanent or dc electromagnets can be used. When the transducer weight is relatively small (200 to 300 g) it is convenient to use permanent magnets. with heavier transducers; it is better to use electromagnets. For greater safety an electromagnet with an exciting voltage of 30 v was used.

Transducers supplied with magnetic bases were used for measuring vibration characteristics of lathes and milling machines. Despite layers of filling, priming and paint, the transducers were held securely.

In order to estimate the force of magnetic attraction and its security in dynamic conditions oscillograms were taken of a milling machine base by means of one transducer fastened by bolts and another secured by a magnet. The oscillograms confirmed the possibility of fixing transducers in complicated and exacting vibration tests by means of magnets.

MEASUREMENTS OF TIME

INTERNATIONAL GEOPHYSICAL YEAR AND MEASUREMENTS OF TIME

D. Iu. Belotserkovskii

Investigations carried out on the basis of materials collected during the International Geophysical Year will throw light on many as yet unclear physical problems of our planet, which in its rotation round its axis and the yearly rotation round the sun serves as a natural standard for one of the three basic units, namely the second of time. In the vast IGY program of work, investigations connected with the study of variations in the velocity of the Earth's rotation and their causes are of the greatest interest for metrology.

Many physical processes occuring on our planet, inside it and in the surrounding atmosphere are causing or could cause these variations. It is known, for instance, that tidal friction in shallow seas is causing a systematic, or as it is usually called, secular, decrease in the velocity of Earth's rotation. As the result of it the day increases and the unit of time changes by $2 \cdot 10^{-8}$ sec per century. The Earth's crust, however, is subject to constant changes. Slow (and in earthquakes, rapid) vertical and horizontal displacements occur in the crust. In time, the depth of seas changes and hence the secular slowing down of the Earth's rotation must also change. The rise and destruction of mountain ranges, displacement of the erosion products, the accumulation of sediments in oceans and the displacement of masses inside the Earth must all influence the rotation velocity of the Earth.

Great attention is paid to the study of slow changing phenomena with the object of subsequently comparing the results with those obtained during the IGY.

Such slowly changing phenomena include the possible "drift" of continents and islands. The old hypothesis, that islands and continents are floating in magma like icebergs in the sea, and in time change their relative positions, has neither been confirmed by science nor completely disproved. It can be checked by repeated determination of the geographical coordinates of various points on the Earth's surface. Longitudes are determined by measuring the difference between the local time (solar or sidereal) in different places at the same physical instant. In this instance, time measurements serve to solve a geophysical problem.

Seasonal atmospheric phenomena also influence the Earth's rotation. Investigation of crystal clocks' operation on the basis of astronomical time determination showed seasonal irregularities in the Earth's rotation round its axis with a yearly and half-yearly period. It is assumed that this phenomenon is caused by periodic exchanges of kinetic energy between the Earth and the surrounding atmosphere with seasonal changes in the direction of winds, especially in mountainous regions. It would appear that periodic changes in the rotation velocity of the Earth are also observed at 14 month periods, which correspond to the periods of free nutation , related to the internal structure and elastic properties of the Earth. Seasonal exchanges of air masses between the north and south hemispheres cause, similar to the free nutation , periodic oscillations of the Earth's poles and hence of the longitudes and latitudes on the Earth's surface. This in turn causes periodic distortions in the astronomical determination of time. One of the basic problems for the IGY is finding the relation between the general circulation of the Earth's atmosphere, the oscillations of the Earth's axis of rotation and the seasonal variations in the speed of rotation of the Earth.

We have already mentioned that for determining a difference in longitude, the difference in local time has to be measured at the same physical instant. Local time is determined from astronomical observations, and in order to read the time in various places at the same physical moment, precise time signals must be transmitted. The reception of these precise time signals can also be used under certain conditions for determining the propagation time of radiowaves. By comparing the data obtained from radio signal reception with the data on atmospheric conditions

it is possible to trace the paths of the radio waves under different conditions and determine the speed of their propagation.

Accurate determination of time is a constant task of the time service. That is why the time service has been charged during the IGY to determine longitude differences, to study by means of high-precision pendulums, crystal and "atomic" clocks, on the basis of astronomical determinations of time, the seasonal irregularities in the Earth's rotation and also to measure the propagation time of radio waves. Among the time services taking part in the IGY program are included the four time services of the Committee of Standards, Measures and Measuring Instruments the VNIIFTRI in Moscow, the VNIIMa in Leningrad, and the VNIIFTRI Laboratory in Irkutsk and the combined time service of the KhGIMIPa and the State University Astronomical Observatory in Khar'kov. These services regularly determine astronomical time by means of transit instruments and regularly receive time signals. They have high quality crystal clocks with which they investigate the seasonal irregularities of the Earth's rotation. The time services in Moscow and Irkutsk are close to the radio stations transmitting precise time signals (in Moscow) and retransmitting them (in Irkutsk), the transmitters working on frequencies close to each other. This arrangement provides conditions necessary for measuring the radio wave propagation time. Together with other Soviet time services, those of the Committee plan their astronomical observations in such a manner as to improve the catalogues of right ascensions of stars observed by the time services. This will lead in future to the establishment of a more even time scale from astronomical observations.

The participation of the time services in the IGY is not limited to this activity. The VNIIFTRI time service, besides providing precise time signals for the ordinary requirements of our country, also sends out special precise radio time signals from the beginning of October 1957 for observing artificial earth satellites. At the end of each hour the radio broadcasting network sends out six short tonal signals. The intervals between their beginnings are equal to a mean solar second and the beginning of the last, sixth signal coincides with the beginning of the hour (0 min. 0 sec.) In addition, over a special radio network, short signals are continuously transmitted over long periods, their intervals equal to a mean solar second and the beginning of each minute is marked by a longer signal and the end of every fifth minute by a still longer six second signal. These signals are used at the artificial Earth satellite observing stations for checking clocks or giving direct indications of time when the passage of a satellite is being recorded.

The Presidium of the Academy of Sciences of the USSR has entrusted the supervision of the work of determining longitudes and time and the responsibility for carrying out the IGY program related to that work to the All-Union Scientific Research Institute for Physico-Technical and Radio-Technical Measurements (VNIIFTRI) of the Committee of Standards, Measures and Measuring Instruments.

INSTRUMENT FOR REPRODUCING AND MEASURING TIME INTERVALS OVER A WIDE RANGE

M. S. Dmitriev

The All-Union Scientific Research Institute for Physico-Technical and Radio-Technical Measurements (VNIIFTRI) developed an instrument for reproducing time intervals in steps of 10 μsec in the range of 10 μsec to 10.48576 sec and measuring time intervals from 10 μsec to 100 sec.

By means of simple switching this instrument can produce:

negative or positive pulses following each other at given intervals;

nonperiodic pulses of either sign whose duration corresponds to a given value;

a series of positive or negative pulses whose number in the series can be predetermined.

It can also measure time intervals in the range mentioned above.

The block schematic of the instrument is given in Fig. 1. The input of the instrument is fed from a highly-

The block schematic of the instrument is given in Fig. 1. The input of the instrument is fed from a highly stable crystal oscillator by a sinusoidal voltage of 100 kc which is amplified in a tuned amplifier and transformed in a shaping stage into short steep front pulses. These pulses are fed to the input of a frequency divider, consisting of 20 symmetrical triggers with 19 feedback circuits (the divider block schematic is given in Fig. 2, and the schematic circuit in Fig. 3).

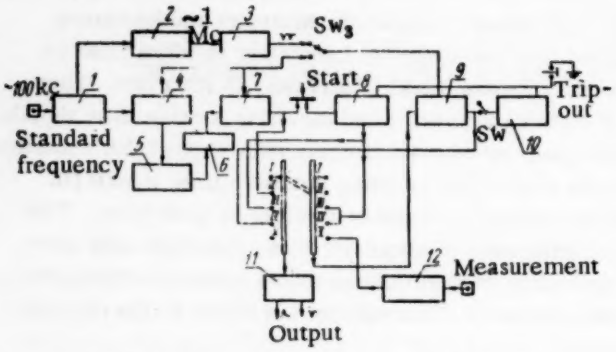

Fig. 1. Block schematic of the instrument.
1) Amplifier; 2) multiplier 1 : 10; 3 and 4) shaping stages; 5) frequency divider; 6) oscillator; 7) and 9) selectors; 8) shaping of nonperiodic pulses; 10) counter; 11) reversing amplifier; 12) shaping of pulses; I) switching off; II) periodic pulses; III) nonperiodic pulses; IV) pulse series; V) time interval measurements.

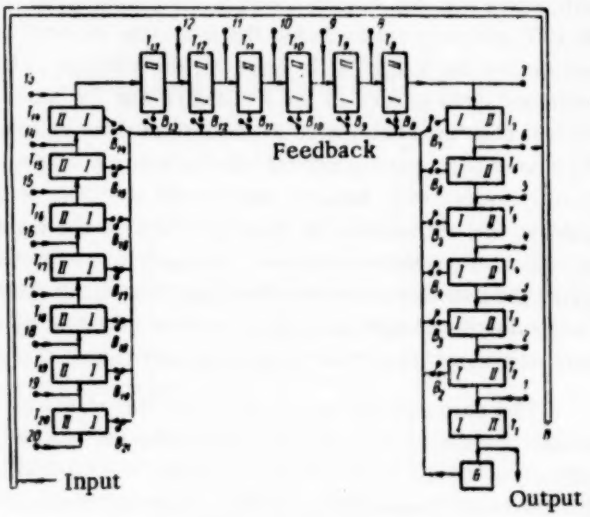

Fig. 2. Frequency divider block schematic.
C) Blocking oscillator; B) tumbler switches; П) switches; T) triggers.

The trigger circuits, with the exception of tube T_2, are identical, therefore circuits T_3 to T_{19} are not shown on the drawing.

In order to ensure reliable trigger operation, the negative triggering pulses are fed to the tube anodes through diodes. The negative pulses which cause an additional change-over of triggers are taken from a blocking oscillator and fed through starting diodes to the right hand grids of the double triodes. The circuit is brought to its initial condition when first switched in by means of the resetting button.

The pulse repetition period T at the output of the frequency divider is equal to 10K μsec, where K is a coefficient of frequency division.

Various feedback arrangements combined with pulses fed to different trigger inputs produce a division coefficient K equal to any integer from 1 to 2^{20} (from 1 to 1048576).

It is not difficult to select the required feedback and trigger input in order to set a desired time interval.

Let us assume that a time interval of 10K μsec is required, where K is a whole number.

In order to obtain the division coefficient K it is necessary:

1. To find the trigger which should receive the input pulses. For this purpose the smallest binary number 2^n is selected which is larger than K in its numerical value. Number n will then be the number of the trigger which should receive the pulses. In this case the output pulses will be repeated at every 2^n input pulses. In order to make the output pulses appear at every $K < 2^n$ input pulses, feedbacks are connected which produce additional triggering. The latter action is equivalent to subtracting pulses from 2^n.

2. To establish the required number of feedback connections in order to obtain K. For this purpose the quantity C by which 2^n has to be decreased in order to obtain K must be found, i.e., $C = 2^n - K$.

We find the largest binary number which is smaller than C and find the remainder C_1, i.e., $C_1 = C - 2^{a_1}$ Next we find the largest binary number which is smaller than C_1 and find the difference C_2, i.e., $C_2 = C_1 - 2^{a_2}$ etc. until the remainder becomes equal to zero.

The number of feedback connections is equal to the number of these binary numerals.

3. To establish what feedback circuits will be required in order to decrease 2^n by the amount C. For this purpose let us calculate:

$$n - a_1 = b_1;\ n - a_2 = b_2;\ n - a_3 = b_3 \text{ etc.}$$

Numbers $b_1, b_2, b_3, \ldots b_k$ correspond to the ordinals of tumbler switches which should be switched in, in order to obtain the required coefficient K.

Example. It is required to obtain a pulse repetition period T = 3.69 msec = $3.69 \cdot 10^3$ μsec.

Let us determine the coefficient of division:

$$K = \frac{3.69 \cdot 10^3}{10} = 369. \qquad (1)$$

Let us select the binary number $2^n : 2^9 = 512 > 369 > 2^8$. Hence n = 9 and the input pulses should be fed to the ninth trigger circuit.

Let us now determine the number of feedback circuits which should be connected:

$C = 2^9 - 369 = 143$; $C_1 = 143 - 2^7 = 15$; $C_2 = 15 - 2^3 = 7$; $C_3 = 7 - 2^2 = 3$; $C_4 = 3 - 2^1 = 1$; $C_5 = 1 - 2^0 = 0$. Hence 5 feedback circuits should be connected.

Let us now determine which of the circuits have to be connected: $n - a_1 = 9-7 = 2$; $n - a_2 = 9-3 = 6$; $n - a_3 = 9-2 = 7$; $n - a_4 = 9-1 = 8$; $n - a_5 = 9-0 = 9$.

Hence, in order to obtain a pulse repetition period of 3.69 msec, tumbler switches B_2, B_6, B_7, B_8, and B_9 should be connected.

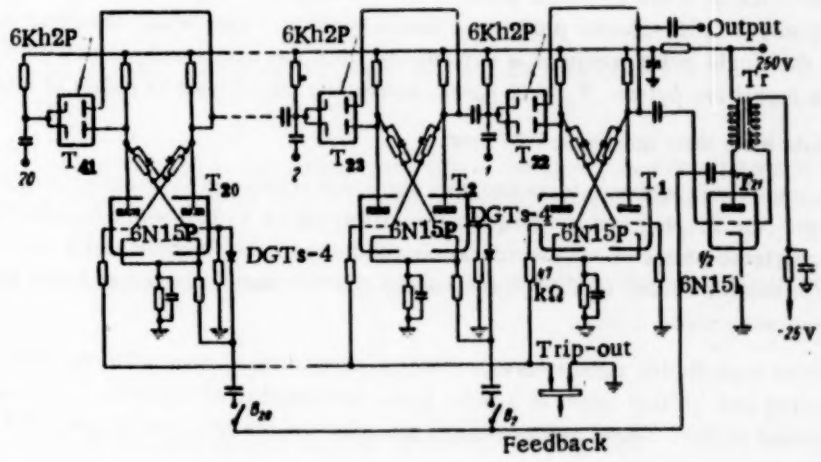

Fig. 3.

It should be noted that dividers with a feedback have a smaller limiting dividing frequency than circuits with straight pulse transmission.

In calculating the limiting division frequency it is necessary to take into account the following:

1. The pulse delay time in frequency divider T_3 consists of the sum of delays in each trigger, τ, the delay in the blocking oscillator τ_1, in the feedback circuit τ_2 and in the trigger with an additional switchover τ_3:

$$T_3 = \sum_1^n \tau + \tau_1 + \tau_2 + \tau_3.$$

where n is the ordinal of the trigger.

2. Maximum delay occurs when input pulses are fed to the 20th trigger, which also receives an additional feedback pulse.

3. For normal operation of the divider it is necessary that $T_{3\,max} < T_n$, where T_n is the repetition period of the input pulses.

The delays in our divider amount to:

$\tau \simeq 0.4$ μsec; $\tau_1 \simeq 0.5$ μsec; $\tau_2 \simeq 0.2$ μsec; $\tau_3 \simeq 0.4$ μsec; $T_{3\,max} = 0.4 \cdot 20 + 0.5 + 0.2 + 0.4 = 9.1$ μsec.

Hence for normal operation of the divider the input pulse repetition period should not be less than 9.1 μsec, which corresponds to a repetition frequency of 110 kc.

The frequency divider output pulses operate a selecting-pulse generator which produces rectangular pulses of 13 μsec duration.

In order to eliminate the phase error introduced by the frequency divider, a selector stage is included in the circuit; this stage consists of a pentode time coincidence pulse selector. The pentode suppressor grid is fed by 13 μsec pulses from the selecting-pulse generator and the control grid by output pulses from the shaping stage. The selected pulses are amplified, shaped in the inverter and fed to the output of the set.

The single pulse producing circuit includes a "nonperiodic pulse" shaping stage, consisting of a trigger with a switch which lets through only the first and second pulses out of the periodic sequence. The first pulse operates the trigger and the second returns it back to normal. Thus, at the trigger output a single pulse is formed, whose length corresponds to the pulse repetition period.

A check of the accuracy of the time intervals produced is achieved by measuring the duration of the single pulses in the "nonperiodic pulse" connection. For this purpose a second pulse time coincidence selector and a pulse counter are included in the circuit.

The second selector is fed by single pulses from the nonperiodic pulse shaping stage and by periodic pulses from the shaping stage. This selector produces a single series of pulses which are counted by the pulse counter. The duration of the single pulse produced is determined from the number of pulses counted, which also determines the period of the repetitive pulses: $T_n = 10\ n$μsec, where n is the number of pulses in a series.

The absolute error does not exceed 20 μsec.

The accuracy of measurement increases with the pulse repetition frequency. For this purpose the instrument includes two stages (the shaping and the frequency multiplying by 1:10), which transform the sinusoidal voltage of 100 kc into a periodic pulses of 0.2 μsec duration and a repetition frequency of 1 Mc. When these pulses are fed to the selector the time interval $T_n = n$μsec, where n is the number of pulses in the series. In this case the absolute error does not exceed 2 μsec.

In addition to reproducing time intervals this instrument can also measure the interval between two single pulses or the leading and trailing edges of a pulse (i.e., the duration of a pulse), or measure the repetition frequency of periodic pulses. These measurements are made in the range of 10 μsec to 100 sec with an absolute error of 2 μsec.

For measuring purposes the circuit includes another shaping stage to which measured pulses of either polarity are fed. The shaping stage produces a single rectangular positive pulse which is fed to a second selector. This selector is also fed by pulses with a repetition frequency of 1 Mc. As the result of selection there appears at the output of the stage a series of pulses, which are counted by the pulse counter. The number of pulses determines the duration of time interval as it has been described previously.

In measuring and testing practice, single series of pulses whose number can be set are sometimes required. They are mostly required for testing pulse counters, for calibrating various electronic indicators, etc.

In the "pulse series" connection the instrument produces a series of positive or negative pulses, whose number can be set. Periodic pulses of different repetition frequencies (100 kc, 1 Mc) are selected by means of a switch and fed to the second selector which also receives single pulses of a known duration. A series of pulses is

obtained from the selector output; the number of pulses in the series is $N = Tf$, where f is the repetition frequency of the periodic pulses and T the duration of the single pulse.

The number of pulses in a series is changed by changing the duration of the single pulse T.

When time intervals are reproduced or measured systematic and random errors arise.

Systematic errors due to delays in the electrical circuit are eliminated by means of the coincidence stage. The systematic error due to changes in the frequency division coefficient (the frequency error) can be determined by the checking circuit of the instrument.

Random errors are due to the timing of pulses (phase errors) and occur mainly in the shaping stage. These errors are negligibly small in a correctly selected pulse shaping circuit. Random errors due to the frequency divider are eliminated in the selector stage.

All the parameters and components of the set were tested in a prototype.

LITERATURE CITED

[1] N. Petrovich and A. Kozyper, "Generation and transformation of electrical pulses," Soviet Radio, M. 1954.

[2] A. Bonch-Bruevich, Application of Electron Tubes in Experimental Physics [in Russian] (GITTL, M., 1954).

[3] L. A Mirovich and L. G. Zelichenko, "Pulse technique," Soviet Radio, M., 1954.

[4] G. Montgomery, Journ. Appl. Phys. 22, 780 (1951).

ELECTRONIC TIME RELAYS

V. S. Zhupakhin and K. S. Zhupakhin

One of the basic characteristics of an electronic time relay, the time transformation coefficient (n_t), is understood to be the relationship between the time interval fixed by the circuit and the time constant of the driving element.

The time interval fixed by the electronic time relay (e.t.r.) circuits in the majority of cases can be determined by expression:

$$T_f = n_t \tau, \qquad (1)$$

where τ is the time constant of the driving element (for instance, $\tau = RC$), and
n_t is the time transformation coefficient (t.t.c.) determined by the circuit design (see below).

Let us examine some possible methods of varying the value of the fixed time intervals (T_f) and of stabilizing it by means of an appropriate circuit design, i.e., by means of varying and stabilizing the t.t.c. (n_t).

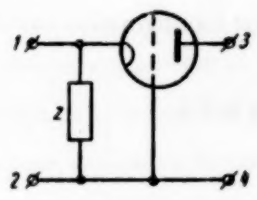

Fig. 1.

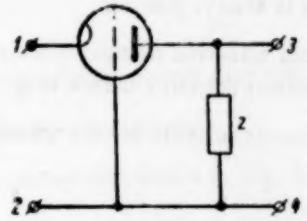

Fig. 2.

The time transformation coefficient can be expressed as

$$n_t = \frac{T_f}{\tau} = n_\tau \ln x, \qquad (2)$$

where n_τ is the transformation coefficient of the driving parameters (see below) and

$\underline{x}$ is the antilogarithm of the time transformation coefficient.

The e.t.r. circuit design determines expressions n_τ and $\underline{x}$ which characterize the quality of the circuit.

Thus the simplest e.t.r. (see circuit No. 1 in the Table of circuits, formulae and graphs) has a small and unstable t.t.c., which depends on the supply voltages, tube parameters and the output relay.

The t.t.c. can be effectively stabilized by means of the so-called stabilization circuit, whose essence consists in supplying an additional positive voltage to the control electrode of the tube and in using potentiometer supplies for the tube electrodes. This leads to an increased rate of voltage change across the condenser and to the possibility of making the ratio of the initial voltage across the condenser to the voltage across it at the time of the output relay operation practically constant ($x \simeq$ const).

In circuits Nos. 2, 3 and 4 given in the Table this method of stabilization was used.

The instability of these circuits is determined in the main by the instability of the driving elements (RC) and can be made small. Thus an actual e.t.r. circuit built on the basis of schematic No. 4 had an error of $\pm 0.2\%$ $\pm 10^{-4}$ sec in the range of $3 \cdot 10^{-3}$ to 10 sec. A variation in the supply voltages of 50% and a simultaneous changing of tubes produced an error in the set time intervals of 1%.

During the three years' operation this circuit did not require any appreciable readjustment.

An increase in the t.t.c. can be achieved according to (2) by increasing either n_τ or $\ln \underline{x}$.

Let us first examine circuits with a large value of $\ln \underline{x}$ and $n_\tau = 1$. Large values of $\ln \underline{x}$ can be obtained with $x \gg 1$ or $x \ll 1$.

a) The simplest e.t.r. circuit (circuit No. 1) can be adjusted in such a way that

$$x = \frac{U_0}{E_{st} - \frac{I_m}{S_\partial}} \gg 1$$

and the time set by the circuit will be large. The stability of the set time intervals, however, becomes very low. This can be easily seen from the graph showing the physical processes in the circuit (see graph of circuit No. 1).

b) In a circuit with small values of x ($x \ll 1$) large values of t.t.c. can be similarly obtained, but with a much greater stability (see circuit Nos. 5, 6 and 7).

In these circuits the value of antilog $\underline{x}$ is close to the reciprocal of the amplification factor of the tube. An interesting feature of these circuits is the use of feedback, which makes the voltage across the condenser vary linearly.

In practice the value of the t.t.c. in either case ($x \gg 1$ or $x \ll 1$) does not exceed a few units. The error in the set time of these circuits, (especially in the case of $x \gg 1$) is considerable (units and tens of percent). With $x < 1$ the value of $\ln \underline{x}$ becomes negative and a -1 factor must be introduced into (2), since the time set by the circuit is always positive.

The most effective method of increasing the t.t.c. is the use of special transformation circuits for the driving parameters (circuits with a large n_τ).

a) A circuit suitable for the transformation of the resistance is shown in Fig. 1.

In fact this circuit can be considered as a delta quadripole. It is represented by the matrix [1]:

$$Z=\frac{1}{y}\begin{vmatrix}1; & -1\\ 1+\mu; & -(1+\mu+y R_l)\end{vmatrix}. \tag{3}$$

where $y=\frac{1}{z}$, and μ and R_l are tube parameters.

Hence, the input impedance of the circuit, viewed from terminals 3 and 4, is

$$z_{in\ 3,4}=z\ (1+\mu+y R_l).$$

Thus we have an obvious resistance transformation (an increase) with a transformation coefficient:

$$n_z=1+\mu+y R_l.$$

b) A circuit suitable for capacity transformation (an increase) is shown in Fig. 2 and is represented by the matrix of the form

$$Z=\frac{1}{y\ (1+\mu)}\begin{vmatrix}1+y R_l; & -1\\ 1+\mu; & -(1+\mu)\end{vmatrix}. \tag{4}$$

If in the circuit of Fig. 2, load $\underline{z}$ is a capacity C, it is easy to show that, viewed from terminals 1 and 2, this circuit can be replaced by its equivalent shown in Fig. 3.

Here:

$$R_e=\frac{R_l\ (2+\mu)}{(1+\mu)^2},$$

$$C_e=C\ (1+\mu).$$

Thus we obtain a capacity transformation with a transformation coefficient

$$n_C=1+\mu.$$

The driving parameters transformation coefficient n_τ is equal to

$$n_\tau=n_R\ n_C.$$

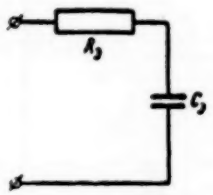

Fig. 3.

Above expressions hold for triodes. Similar expressions can be obtained for pentodes if they are treated as equivalent triodes. Thus, for circuit of Fig. 4 the input impedance, viewed from terminals 3 and 4, is determined by the expression

$$z_{in\ 3,4}=z\left(1+\mu+y R_l+\frac{D_2}{D}\right),$$

and for the circuit of Fig. 5 by the expression

$$z_{in\ 3,4}=z\left(1+\mu+y R_l+\frac{D_2}{D}+\frac{D_3}{D}\right).$$

It is obviously expedient to use pentodes, since they have a considerably greater amplification factor.

If a large t.t.c. is required, series connected similar delta quadripoles can be used.

In this connection let us examine, for instance, the two-stage connection shown in Fig. 6.

No.	Electronic time relay circuits	Time transformation coefficient n_t	Circuit operation graphs and remarks
1	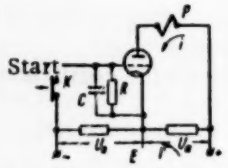	$n_t = \ln \dfrac{U_0}{E_{st} - \dfrac{I_m}{S_\partial}}$, $E_{st} = E_{g_0} - DU_a$. I_m — relay operation current P; S_∂ — dynamic mutual conductance of the tube; $D = \dfrac{1}{\mu}$ — reciprocal amplification factor; $i' > i$	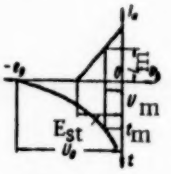
2	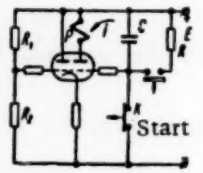	$n_t = \ln \left[\dfrac{I_0 - I_m}{SE} + \dfrac{R_1}{R_1 + R_2} \right]$ at $\dfrac{R_1}{R_1+R_2} \gg \dfrac{I_0 - I_m}{SE}$; $n_t \simeq \ln \dfrac{R_1}{R_1+R_2}$; I_0 — tube current at rest	Graph similar to that of No. 3, see [3]
3	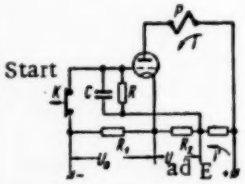	$n_t = \ln \dfrac{U_0 + U_{ad}}{U_{ad} + E_{st} - \dfrac{I_m}{S_\partial}}$ at $U_{ad} \gg E_{st} - \dfrac{I_m}{S_\partial}$; $n_t \simeq \ln \left(1 + \dfrac{R_1}{R_2}\right)$; $E_{st} = E_{g_0} - DU_a$; $i' > i$	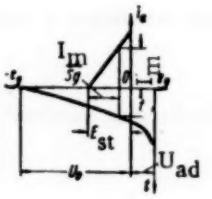
4	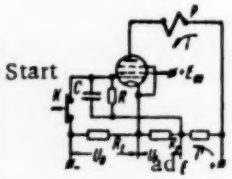	$n_t = \ln \dfrac{U_0 + U_{ad}}{U_{ad} + E_{st} - \dfrac{I_m}{S_\partial}}$ at $U_{ad} \gg E_{st} - \dfrac{I_m}{S_\partial}$; $n_t \simeq \ln \left(1 + \dfrac{R_1}{R_2}\right)$; $E_{st} \simeq E_{g_0} - D_2 E_{g_2} - DU_a$; $i' > i$; D_2 — Recip. ampl. factor w/resp. to 2nd grid	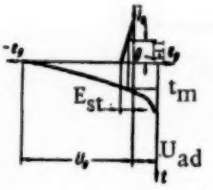

Table of Circuits, Formulae and Graphs (Continued)

No.	Electronic time relay circuits	Time transformation coefficient n_t	Circuit operation graphs and remarks
5	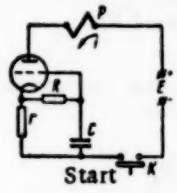	$n_t = \ln D\left[\frac{E}{r I_m} - 1 - \frac{R_l}{r}\left(1+\frac{SE_{g_0}}{I_m}\right)\right]$, E_{g_0}, D, R_l, S – tube parameters	Condition for circuit operation: $E > I_m\left[r + R_l\left(1+\frac{SE_{g_0}}{I_m}\right)\right]$
6	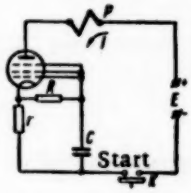	$n_t = \ln \frac{D}{1+D_2+D_3}\left[\frac{E}{rI_m} - - 1 - \frac{R_l}{r}\left(1+\frac{SE_{g_0}}{I_m}\right)\right]$, D_3 – recip. ampl. factor with respect to 3rd grid	Conditioned for circuit operation similar to No. 5
7	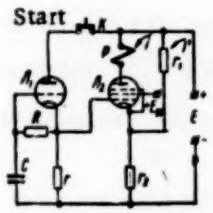	$n_t = \ln D_1\left[\frac{r_1}{r_2} - \frac{R_{i_1}}{r} - \left(1+\frac{r_1}{r_2}\right)\frac{E_{g_{01}}}{D_1 E}\right]$ at $\frac{Er_2}{r_1+r_2} \gg \frac{I_m}{S_2} - E_{st_2}$ where D_1, R_{i_1}, $E_{g_{01}}$ – parameters for tube T_1; S_2 и E_{st_2} – tube T_2	$t' > t$ See [4] and [5]
8	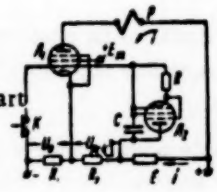	$n_t = \left(1+\mu+\frac{R_l}{R}+\frac{D_2}{D}\right)\cdot \ln\left(1+\frac{R_1}{R_2}\right)$, where μ, R_l, D_2, D – parameters, tube T_2. This expression holds at $U_{ad} \gg E'_{g_0} - D'_2 E_{g_2} - D' U_a$, where D'_2, D', E'_{g_0} – parameters, tube T_1	Graph similar to No. 4

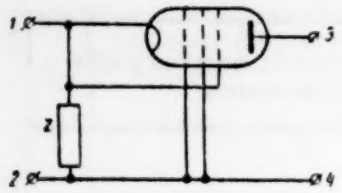

Fig. 4.

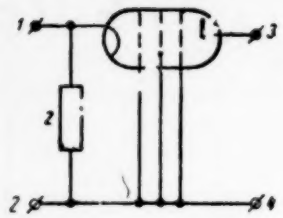

Fig. 5.

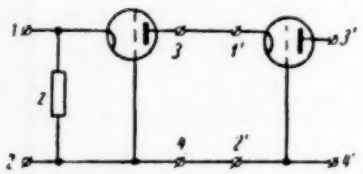

Fig. 6.

It is possible to represent this circuit by a matrix of the form

$$a=\frac{1}{(1+\mu)^2}\begin{vmatrix}1; & R_l\,(2+\mu)\\ y; & (1+\mu+y\,R_l)\cdot(1+\mu)\end{vmatrix}, \qquad (6)$$

whence

$$z_{in3,4}=z\,(1+\mu)\cdot(1+\mu+y\,R_l).$$

Thus with a two-stage connection we raise the transformation n_t by more than $(1+\mu)^2$ times:

$$n_z=(1+\mu)\cdot(1+\mu+yR_l). \qquad (7)$$

A similar condition obtains with capacity transformation. In a general case of an n-stage connection of similar quadripoles, with the condition that

$$1\ll\mu\gg yR_l,$$

the t.t.c. can be evaluated by the expression

$$n_t\simeq\mu^n\ln x. \qquad (8)$$

It should be noted that (8) is relatively accurate only for the following values of the transforming parameter $\underline{z}$:

$$\frac{1}{S}\ll z\ll\frac{z_y}{n_z},$$

where z_y is the capacitor leakage resistance. If $z\propto\frac{1}{S}$, expression (8) will give a lower value than the actual t.t.c. If $z=\frac{z_y}{n_z}$ expression (8) will give a value higher than the actual value of the t.t.c., since it does not take into account the shunting effect of the stray leakages in the circuit.

An expression for an actual t.t.c., taking into account the stray leakages, will have the form:

$$n_{t\,act}=\frac{n_z\,z_y}{n_z\,z+z_y}\ln x. \qquad (9)$$

In order to obtain stability when driving parameters are transformed. according to express (8), factors $\ln \underline{x}$ and μ should be stabilized.

Factor $\ln \underline{x}$ can be stabilized by the method of circuit stabilization outlined above.

Under normal conditions the amplification factor (μ) of a tube is the most stable of its parameters. In the case of microcurrent operation, when the amplification factor depends on the current flowing through the tube, one can obviously speak only of a certain mean value of the amplification factor.

Thus in this case when a stable value for the t.t.c. is required, the tube supply voltage should be stabilized. E.t.r. circuits with driving elements transformation (circuit No. 8 and others), but without heater voltage stabilization were tested out. They provided time intervals within the limits of 1 to 120 min, with an error of the order of 3%. The actual t.t.c. values in this case amounted to tens and hundreds of thousands.

The article describes only the most efficient methods of stabilization and time interval amplification; the problem was solved by selecting e.t.r. circuits with appropriate t.t. coefficients.

The knowledge of the t.t.c. as a function of actual circuit parameters and supply voltages permits one to make optimum use of the given circuit potentialities.

The t.t.coefficients given in the Table have been derived with the assumption that the mutual tube characteristics are linear, and they serve as qualitative evaluations of the properties of various circuits.

Tests have also provided satisfactory agreement of the quantitative relations. The measurement of the set time intervals was made by means of an electronic recording stop-watch, type 521 [2], with a precision of 10^{-4} sec.

LITERATURE CITED

[1] E. V. Zeliakh , Foundations of the General Theory of Linear Electrical Circuits, [in Russian]. (AN SSSR Press, 1951).

[2] V. S. Zhupakhin, Electronic Stop-Watches, Type 521 and 521-U [in Russian] (INTI AN SSSR Press, Instruments and Assemblies, 1956).

[3] A. M. Pazygraev, Electronic Control of Metal-Cutting Lathes [in Russian] (Mashgiz, 1953).

[4] "Ein zuverlässiger elektronischer Zeitschalter" Funk-Technik, No. 24, 1954.

[5] Radio-Television News, October, 1954.

ELECTRICAL MEASUREMENTS

A MAGNETIC TRANSDUCER WITH A PERMANENT MAGNET

V. N. Mil'shtein and N. A. Palibina

This article deals with the principles of operation and some theoretical considerations of magnetic transducers with a permanent magnet used to measure direct current by the balancing method.

The transducer's principle of operation. Let us examine a system (Fig. 1a) consisting of a permanent magnet in a closed magnet circuit.

The permanent magnet flux can be represented as a sum of a longitudinal flux Φ_p entering the magnetic circuit at cross-section AA_1 and a transverse flux Φ_q entering the magnetic circuit at cross section GG_1.

It is obvious that in expressing the resultant value of the magnetic flux Φ_s, which is equal to

$$\Phi_s = \sqrt{\Phi_p^2 + \Phi_q^2}, \tag{1}$$

the relation between Φ_p and Φ_q will be determined by angle α, which specifies the position of the magnet.

It can be considered as the first approximation that

$$\Phi_p = \Phi_s \cos\alpha, \quad \Phi_q = \Phi_s \sin\alpha. \tag{2}$$

The transverse component has but a small influence on the basic performance of the system. Hence the turning of the permanent magnet will be considered as a means of changing the longitudinal component of the flux, which determines the performance of the system.

Let us now examine the same magnetic circuit without the permanent magnet but with two windings 2 and 2' (Fig. 1b). The windings are connected in series and a direct current I is flowing through them. The direction of the windings is such that the sum of ampere turns of the windings along the magnetic circuit is zero, but the flux in the space round the magnetic circuit due to each winding is $\frac{\Phi_=}{2}$, flowing as shown in Fig. 1b.

It should be noted that in reality the magnetic transducer represents a three-dimensional system of magnetic field distribution. The ideal representation assumed in Fig. 1b facilitates investigation, without violating in principle any relationships; for quantitative calculations, however, it is necessary to take into consideration the actual field distribution.

Let us assume then that the flux $\Phi_=$ due to both coils is concentrated and coincident with axis O_1O_2, i.e., with the longitudinal component Φ_p of the permanent magnet flux.

It is obvious that in the presence of both sources of magnetic fields, the permanent magnet and coils 2 and 2', the resultant value Φ_{res} of the longitudinal component of the magnetic flux is according to (2) equal to

$$\Phi_{res} = \Phi_s \cos\alpha - \Phi_=. \tag{3}$$

It is required to have at the transducer output an alternating voltage whose amplitude and phase should correspond to the magnitude and direction of flux Φ_{res}.

In order to achieve this result the magnetic circuit is periodically magnetized and demagnetized by means of two similar windings 1 and 1' (Fig. 1c), which carry current pulses of a definite polarity and of industrial frequency.

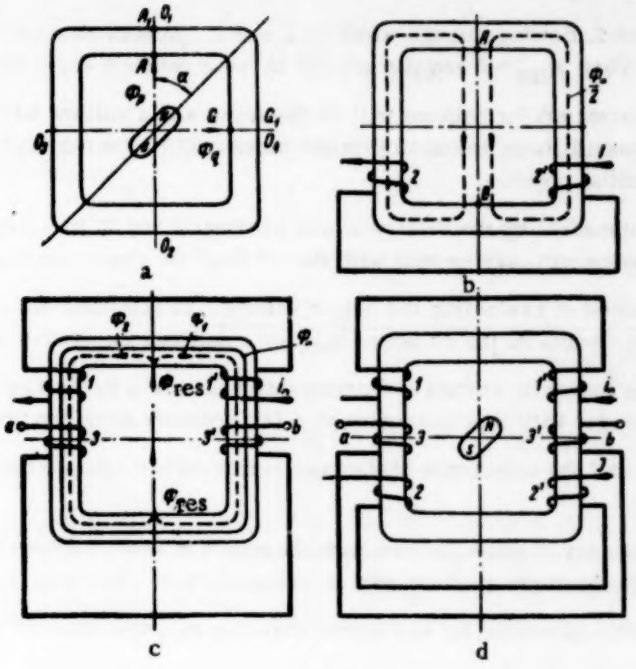

Fig. 1.

Fig. 2.

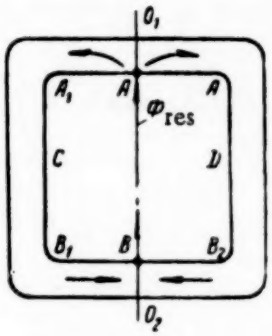

Fig. 3.

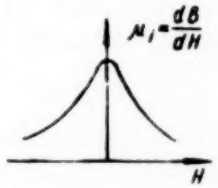

Fig. 4.

Windings 1 and 1', as distinct from winding 2 and 2', are connected in series aiding so that the resulting flux $\Phi_{\sim}$ passes in the main through the magnetic circuit. During the time pulses pass through the winding the magnetic circuit becomes saturated and its permeability for any "extraneous" magnetic fields becomes very low. In the intervals between the pulses the magnetic circuit is not saturated and the permeability is very high.

The permanent field Φ_{res} due to the permanent magnet and the direct current in coils 2 and 2', not shown in Fig. 1c, can be considered an "extraneous" magnetic field. Alternating output voltages appear in the similar winding 3 and 3' (Fig. 1c), which although connected in series opposing produce in-phase voltages induced by the components of flux Φ_{res}.

Let us first assume that $\Phi_{res} = 0$. Then the only source of a magnetic field will be the current in windings 1 and 1'. Under this condition the magnetic flux in all the sections of the circuit can be considered the same, hence the emf induced in winding 3 and 3' will be equal in amplitude and opposite in phase. The voltage between points a and b will then be equal to zero.

If flux Φ_{res} is now assumed to appear in the circuit, it will become pulsating owing to the periodic changes in the permeability of the core. In entering the magnetic circuit, flux Φ_{res} splits into two parts, Φ_1 and Φ_2, which can be assumed equal (Fig. 1c).

If in one half of the magnetic circuit, flux, Φ_1 is in phase with flux $\Phi_{\sim}$, due to windings 1 and 1', in the other half flux Φ_2 will be in anti-phase with $\Phi_{\sim}$. Hence, the alternating emf's induced in windings 3 and 3' by the alternating components of fluxes Φ_1 and Φ_2 will add instead of subtracting and a voltage will appear between terminals a and b.

Figure 1d shows the complete schematic of the device.

Let the direct current I, flowing through windings 2 and 2', produce at some instant flux $\Phi_=$ which completely balances flux $\Phi_s \cos \alpha$. Then $\Phi_{res} = 0$ and the voltage between points a and b will be zero.

If current I is now increased, the balance will be destroyed and a voltage will appear between terminal a and b. In order to restore balance, it is sufficient to turn the permanent magnet through a certain angle (counter-clockwise) with respect to its initial position.

By using a system controlled by the voltage across windings 3 and 3', it is possible to relate automatically the angle of rotation of the permanent magnet axis with the value of the direct current through windings 2 and 2'.

An approximate method of evaluating the output voltage. In designing the transducer it should be remembered that under normal working conditions the values of Φ_{res} are small and the system is close to balance.

The condition of the magnetic curcuit is determined, in the main, by, the flux due to the current in windings 1 and 1'. This current changes with time according to a law approximating the graph shown in Fig. 2.

Since flux Φ_{res} is small, the reluctance of the core is determined by the incremental permeability of the core.

Considering the similarity of above process with the effect of small currents and emf's in nonlinear circuits, it is possible to apply to this problem methods used in calculations of electrical circuits [1].

In conformity with this statement, let us consider that flux Φ_{res} branches off in the magnetic circuit as shown in Fig. 3.

The incremental reluctance of each half of the magnetic circuit (ACB and ADB) is equal to:

$$R_{i_m} = \frac{l_m}{2} \cdot \frac{1}{Q_m} \cdot \frac{1}{\mu_i}, \tag{4}$$

where l_m is the total length of the magnetic circuit,
Q_m its cross-sectional area, and
μ_i the incremental permeability of the core.

The value of μ_i for a given core material is determined by the field strength $H_\sim$ due to the pulsating current $i_\sim$ in windings 1 and 1'.

Neglecting the core losses it is possible to plot a graph of the relationship between $\mu_i = \frac{dB}{dH}$ and the field strength H, where B is the flux density (Fig. 4).

The field strength is in the main determined by the current in windings 1 and 1' and equals to:

$$H = 2 \frac{I_\sim W_1}{l_m}, \tag{5}$$

where W_1 is the number of turns in each winding, and
l_m is the length of the magnetic circuit.

By using graph (Fig. 4) and formula (5) it is possible to determine graphically the law of μ_i variations with time.

Similarly it is possible to find the variations with time of $\frac{1}{\mu_i}$ (Fig. 5).

By using the relationship thus obtained

$$\frac{1}{\mu_i} = f(t), \tag{6}$$

it becomes possible to determine on the basis of (4) that:

$$R_{l_m} = F(l) = \frac{l_m}{2} \cdot \frac{1}{Q_m} f(l). \tag{7}$$

The reluctance to flux Φ_{res} is determined by the existence of two parallel paths in the magnetic circuit, each of which has the reluctance of R_{l_m}.

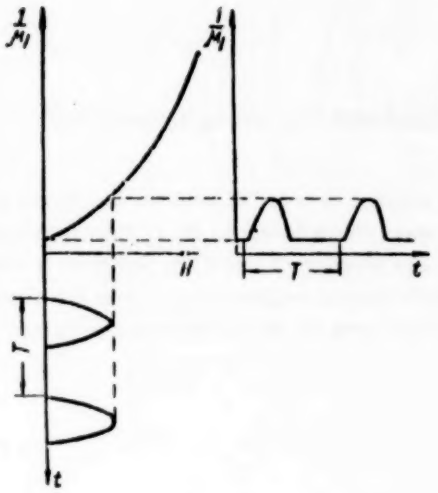

Fig. 5.

The drop in the magnetic potential between points A and B of the magnetic circuit (Fig. 3) is equal to*

$$U_m = \frac{1}{2} R_l \Phi_{res} = \frac{l_m}{4} \cdot \frac{1}{Q_m} f(l) \Phi_{res} \tag{8}$$

On the basis of (8) and Fig. 5 it is not difficult to find the variations of U_m with time.

U_m consists of a direct $U_{m=}$ and an alternating $U_{m\sim}$ component. The alternating component of the flux $\Phi_{\sim}$, due to the alternating component of the magnetic tension $U_{m\sim}$, splits up in the magnetic circuit similarly as the permanent flux Φ_{res}

$$\Phi_{\sim}(l) = g_b U_{m\sim}, \tag{9}$$

where g_b is the permeance between the opposite sides of the magnetic circuit marked in Fig. 3 as A_1AA_2 and B_1BB_2.

The alternating flux $\Phi_{\sim}(t)$ induces in winding 3 and 3' (Fig. 1d) an emf ϵ:

$$\epsilon = W_3 \frac{d\Phi_{\sim}(l)}{dt}. \tag{10}$$

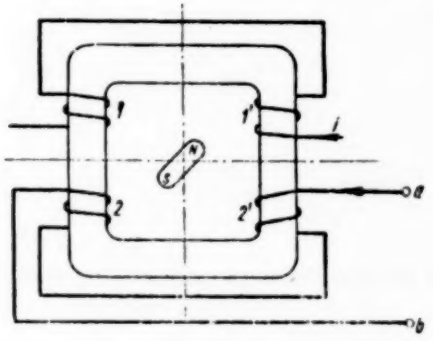

Fig. 6.

Where W_3 is the number of turns in each winding 3 and 3'. Quantity $\frac{d\Phi_{\sim}}{dt}$ can be found by means of graphic differentiation of $\Phi_{\sim}(t)$.

The actual instruments are wound with only two pairs instead of three pairs of windings. The function of windings 2 and 2' becomes more complex. They are simultaneously used as windings 3 and 3'. The replacement of two pairs of windings by one pair is made possible by the use of a two-channel filter which divides the output of windings 2 and 2' into two independent circuits carrying direct and alternating currents respectively. Figure 6 shows an arrangement using two pairs of windings.

Finding optimum relations between the transducer parameters. In designing the device it is necessary to choose the parameters in such a way that the induced emf ϵ is at the maximum for a given value of the dc input signal.

The basic parameters determining the value of the output voltage for a given size of the core laminations are the ratio of the areas occupied by the first and second windings and the cross-sectional area of the magnetic circuit.

*Here Φ_{res} is the initial permanent magnetic flux. The alternating component $\Phi_{res\sim}$ is found from second approximation formulae.

Choice of the sectional areas ratio of windings 1 and 1' and 2 and 2'. Let us denote the combined sectional area of windings 1 and 1' and 2 and 2' by S_1 and S_2 respectively and the total winding area by S_0, then obviously

$$S_2 = S_0 - S_1. \tag{11}$$

In order to produce certain ampere-turns $(AW)_2$ in windings 2 and 2' it is necessary to dissipate a certain power $P_{=}$. The relation between $(AW)_2$ and $P_{=}$ is expressed by the equation

$$P_{=} = \frac{\rho l_m}{k S_2}(AW)_2^2, \tag{12}$$

where ρ is the resistivity of the wire,

l_m the mean length of a winding turn,

k the coefficient showing the extent to which the core port is filled with conducting material and

S_2 is the combined section area of windings 2 and 2'.

Since in practice we can always choose a sufficiently powerful magnet in order to balance the fluxes due to the ampere-turns $(AW)_2$, it is desirable to provide conditions for ampere-turns $(AW)_2$ to be at their maximum for a given $P_{=}$. This will also increase the sensitivity of the device. Let windings 2 and 2' be fed from a certain source (which could be the output of a dc amplifier) with an emf ϵ and internal resistance r_i. Then for maximum power in the windings 2 and 2', the wire diameter and the total number of turns W_2 should be selected in such a way as to make the winding resistance equal to r_i:

$$\frac{\rho l_m}{k S_2} W_2^2 = r_i. \tag{13}$$

Then the power will be

$$P_{=} = \frac{E^2}{4 r_i} = P_{= \max} \tag{14}$$

and on the basis of (12)

$$(AW)_2 \max = \sqrt{\frac{k S_2}{\rho l_{m_2}}}\sqrt{P_{= \max}} \tag{15}$$

From this it follows that $(AW)_2 \max$ and, hence, the sensitivity of the transducer are proportional to the square root of S_2.*

It should be noted that the magnetic transducer output voltage is fed from windings 2 and 2' to the amplifier through a step-up transformer; therefore the number of turn W_2 can be determined from (13) without taking into consideration that the alternating emf in windings 2 and 2' increases when W_2 is increased.

Thus, it follows on the basis of (15) that S_2 should be large; this however is possible according to (11) only by decreasing S_1. In turn the decreasing of S_1 will lead to a decreased sensitivity. In fact when a pulsating current runs through windings 1 and 1' (see Fig. 2) the maximum ampere-turns $(AW)_{1\max} = 2I_{\max}W_1$ can be represented by

$$(AW)_{1\max} = \Delta k_a k S_1,$$

where Δ is the effective value of current density,

k_a the current curve form factor,

* Variation of l_m due to S_2 can be neglected in the first approximation.

k the core port stacking coefficient, and
S_1 is the combined section area of windings 1 and 1'.

In order to avoid overheating Δ must not exceed a certain value.

Thus in designing the device, $(AW)_{1\,max}$ should be considered proportional to S_1.

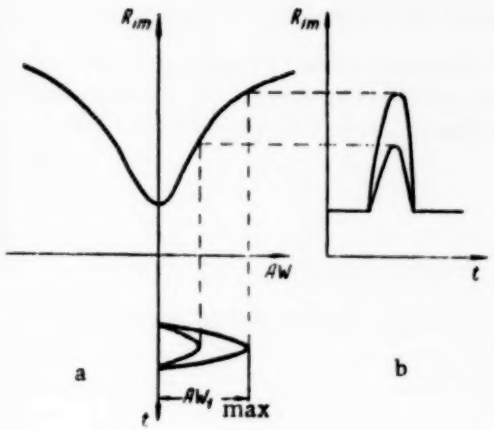

Fig. 7.

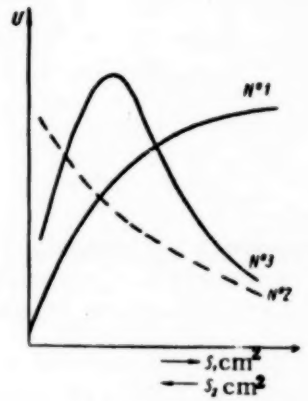

Fig. 8.

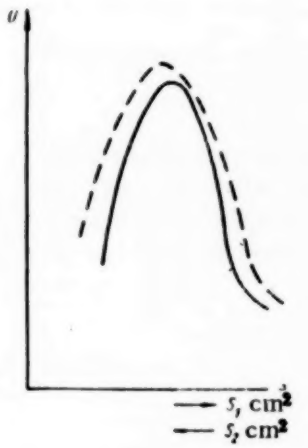

Fig. 9.

Figure 7 gives curves of R_{i_m} plotted against time for two values of $(AW)_{max}$. From these curves it follows that a decrease in $(AW)_{1\,max}$ leads to a decrease in the depth of modulation of R_{i_m}.

According to (8) this will also decrease the alternating component of the magnetic tension U_m which determines the value of $\Phi_{\sim}$, see (9).

It follows from the above that a decrease of S_1 will cause a fall in sensitivity. By means of the graphical analytical method used above it is also possible to find the relation between $\Phi_{\sim}$ and S_1. Figure 8 curve No. 1 shows $\Phi_{\sim} = f(S_1)$ for the following parameters of the transducer: core made of transformer steel type E-330, core section area 0.28 cm², $W_I = 2 \times 700$ turns, $W_{II} = 2 \times 10{,}000$ turns.

In the same figure the dotted line shows $(AW)_{2\,max} = f_2(S_1)$ found from (15) and (11):

$$(AW_2)_{max} = \sqrt{\frac{\kappa}{l_{cp}}}\sqrt{P_{-max}}\sqrt{S_0 - S_1} = \kappa\sqrt{S_0 - S_1} \quad \text{(curve № 2).}$$

By multiplying the ordinates of graphs No. 1 and 2, the region of suitable values for S_1 is obtained. (Curve No. 3).

Figure 9 shows the values of the transducer alternating output voltage plotted against the sectional areas of S_1 and S_2.

The full line curve was obtained experimentally and the dotted one by calculation. The experiment consisted in measuring the output voltage of several laboratory models with different winding area ratios but the same current density.

It will be seen that the agreement is satisfactory.

Choice of the core cross section. By means of the analytical methods described it is possible to choose an optimum cross section for the core. In order to be able to do it, however, more precise methods should be used in certain respects.

Up to the present we assumed that the magnetic tension U_m was caused by the magnetic flux in the two limbs of the core. We neglected the flux outside the core. If this is taken into account expression (8) will take the form:

$$U_m = \frac{\frac{1}{2}}{\frac{1}{R_i} + g_b} \Phi_{res}, \tag{17}$$

where R_i is the reluctance of one of the core limbs, and
g_b is the permeance of the shunting "air" path.

According to (17) U_m is maximum when $R_i = R_{i\,max}$.

$$(U_m)_{max} = \frac{\frac{1}{2}}{\frac{1}{R_{i\,max}} + g_b} \Phi_{res},$$

and it is minimum when $R_i = R_{i\,min}$:

$$(U_m)_{min} = \frac{\frac{1}{2}}{\frac{1}{R_{i\,min}} + g_b}.$$

The difference between $U_{m\,max}$ and $U_{m\,min}$ determines the amplitude of the alternating component of the magnetic flux Φ_{res}, see (9).

$$(U_m)_{max} - (U_m)_{min} = \frac{1}{1 + \frac{1}{R_{i\,max} g_b}} - \frac{1}{1 + \frac{1}{R_{i\,min} g_b}} \cdot \frac{1}{2} \Phi_{res} R_b$$

As the cross-sectional area Q of the core decreases, $R_{i\,max}$ and $R_{i\,min}$ increase and the difference

$$F = \frac{1}{1 + \frac{1}{R_{i\,max} g_b}} - \frac{1}{1 + \frac{1}{R_{i\,min} g_b}} \tag{18}$$

acquires a maximum at a certain value of $Q = Q_{opt}$.

According to (4)

$$R_{i\,max} = \frac{l_m}{2} \cdot \frac{1}{Q} \cdot \frac{1}{\mu_{min}},$$
$$R_{min} = \frac{l_m}{2} \cdot \frac{1}{Q} \cdot \frac{1}{\mu_{max}}. \tag{19}$$

Substituting (19) and (18) we obtain

$$F = \frac{1}{1 + \frac{\mu_{i\,min} Q}{A}} - \frac{1}{1 + \frac{\mu_{i\,max} Q}{A}}, \tag{20}$$

where

$$A = \frac{l_m}{2} g_b \tag{21}$$

F is at a maximum when

$$Q_{opt} = \frac{A}{\sqrt{\mu_{l\max}\,\mu_{l\min}}} = \frac{\frac{l_m}{2} - g_b}{\sqrt{\mu_{l\max}\,\mu_{l\min}}}. \qquad (22)$$

Conclusions. At present the development of magnetic transducers of the type described is in its infancy.

The investigation carried out cannot be considered as exhaustive, since a complete evaluation of the possibilities of the new system can only be made after considerable experimental material has been accumulated and the theory developed still further. The outlines method of designing magnetic transducers, however, may be found useful.

LITERATURE CITED

[1] V. N. Mil'shtein, Elektrichestvo, No. 5, 1950.

[2] V. N. Mil'shtein and N. A. Palibina, Scientific Technical Information Bulletin, (Niiteplopribora, No. 3, 1956).

DESIGN OF FERRO-DYNAMIC GALVANOMETERS

A. M. Melik-Shakhnazarov

The design of a ferro-dynamic galvanometer differs from that of normal ferro-dynamic instruments and ratiometers [1, 7] basically in the application to the moving system of the instrument of two equal counteracting moments, an electrical and a mechanical one.

The basic components of a ferro-dynamic galvanometer are: (Fig. 1) the magnetic circuit, the excitation winding W_b and the coil W of an area S_p. A sinusoidal voltage U, of angular frequency ω, is applied to the excitation winding. The flux due to this winding has a density B in the air gap.

When the coil of the instrument is in a position coinciding with the direction of the flux axis, no emf will be induced in the coil. This position can be called the electrically neutral line.

When the coil is deflected from the neutral position by an angle α the emf induced in it will be:

$$E_p = \omega WBS_p\alpha.$$

If the moments acting on the coil of the ferro-dynamic galvanometer are considered separately as moment M_x produced by the current due to the voltage U_x applied to the coil, and moment M_p produced by the current due to the induced emf E_p, we shall obtain, from the position of vectors shown on the vector diagram (Fig. 2), the following values for the moments:

$$M_x = \frac{U_x BS_p W\cos(\delta+\varphi)}{z},$$

$$M_p = -\frac{B^2 S_p^2 W^2 \omega \alpha \sin\varphi}{z},$$

where the meaning of the phase angles δ and φ becomes clear from the diagram (Fig. 2).

In the balanced position both these moments M_x and M_p are balanced out by the counteracting mechanical moment $M_M = W_M \gamma$, where W_M is the stiffness of the compressing or extending spring and γ is the angle of the coil deflection from the mechanical neutral line (a position of the coil determined by the compression or extension of the spring).

If the operation of a ferro-dynamic galvanometer is analyzed the following conclusions can be drawn [2, 3]:

1) For a normal operation of a ferro-dynamic galvanometer, a coincidence of the electrical and mechanical neutral lines is required. If the position of the two neutral lines differs by angle β, the moving system will, in the absence of voltage U_x, be displaced from the position of the electrical neutral line by angle α_0:

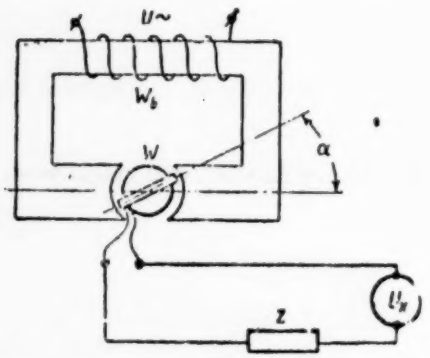

Fig. 1.

$$\alpha_0 = \frac{\beta}{1 + \frac{B^2 S_p^2 W^2 \omega \sin\varphi}{z W_M}},$$

moreover the displacement will depend, as it will be seen from the formula, on the parameters of the measuring circuit (z, φ).

2) The sensitivity of the ferro-dynamic galvanometer is determined from the formula:

$$S = \frac{\alpha}{U_x} = \frac{BS_p W \cos(\delta + \varphi)}{z\left(W_M + \frac{B^2 S_p^2 W^2 \omega \sin\varphi}{z}\right)} =$$

$$= \frac{BS_p W \cos(\delta + \varphi)}{z(W_M + W_e)},$$

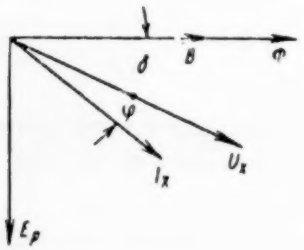

Fig. 2.

where the term

$$\frac{B^2 S_p^2 W^2 \omega \sin\varphi}{z} = W_e$$

can assume various values depending on the magnitude and sign of angle φ in the measuring circuit.

If the measuring circuit impedance is inductive, the term W_e acts as an electrical counteracting moment (electrical spring). If the measuring impedance is resistive, term $W_e = 0$. If it is capacitative term, W_e becomes negative. In this instance there are two possibilities:

$$W_M > |W_e| \;\&\; W_M < |W_e|.$$

In the first case, term W_e virtually tends to balance the mechanical counteracting moment and decrease the resulting counteracting moment of the instrument, thus increasing the sensitivity of the galvanometer. In the second case, the coil tends to take up a position normal to the direction of the flux axis and the moving system looses zero stability.

3) In order to raise the sensitivity of the ferro-dynamic galvanometer, it becomes advisable in certain cases to decrease angle φ in the measuring circuit by connecting a capacitative impedance either in parallel or in series with the coil. In the case when the impedance of the measuring circuit can change in the course of measurement it is not always advisable to obtain condition $\varphi < 0$, since in the process of measurement condition $W_M < |W_e|$ may then occur with the resulting zero instability. Therefore schemes with a fixed galvanometer coil circuit impedance have certain advantages [6].

4) With given measuring circuit parameters the sensitivity of the galvanometer can be increased by providing an optimum flux density in the airgap. This flux density can be determined by finding a maximum for the

sensitivity formula. The optimum flux density is equal to

$$B = \frac{1}{WS_p}\sqrt{\frac{W_M z}{\omega \sin\varphi}}.$$

In this case the sensitivity is expressed by the formula:

$$S = \frac{\cos(\beta+\varphi)}{\sqrt{W_M \omega \sin\varphi z}}.$$

5) When the measuring circuit impedance is inductive, i.e., when term W_e has the effect of an electrical counteracting moment, the galvanometer will operate without the mechanical counteracting moment (frameless coil, flexible leads). In this case the ferro-dynamic galvanometer is similar to the ferro-dynamic ratiometer [1] and its sensitivity is determined by formula:

$$S = \frac{\cos(\beta+\varphi)}{BS_p W \omega \sin\varphi}.$$

In this instance sensitivity is maximum when the flux density in the airgap is reduced to a minimum. The practical limit for the reduction of the flux density is determined by the value of the friction moment. The value of the minimum permissible flux density can be determined from expression

$$W_e \Delta\alpha_{min} > M_{mp},$$

where $\Delta\alpha_{min}$ is the permissible absolute error in the pointer zero position, and
W_e is the specific electric restoring moment.

The use of the ferro-dynamic galvanometer without a mechanical counteracting moment is especially expedient in measuring circuits with an incomplete balance.

6) The ferro-dynamic galvanometer also has some peculiarities in the moving system parameters. The moving system can have four types of movement: damped oscillations, undamped oscillations, aperiodic and critical damping [2]. In some cases it is possible to control the movement by means of an additional excitation winding fed by a direct current.

It is possible by means of the relations given above to calculate the basic parameters of a ferro-dynamic galvanometer for various initial conditions. The same relations can be used for calculating induction converters for the galvanometer amplifiers [4, 5].

Let us examine numerical calculations of parameters for a galvanometer in a static operating condition.

The galvanometer has a coil of W = 85 turns and an area $S_p = 3.5\ cm^2 = 3.5 \cdot 10^{-4}\ m^2$. The value of the specific mechanical counteracting moment is:

$$W_M = 0.0306\ gcm/rad = 30.6\ mgcm/rad.$$

The position of the electrical and mechanical neutral lines coincides.

$$(\beta = 0).$$

The vector of the measured voltage U_x is in phase with the flux vector ($\delta = 0$). The alternating current frequency is equal to $f = 50$ cps.

1. Evaluation of the operating moment M_x, the specific electric counteracting moment W_e and the sensitivity of the galvanometer with the following initial conditions:

$B = 0.15\ weber/m^2$ (effective value)
$U_x = 20$ mv, $z = 13$ ohms, $\varphi = 4°$.

The operating moment is equal to

$$M_g = \frac{U_x B S_p \cos(\delta+\varphi)}{z} \cdot \frac{10^8}{9810} \text{ g}\cdot\text{cm},$$

$$M_g = \frac{20\cdot10^{-3}\cdot0.15\cdot3.5\cdot10^{-4}\cdot85\cdot0.998\cdot10^8}{13\cdot9810} =$$

$$= 0.07 \text{ g}\cdot\text{cm} = 70 \text{ mg}\cdot\text{cm}$$

The specific electrical counteracting moment is equal to:

$$W_e = \frac{B^2 S_p^2 W^2 \omega \sin\varphi}{z} \cdot \frac{10^8}{9810} \text{ g}\cdot\text{cm/rad},$$

$$W_e = \frac{0.15^2\cdot3.5^2\cdot10^{-8}\cdot85^2\cdot314\cdot0.07\cdot10^8}{13\cdot9810} =$$

$$= 0.34 \text{ g}\cdot\text{cm/rad} = 340 \text{ mg}\cdot\text{cm/rad}$$

The galvanometer sensitivity is equal to:

$$S = \frac{B S_p W \cos(\delta+\varphi)\cdot10^7}{z\,(W_M + W_e)\cdot981} =$$

$$= \frac{0.15\cdot3.5\cdot10^{-4}\cdot85\cdot0.998\cdot10^7}{13\cdot(0.0306+0.340)\cdot981} =$$

$$= 9.5 \text{ rad/v} = 0,54 \text{ degree/mv}$$

It will be seen from the calculation that the electrical counteracting moment W_e (the electrical spring) is considerably larger then the mechanical countering moment and the sensitivity of the galvanometer is small.

2. Evaluation of an optimum flux density in order to obtain maximum sensitivity for given measuring circuit parameters.

The optimum flux density is determined from the formula

$$B_1 = \frac{1}{W S_p \cdot 10^4} \sqrt{\frac{9810 W_M z}{\omega \sin\varphi}} \text{ weber/m}^2$$

$$B_1 = \frac{1}{85\cdot3.5\cdot10^{-4}\cdot10^4} \sqrt{\frac{9810\cdot0.0306\cdot13}{314\cdot0\ 07}} =$$

$$= 0\ 045 \text{weber/m}^2 = 450 \text{ gauss}$$

With this value of flux density the specific electric counteracting moment is equal to:

$$W_e = \frac{B_1^2 S_p^2 W^2 \omega \sin\varphi \cdot 10^8}{9810\ z} =$$

$$= \frac{0,045^2\cdot3.5^2\cdot10^{-8}\cdot85^2\cdot314\cdot0.07\cdot10^8}{9810\cdot13} =$$

$$= 0.0306 \text{ g}\cdot\text{cm} = 30.6 \text{ mg}\cdot\text{cm}$$

Thus the condition for maximum sensitivity corresponds, for given measuring circuit parameters, to equal specific electrical and mechanical moments.

Under this condition the galvanometer sensitivity is equal to:

$$S=\frac{B_1 S_p W\cos(\delta+\varphi)\cdot 10^7}{z\,(W_M+W_e)\cdot 981}=$$

$$=\frac{0.045\cdot 3.5\cdot 10^{-4}\cdot 85\cdot 0.998\cdot 10^7}{13\cdot(0.0306+0.0306)\cdot 981}=17\ \text{rad/v}=1\ \text{degree/mv}$$

Thus the galvanometer sensitivity is raised by a factor of 2 as compared with the preceding case (An experimental evaluation of the optimum flux density and sensitivity agrees with the calculated values).

3. Evaluation of the galvanometer sensitivity at flux density of B = 1.5 weber/m², with the electrical counteracting moment eliminated by means of compensating the inductance of the galvanometer coil ($\varphi = 0$).

In order to compensate the inductance of the coil a capacitor shunted by a resistor (Fig. 3) is connected in series with the coil. For a given value of the capacitor C = 20 μf (an electrolytic capacitor may be used) the value of the resistance can be determined from the formula:

$$R_c=10^3\sqrt{\frac{z\sin\varphi}{\omega C\,(1-\omega C z\sin\varphi\cdot 10^{-6})}},$$

where C is the capacity in microfarads.

At a frequency of 50 cps and a small angle φ it is possible to neglect the second term in the denominator, then

$$R_c=10^3\sqrt{\frac{z\sin\varphi}{\omega C}}=10^3\sqrt{\frac{13\cdot 0.07}{314\cdot 20}}=12.1\ \text{ohm}$$

The total impedance of the circuit after compensation is equal to z_1 = 25 ohms, φ = 0. The galvanometer sensitivity is then equal to:

$$S=\frac{BS_p W\cos\delta\cdot 10^7}{z_1 W_M\cdot 981}=$$

$$=\frac{0.15\cdot 3.5\cdot 10^{-4}\cdot 85\cdot 1\cdot 10^7}{25\cdot 0.0306\cdot 981}=60\ \text{rad/v}=3.4\ \text{degree/mv}$$

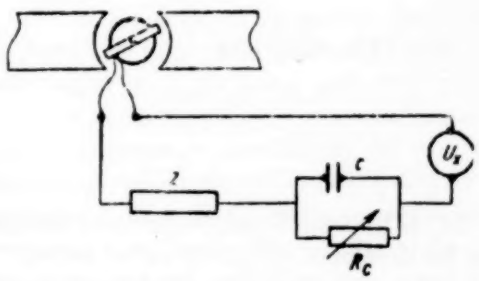

Fig. 3.

The sensitivity of the galvanometer can be still further increased if the coil is over-compensated (a negative φ angle). In this case the specific electrical moment W_e acquires a negative sign, stops being counteracting and the sensitivity formula becomes:

$$S=\frac{B_1 S_p W\cos(\delta-\varphi)\cdot 10^7}{z\,(W_M+W_e)\cdot 981},$$

Moment W_e compensates moment W_M thus increasing the galvanometer sensitivity.

Under condition $W_M + W_e = 0$, $S = \infty$. In practice, under this condition, the galvanometer looses zero stability and is deflected to the maximum value at random in either direction.

4. Evaluation of the negative angle φ, at which the galvanometer looses its stability, for a given value B = 1.5 weber/m² and a total impedance of the measuring circuit previously obtained; z_1 = 25 ohms.

Angle φ is determined from the relationship $W_M + W_e = 0$.

$$\sin\varphi = -\frac{W_M z \cdot 9810}{B^2 S_p^2 W^2 \omega \cdot 10^8} =$$

$$= -\frac{0.0306 \cdot 25 \cdot 9810}{0.15^2 \cdot 3.5^2 \cdot 10^{-8} \cdot 85^2 \cdot 314 \cdot 10^8} = -0.012,$$

$$\varphi \simeq -40'.$$

Thus with a negative angle φ of 40' only, over-compensation occurs. Hence when it is required to increase the galvanometer sensitivity by means of compensating the mechanical counteracting moment, a smooth variation of angle φ should be provided.

It should also be noted that when the counteracting moment is compensated, the resulting specific restoring moment is decreased, which leads to a deterioration of the zero stability; the compensation of the mechanical moment should, therefore, be carried out only within certain limits.

Above examples only dealt with the calculation of the basic galvanometer parameters.

The technique of designing the galvanometer for maximum efficiency, maximum sensitivity, etc. is in the main the same as for moving coil instruments.

LITERATURE CITED

[1] V. O. Arutiunov, Design and Construction of Electrical Measuring Instruments [in Russian] (GEI, 1949).

[2] A. M. Melik-Shakhnazarov, Some Peculiarities of the Operation of Ferro-Dynamic Null Indicators [in Russian] (Works of the Azerbaidzhan Industrial Institute, ed. 11, 1955).

[3] A. M. Melik-Shakhnazarov, G. A. Alizade and T. M. Aliev, Zavod. Laboratoriia , No. 7, 1953.

[4] N. P. Volkov, Priborostroenie, No. 2, 1957.

[5] A. M. Melik-Shakhnazarov, Izmerital'naia Tekhika, No. 1, 1957.

[6] A. M. Melik-Shakhnazarov, G. A. Alizade and T. M. Aliev, Zavod. Laboratoriia , No. 6, 1955.

[7] A. F. Kulikovskii, Electrical Measuring Instruments for Checking Boring Processes [in Russian] (Gostoptekhizdat, 1952).

A PORTABLE SET FOR TESTING ELECTRICITY METERS

V. S. Sheiko

Following a suggestion made by the author of this article the VNII (All-Union Scientific Research Institute) of the Committee for Standards, Measures and Measuring Instruments has developed a portable set for testing electrical power and va meters as well as phase meters, wattmeters, ammeters and voltmeters of class 1.5 at the factory premises and in particular during inspection testing.

Although relatively light and small this set is technically as good as rack-mounted devices and in some respects even better.

Figure 1 gives the schematic circuit of the set. Current and voltage adjustments are made by means of autotransformers RT of the LATR-2 type. In order to ensure smoother current and voltage adjustment in single-phase measurements the set includes a switch Sw which transfers the first phase autotransformer to the "load" terminals of the second phase. It is then used as a second adjusting stage (fine adjustment).

In order to decrease the weight of the set, specially made light load-transformers L_1T-L_2T are used, and all the adjusting and standard transformers ST type LATR-2 and I-54 are mounted without their cases.

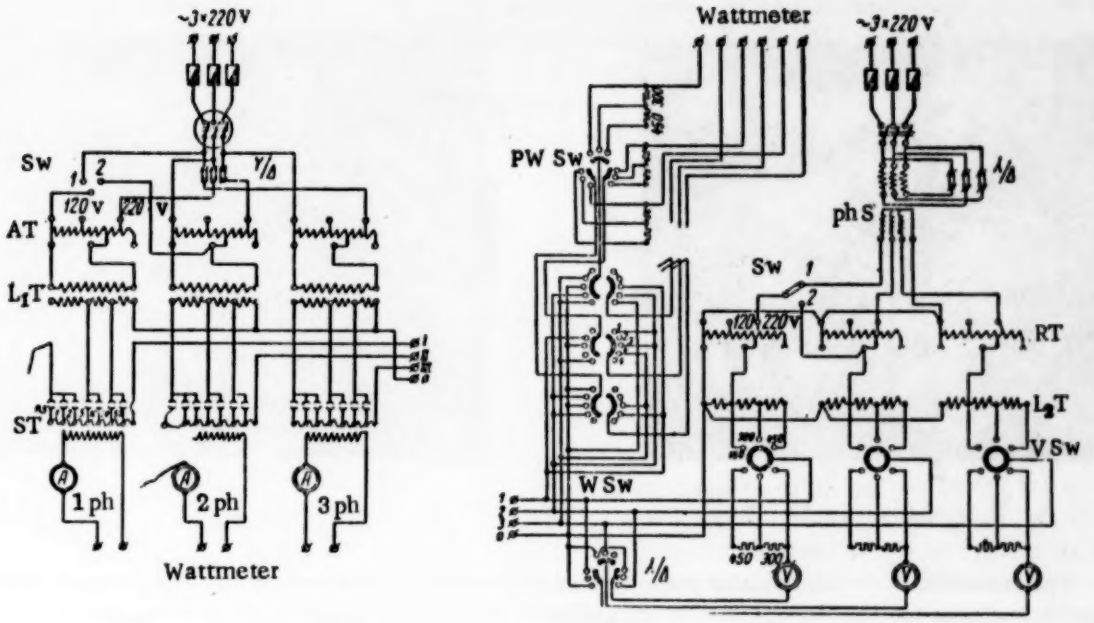

Fig. 1.

The phase shifter PhS is made up of components of two motors, the rotor being the moving part of the electric plane type I-24a of the "Elektroinstrument" plant (Daugavpils), which has a three-phase star-connected winding, and the stator belongs to the motor made by the 2nd Mechanical Artel (Moscow) which has a special winding for working from a supply of 220 or 380 v.

The phase shifter weights 8.5 kg and its dimensions are 180 × 180 × 180 mm.

The set is mounted in two cases, one contains all the voltage circuit components including the phase shifter, the other all the current circuit components. Each case weighs 40 kg and has the dimensions of 50 × 40 × 25 cm.

The set works from a three-phase supply of 220 or 380 v. The phase shifter and the adjusting transformers can be set to operate from either voltage.

In Fig. 1 the set is shown to be connected to a supply of 220 v without a neutral conductor.

The top panel of the voltage case contains (Fig. 2) terminals for connecting the set to a three-phase supply of 220 or 380 v; a three-pole switch 2; fuses 3 for a nominal current of 2 a; terminals 4 for connecting the instruments to be measured; three pairs of terminals 5 for connecting standard instruments (wattmeters or voltmeters); switch 6 which transfers the autotransformer for fine adjustment purposes; (Sw in Fig. 1); switch 7 for adjusting voltmeter ranges to 150-300 and 450 v (VSw in Fig. 1); switch 8 which provides wattmeter circuits for testing various electricity meters without changing connections on the wattmeters themselves (W Sw in Fig. 1); switch 9 for parallel wattmeter circuit ranges (PW Sw in Fig. 1); switch 10 connecting voltmeters for phase or line voltage measurements; three voltmeters 11 of the E-421 type, each with three ranges of 150-300-450 v, for measuring phase voltages and selected in such a way that their basic errors do not exceed those for class 1.5 instruments.

In the center of the panel there is knob 12 connected to the phase shifter worm-gear. The phase shifter provides an adjustment of the voltage phase with respect to the current from 0 to 120°. At the bottom of the panel regulators 13 are mounted; they consist of three autotransformers type LATR-2 which provide a voltage adjustment from 0 to 450 v.

The upper current case panel (Fig. 3) contains: terminals 1 for connecting the set to the three-phase supply; a three pole switch 2; fuses 3 for a nominal current of 2a; test terminals 4; three pairs of terminals 5 for standard instruments; switch 6 which transfers the autotransformer for fine adjustment purposes (Sw in Fig. 1); three type E-421 ammeters connected by means of instrument current transformers type I-54 for measuring phase currents.

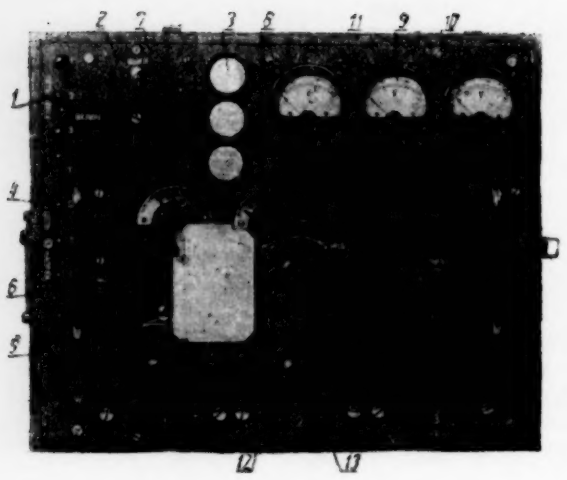

Fig. 2.

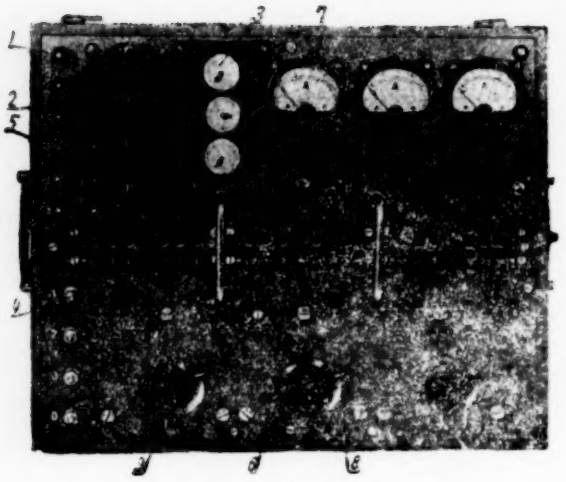

Fig. 3.

The middle of the panel contains jacks 8 connected to three instrument current transformers supplying wattmeter and ammeter testing circuits. Transformer ST switches are ganged with load transformer L_1T switches so that measuring ranges and loads are switched simultaneously. The bottom of the panel contains current regulators 9 which consist of three autotransformers type LATR-2.

Standard instruments are not provided in the set since they are usually available on the spot, and since their inclusion would have increased considerably the weight and size of the set.

The set can be used in travelling laboratories particularly in GAZ-69 vans which have been adopted by the Committee for Standards, Measures and Measuring Instruments for inspection laboratories. In this connection it is convenient to have permanent racks in the van for mounting electricity meters.

For testing purposes the two halves of the set are placed side by side on a bench with three wattmeters between them connected to terminals on both cases marked "Wattmeter." The wattmeters must be of the ASTD type, since range multipliers for this type of wattmeters are provided in the set. One model set of this type was made in the VNII Laboratory of the Committee and is at present being used.

Tests have shown that the voltage in the secondary circuit of the phase shifter changes by less than 1% when the rotor is moved through 120°; the shape of the current and voltage are practically sinusoidal; the adjustments of the phased voltage and current are independent of each other and provide an easy setting of the standard wattmeter at any point on the scale.

Experience gained in operating the set has shown that it is convenient and fully satisfies its design requirements.

Conclusions. This portable set may find a wide application both in State Inspection Laboratories for Measuring Equipment and in establishments connected with the testing and repair of electricity meters, in particular in Base Laboratories for Departmental Inspection. It is therefore advisable to organize mass production of these sets.

AN ELECTRONIC PHASE METER FOR SUPPLY FREQUENCY CIRCUITS

I. M. Vishenchuk, A. F. Kotiuk and V. A. Sheremet'ev

In many investigations of transients in supply frequency circuits it is required to know the phase shift between two voltages.

The common double channel electronic phase meters with permanent magnet oscillographs [1, 2, 3] have a number of important defects, the basic ones being, the limited range (0 to 180°) and a considerable error (up to 5%). The total error of these phase meters consists of the null error, which produces the same absolute error in measuring different angles, and the sensitivity error which produces the same relative error in measuring different angles. Among other defects of these phase meters one should also mention the time lag in taking oscillograms, which amounts to 15-18 msecs.

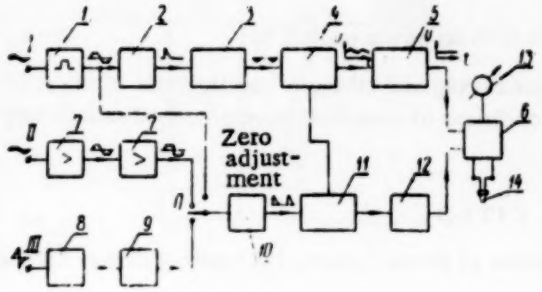

Fig. 1.

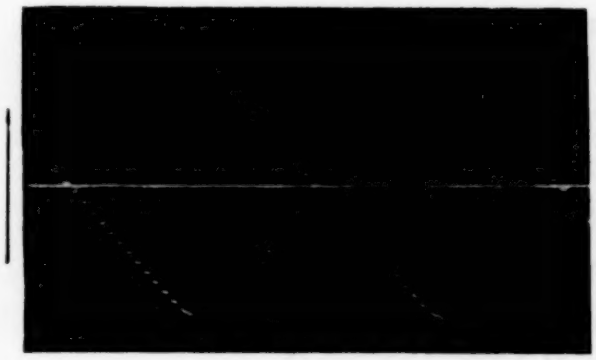

Fig. 2.

Below we describe a phase meter which largely eliminates above defects.

Figure 1 gives its block schematic. The supply sine-wave reference voltage in channel I is fed to limiter 1, whose output voltage has a trapezoidal shape with steep sides. After differentiation in stage 2, this voltage assumes the shape of short triangular pulses. Positive pulses trip the starting multivibrator of phantastron 3, which shapes short negative pulses, closing the saw-tooth phantastron generator 4 during the flyback. At the end of each pulse, the generator is released producing the linearly decreasing portion of the saw-tooth voltage. Thus the phantastron generator produces a saw-tooth 50 cps voltage, closely synchronized with the supply voltage, since the flyback occurs as the supply voltage passes through zero in the positive direction. Low pass filter 5 passes the saw-tooth voltage direct component, which is fed to the input of the differential tube voltmeter 6. The voltage whose phase requires to be measured is fed to the input of one of the two channels: to channel II, if the voltage is sinusoidal and to channel III, if it has the shape of a zigzag pulse with a positive edge slope of the order of 0.2-0.5 v/elect. degree. (Channel III is designed to measure the angle of retard of synchronous machines; the voltage to the input of the channel was fed from an electromagnetic phase transducer of the measured generator emf).

Channel II consists of two similar stages of amplifier-limiters 7. Their purpose is to transform the sinusoidal voltage into short pulses for starting the multivibrator at the instant the voltage passes through zero in the positive direction. Channel II operates normally with an input voltage of 0.5 to 60 v.

Channel III consists of an input amplifier with a delay phantastron 9 used as a phase shifter. The purpose of the delay phantastron is to change if required the phase of the tripping pulse at the input of the channel.

The voltage from either channel II or III is fed through the differentiating RC circuit to the input of the single-period multivibrator 10. At its output positive voltage pulses are produced whose time delay with respect to the reference voltage is proportional to the required phase shift. These pulses operate the electronic switch 11. At the instant a pulse reaches the switch, it opens and the "memory" capacitor 12 is charged up to the instantaneous value of the phantastron generator voltage. Until the next pulse is received the capacitor "remembers" this voltage fed to the second input of the differential tube voltmeter. An indicating instrument 13 and the loop of a permanent magnet oscillograph 14 are connected to its output.

Investigation of separate units and the instrument as a whole have shown that the component errors due to zero drift in channel I are eliminated by the zero adjustment of the phase meter. There remains the error due to changes in sensitivity which does not exceed 1%. The component error due to the units of channel III caused by variations in the anode and heater voltages of the delay phantastron does not exceed 0.5°. The same error is obtained in channel II with a constant amplitude input signal. In order to obtain this small error in channel II, its limiters must be balanced beforehand. Thus the basic error of the phase meter, when used with a class 0.5 microammeter for an indicating instrument, and when it is zero adjusted and balanced before measuring, does not exceed 0.5° + 1%.

Its range is ±180 elect. degrees. It also has smaller ranges of ±90 and ±45 elect. degrees. The instrument has a center zero linear scale. The measured angle is recorded on the oscillogram every 0.02 sec, which is quite satisfactory for industrial and research purposes. Oscillograms were taken by means of oscillograph MPO-2 with loop No. VIII. Figure 2 shows an oscillogram of phase angle changes in a transient process obtained by means of the phase meter. The angle changed linearly in the range of +180 to −180°, then suddenly from −180 to +180° etc.

The phase meter is designed for measurement at supply frequency only. The frequency error within limited deviations is proportional to the deviation.

The meter power consumption is 50 va. It weighs together with its power pack 5 kg.

Conclusions. Field tests of the phase meter, consisting of measuring and taking of oscillograms of the rotor retard angle of a 15,000 kw synchronous generator at different conditions of operation, have produced satisfactory results.

LITERATURE CITED

[1] Iu. M. Gorskii, Measuring Devices in Physical Simulation of Power Systems [in Russian] (Trudy MEI, ed. 20, 1956).

[2] Electronic Instrument for Measuring and Recording Phase Shift Between Two ac Voltages [in Russian] (Technical Information of the V. I. Lenin All-Union Electrotechnical Institute, 1952).

[3] Instruction for the Use of Electronic Phase Meters, Type EFU-2 [in Russian] (Gidroenergoproekt, MES. SSSR, 1956).

CERTAIN ERRORS IN THREE-WINDING ELECTRODYNAMIC PHASE METERS

A. D. Nesterenko and E. S. Polishchuk

Double coil, double winding phase meters are widely used for power factors and phase shift measurements in single and three-phase circuits of supply and higher frequencies.

The basic defect of such phase meters is the variation of their readings with frequency. Hence in the overwhelming majority of cases, they are designed to work at one fixed frequency only.

There exist two types of phase meters whose readings are made less dependent on frequency. In one of these types (made by the firm Hartmann and Braun, type Eph, and the combined phase and frequency meter proposed by V. O. Arutiunov [1]) the frequency compensation is made manually by means of changing the impedance in the moving coil circuit. In another type (proposed by Pratt) one of the moving coils (Fig. 1) is divided into two parts, one having an inductive and the other a capacitative impedance series connection. With changing frequency the total current, which determines the turning moment, remains substantially constant. Such a phase meter is in essence a three-winding instrument.

By a correct choice of parameters it is possible, according to Pratt, to reduce the error due to mutual induction between the moving and stationary coils to a minimum. The latter is particularly important in higher frequency circuits where above error can reach excessive values.

Due to these advantageous properties the three-winding phase meter was made at the "Tochelektropribor" plant for measuring power factors in higher than supply frequency circuits.

An analysis of errors in three-winding phase meters is given below.

Errors due to variations in the phase meter parallel circuit parameters. Let us first investigate a two-winding phase meter, whose schematic and vector diagram are given in Figs. 2 and 3 respectively.

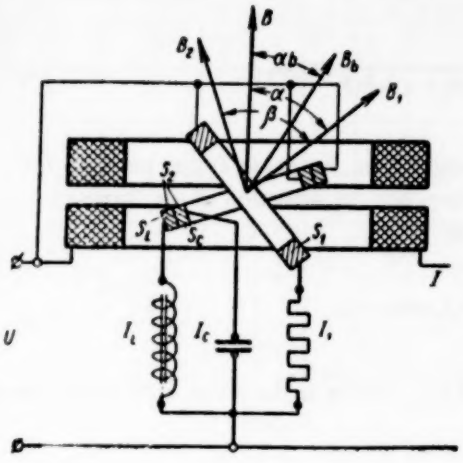

Fig. 1.

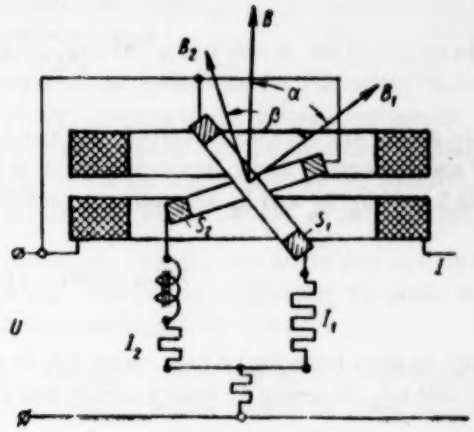

Fig. 2.

The basic relationship between the angle of rotation α of the instrument's moving part and the phase angle φ has the form [2]:

$$\operatorname{ctg}\alpha = \frac{k_1 I_1}{k_2 I_2} \cdot \frac{\cos(\varphi - \psi)}{\cos(\gamma - \varphi + \psi)\sin\beta} + \operatorname{ctg}\beta, \qquad (1)^*$$

where I_1 and I_2 are currents in the first and second coils respectively,

γ the phase difference between currents I_1 and I_2,

φ the phase difference between current I_1 and voltage U, fed to the instrument terminals,

β the angle in space between the directions of fluxes in coils 1 and 2, and

k_1 and k_2 are the constant coefficients depending on the absolute and relative dimensions of the coils.

Error due to the deviation of the phase meter parallel circuit parameters $\left(k_1 I_1 / k_2 I_2 = k,\ \gamma \text{ and } \psi\right)$ from their set values by Δk, $\Delta\gamma$ and $\Delta\psi$ is equal to [2]:

$$\Delta\alpha = -\frac{\sin\alpha\sin(\beta-\alpha)}{\sin\beta} \cdot \left[\frac{\Delta k}{k} - (\Delta\gamma - 2\Delta\psi)\operatorname{ctg}\gamma\right] - \\ - \frac{1}{\sin\beta\sin\gamma}\left[(\Delta\gamma + \Delta\psi)\sin^2(\beta-\alpha) + k^2\Delta\psi\sin^2\alpha\right]. \qquad (2)$$

Let us now determine the basic relationship between the rotation angle α of the instrument's moving part and the phase difference angle φ for a three-winding phase meter, whose schematic is shown in Fig. 1. The vector diagram of the currents and voltages in this circuit is shown in Fig. 4. Due to the interaction of the fluxes of the moving and stationary coils of the instrument, two turning moments D_1 and D_2 act on the moving part of the instrument. A balance of the moving part is obtained when:

$$D_1 = -D_2. \qquad (3)$$

It is easy to find that

$$D_1 = k_1 I_1 I \cos\varphi \sin\alpha,$$

$$D_2 = D_L + D_c = -[k_L I_L I \cos(\Theta_L - \varphi) - \\ - k_c I_c I \cos(\Theta_c + \varphi)] \sin(\beta - \alpha).$$

* ctg = cot.

By substituting the values of D_1 and D_2 into (3) and performing the required transformations we obtain:

$$\operatorname{ctg}\alpha = \frac{k_1 I_1 \cos\varphi}{[k_L I_L \cos(\theta_L - \varphi) - k_c I_c \cos(\theta_c + \varphi)]\sin\beta} + \operatorname{ctg}\beta, \tag{4}$$

where I_1, I_L and I_C are currents in coils S_1, S_L and S_C respectively, θ_L and θ_C are the phase angles between the voltage U and currents I_L and I_C respectively, β is the angle in space between the direction of the fluxes in coils 1 and 2, and k_1, k_L and k_C are constant coefficients. Let us denote

$$[k_L I_L \cos(\theta_L - \varphi) - k_c I_c \cos(\theta_c + \varphi)] = k_2 I_2 \cos(\gamma - \varphi). \tag{5}$$

It will be seen from Fig. 4 that vector $k_2 I_2$ is the sum of $k_C I_C$ and $k_L I_L$ and γ is the phase shift angle between voltages U and $k_2 I_2$ obtaining in Pratt's circuit and equal to $\pi/2$.

Fig. 3.

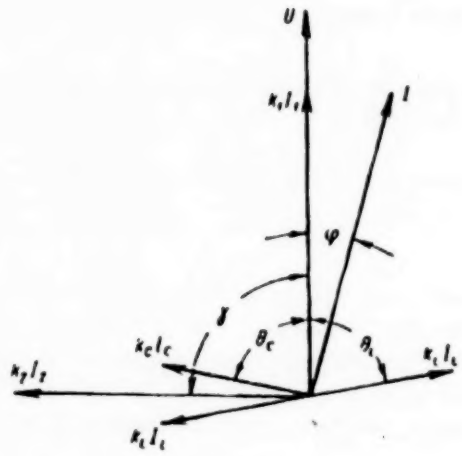

Fig. 4.

It is possible by means of (5) to transform (4) into

$$\operatorname{ctg}\alpha = \frac{k_1 I_1}{k_2 I_2} \cdot \frac{\cos\varphi}{\cos(\gamma - \varphi)\sin\beta} + \operatorname{ctg}\beta. \tag{6}$$

Expression (6) is similar to (1) and can be regarded as a particular case of the latter, (when $\psi = 0$). Hence expression (2) used for determining errors in two-winding phase meters can also be used in the case of Pratt's circuit.

In order to obtain the maximum specific restoring moment, with other conditions being equal, angle β in Pratt's circuit is usually made equal to $\pi/2$ [3]. Rembering also that in Pratt's circuit $\psi = 0$ and $\gamma = \pi/2$, it becomes possible to transform (2) to the form

$$\Delta\alpha = -0{,}5 \sin 2\alpha \frac{\Delta k}{k} - \Delta\gamma \cos^2\alpha. \tag{7}$$

It will be seen from (7) that $\Delta\alpha$ is not a constant, but depends on the position of the instrument's moving part. Making the derivative of $\Delta\alpha$ with respect to α equal zero, we obtain the scale point $\alpha_{\Delta m}$ which corresponds to the maximum error $(\Delta\alpha)_m$

$$\alpha_{\Delta m} = \frac{1}{2} \operatorname{arcctg}\left(k \frac{\Delta\gamma}{\Delta k} \right). \tag{8}^*$$

* arcctg = $\cot^{-1}$.

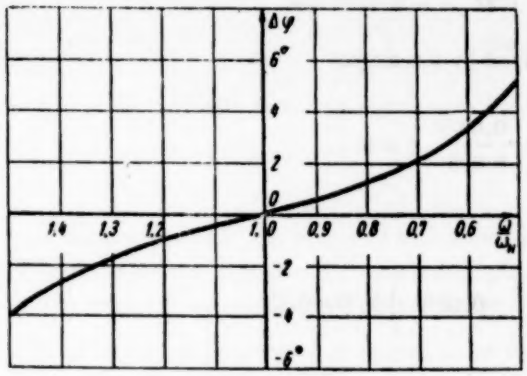

Fig. 5.

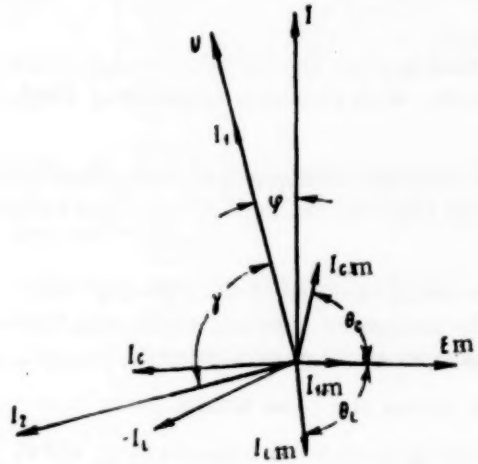

Fig. 6.

By substituting the value of $\alpha_{\Delta m}$ in (7) we obtain the maximum error $(\Delta\alpha)_m$.

The causes of errors due to the variation of basic parameters of the system are the following: variations in frequency; changes in the voltage and current of external circuit; changes in the external temperature; heating up of the set components by the operating currents; nonlinearity of the circuits containing iron.

Let us now examine the errors due to frequency changes and those due to connecting the phase meter through instrument transformers.

It is easy to show that Pratt's circuit posesses frequency stability within certain limits of frequency variations. Let us, for instance, determine what is the error with a frequency variation of ±10%. For this purpose let us examine the circuit of the "Tochelektropribor" plant's phase meter ELF-1 which has the following characteristics: $k = \sqrt{3}$; $\theta_L = 86°$; $\theta_c = 89.5°$; $\gamma = 90°$; $\beta = 90°$; $r_1 = 600$ ohms; $|Z_L| = |Z_c| = 2100$ ohms. The instrument's parallel circuit is connected through a transformer with an output voltage of 36 v. The nominal frequency is 500 cps. The maximum value of mutual inductance between the stationary coil and each of the moving coils is 0.97 mh.

A fall in frequency by 10% decreases impedance Z_L and increases Z_c by about 10%, changes the value of current I_2 to

$$I_2' = I_2\left(\frac{1{,}1 + \frac{1}{1{,}1}}{2}\right) = 1.005 I_2.$$

Then

$$\Delta k = \left(\frac{k_1 I_1}{k_2 \cdot 1.005 I_2} - \frac{k_1 I_1}{k_2 I_2}\right) = -0.005k.$$

Variations in frequency change the reactance of coils S_L and S_c; hence the ratios $\frac{x_L}{r_L} = \operatorname{tg}\theta_L$ and $\frac{x_c}{r_c} = \operatorname{tg}\theta_c$ (here x_L, x_c, r_L and r_c are respectively the reactive and resistive components of coils S_L and S_c). Therefore with a 10% fall in frequency, the deviation of phase angles θ_L and θ_c from the normal values can be determined from expressions:

$$\Delta\theta_L = \operatorname{arctg}\left(0.9\frac{x_L}{r_L}\right) - \theta_L = \operatorname{arctg}\left(0.9\operatorname{tg}86°\right) - 86° = -0°25',$$

$$\Delta\theta_c = \operatorname{arctg}\left(1.1\frac{x_c}{r_c}\right) - \theta_c = \operatorname{arctg}\left(1.1\operatorname{tg}89.5°\right) - 89{,}5° = 0°02'.$$

It is easy to show that at

$$\theta_L \simeq \theta_c \simeq \frac{\pi}{2}$$

$$\Delta\gamma \simeq \Delta\theta_L - \Delta\theta_c = -0°27' = -0{,}0079 \text{ rad}$$

The error reaches its maximum value at the point determined by the angle:

$$\alpha_{\Delta m} = \frac{1}{2}\operatorname{arcctg}\left(\frac{0.0079}{0.005}\right) = 16°.$$

At that point the error is:

$$\Delta_m\alpha = 0.5\sin 32° \frac{-0.005k}{k} - \left(-0.0079\right)0.92 = 0.45°.$$

It will be seen that with a 10% change in frequency, the error does not exceed 0.45°, whereas in the ordinary phase meter circuit type ELF (two-winding) this error attains 6.25° [2].

The graph (Fig. 5) gives the values of the maximum frequency error of phase meter ELF-1 plotted against the frequency deviation from the normal.

It will be seen from the graph that readings of the three-winding phase meters, within certain limits of frequency deviation, are almost independent of frequency variations. With frequency deviations of ±50% the instrument errors do not exceed 5°.

Additional errors due to the changes in the phase shift of instrument transformers are determined by the angular errors in the transformers. Owing to the small value of the latter (of the order of 0.5°) these additional errors can be considered insignificant.

Errors due to additional turning moments. These moments can be produced by the following causes: mutual inductance between the stationary and moving coils of the instrument; effects of an external field on the working fields of the system; effect of external fields on the inductance of the phase shifting device, etc.

Distortions in the shape of the measuring circuit current or voltage also cause similar errors.

Let us assume that in addition to the turning moments D_1 and D_2, another two moments $D_{1\,ad}$ and $D_{2\,ad}$ are acting on coils one and two respectively. The balance condition of the moving part of the instrument will then be:

$$D_1 + D_{1\,ad} = -(D_2 + D_{2\,ad}). \tag{9}$$

After substituting values of D_1 and D_2 in (9) and appropriate transformations we obtain:

$$\operatorname{ctg}\alpha' = \frac{k_1 I_1 \cos\varphi}{k_2 I_2 \sin\varphi \sin\beta}\left[1 + \frac{D_{1\,ad}}{k_1 I_1 \cos\varphi \sin\alpha} - \frac{D_{2\,ad}}{k_2 I_2 \sin\varphi \sin(\beta-\alpha)}\right] + \operatorname{ctg}\beta. \tag{10}$$

Since $D_{1\,ad}$ and $D_{2\,ad}$ are normally much smaller than D_1 and D_2, the value of α can be first found from (4) and substituted in (10).

The effect of such additional turning moments causes an extra deflection of the moving part of the instrument by the angle:

$$\Delta\alpha = \alpha' - \alpha.$$

$\Delta\alpha$ can be calculated from the expression

$$D_{ad} = D_{res}\Delta\alpha,$$

whence

$$\Delta\alpha = \frac{D_{ad}}{D_{res}}, \tag{11}$$

where D_{res} is the specific restoring moment at the given point of the scale [3];

$$D_{ad} = D_{1\,ad} + D_{2\,ad}.$$

Let us now examine the effect of additional turning moments due to mutual inductance between the stationary and moving coils. In ordinary two-winding phase meters, mutual inductance errors attain considerable values even at the supply frequency; hence, these meters cannot be used for any higher frequencies.

Let us determine the value of this error for Pratt's circuit. For this purpose let us calculate the additional turning moments $D_{1\,m}$ and $D_{2\,m}$, due to mutual inductance and acting on coils S_1 and S_2, respectively.

$$D_{1\,m} = k_1 I_{1m} I \sin\theta_1 \sin\alpha = -\omega I^2 \frac{M_1}{r_1} \sin\theta_1 \sin\alpha, \tag{12}$$

$$D_{2\,m} = \omega I^2 \left[k_L M_L \frac{1}{Z_L} \sin\theta_L - k_c M_c \frac{1}{Z_c} \sin\theta_c \right] \sin(\beta - \alpha), \tag{13}$$

where M_1, M_L and M_c are values of mutual inductance between the stationary and the corresponding moving coils, and θ_1, θ_L and θ_c are the phase angles between the mutual inductance emf's and the corresponding currents caused by these emf's (Fig. 6).

Since the coil S_1 circuit is resistive, $\theta_1 = 0$ and hence $D_{1\,m} = 0$.

In order to obtain frequency stability within certain limits and eliminate mutual inductance errors in Pratt's phase meters, the following conditions must be fulfilled [3]:

$$k_L = k_c; \quad |Z_L| = |Z_c|; \quad \theta_L = -\theta_c \simeq \frac{\pi}{2} \tag{14}$$

Since $M_L = k_L a$ and $M_c = k_c a$, equality $M_L = M_c$ will hold, and the expression in brackets of formula (13) will equal zero, i.e., $D_{2\,m} = 0$.

Theoretically, therefore, (since $D_{1\,m} = 0$ and $D_{2\,m} = 0$) there will be no mutual inductance error in three-winding phase meters. Conditions (14), however, cannot be strictly observed owing to purely technical reasons.

Let us assume that quantity $k_L M_L \frac{1}{Z_L} \sin\theta_L$ differs from quantity $k_c M_c \frac{1}{Z_c} \sin\theta_c$ by 20%. Then, considering that $\theta_L \simeq -\theta_c \simeq \frac{\pi}{2}$ and that $M_L = M_{Lm} \sin\alpha$ (M_{Lm} is the maximum value of mutual inductance occurring when the direction of the coil axes coincide), we obtain from (13):

$$D_{2m} = \omega I^2 \left(0{,}2 k_L M_{Lm} \frac{1}{Z_L}\right) \sin\alpha \sin\left(\beta - \alpha\right).$$

By substituting the values of $D_{1\,m}$ and $D_{2\,m}$ in (10) we obtain:

$$\operatorname{ctg}\alpha' = k \frac{\operatorname{ctg}\varphi}{\sin\beta} \left[1 - \frac{\omega I^2 \sin\alpha \sin(\beta - \alpha)\, k_L M_{Lm} \frac{1}{Z_L} \cdot 0{,}2}{k I_1 I \sin\varphi \sin(\beta - \alpha)} + \operatorname{ctg}\beta \right]. \tag{15}$$

The Table gives mutual inductance errors for ELF-1 phase meter (nominal frequency of 500 cps) determined from (15).

TABLE

φ	−60°	−45°	−30°	−15°	0°	15°	30°	45°	60°
α	−45°	−30°	−18,27°	−8,50°	0°	8,50°	18,27°	30°	45°
Δα	−0,13°	−0,10°	−0,05°	−0,02°	0,00°	0,02°	0,05°	0,10°	0,13°

It will be seen that the mutual induction error at 500 cps does not exceed 0.13°, whereas in two-winding phase meters ELF, at as low a frequency as 50 cps, it reaches 0.33° as calculated from formula given in [2].

Conclusions. 1. As compared with normal double coil, two-winding phase meters, the three-winding meters have the advantage that their readings hardly depend on frequency variations within certain limits. Thus, for instance, a frequency change of ± 10% produces an error, in the three-winding phase meter examined, not exceeding 0.45°, whereas in the two-winding phase meter, a similar error attains 6.25°.

2. The use of normal double coil electrodynamic phase meters at frequencies higher than the supply frequency is made difficult by the substantial mutual inductance error. The Pratt circuit is theoretically free from such errors; in practice it is impossible to eliminate these errors completely; however they are reduced to insignificant values (for instance in the ELF-1 phase meter the mutual inductance error does not exceed 0.2°).

LITERATURE CITED

[1] V. O. Arutiunov, Electrical Radio Meters [in Russian] (GEI, 1956).

[2] A. D. Nesterenko, Collection of Works of the Electrotechnical Institute [in Russian] (AN UkSSR press ed. 12, 1955).

[3] E. S. Polishchuk, Bulletin of the Kiev Order of Lenin Polytechnical Institute [in Russian] (v. XXII, 1957).

DESIGN OF TUNED CIRCUITS FOR FREQUENCY-METERS OF SUPPLY FREQUENCY

M. L. Fish

It is often expedient to select and calculate circuits for supply-frequency frequency-meters, which use as their frequency-sensitive element a series tuned circuit, consisting of an induction coil and capacitor, on the basis of power relations which provide a graphic expression for various interrelated requirements of the instrument [1-5].

In this article we examine principles for a rational design of a tuned circuit, which is one of the basic elements of an industrial-frequency resonance type frequency-meter.

The analysis of power relations and calculations on their basis of frequency meter circuits give in each concrete case a fixed value for the product QP_L, in which both factors are determined by the construction of the tuned circuit induction coil and the method of its use in the instrument (Q is the quality factor and P_L the reactive power of the coil).

A rational design method should provide on the basis of a given QP_L a minimum size, weight and cost for the coil and hence the capacitor, and at the same time limit inductance L variations caused by the supply voltage fluctuations, temperature changes, etc.

Ferromagnetic cores have to be used with the coils in question in order to obtain a large P_L with a small coil size. The core, however, is always provided with an airgap which stabilizes the coil inductance, although it does increase the reluctance of the core.

It is obvious that the higher the precision of frequency measurement required, the greater must the accuracy of inductance stabilization be made. In fact the relative change in the tuned frequency $\frac{\Delta\omega_0}{\omega_0}$ is always equal to half the relative change in inductance $\frac{\Delta L}{L}$ which produced it. The effect on the instrument produced by the change in the tuned frequency is the same as that produced by the measured frequency. Hence in every concrete case it is important to be able to determine the value of the airgap in the core.

Design method. The reactance of the coil with an airgap δ (in cm) can be calculated from the formula

$$x_L = \omega L = \frac{0.4\,\pi\,W^2\,\omega\cdot 10^{-8}}{\frac{l_c}{\mu_\sim S_c} + \frac{\delta}{S_c}}, \qquad (1)$$

where ω is the nominal frequency, sec^{-1},

W the number of turns in the winding,

$\mu_\sim$ the dynamic permeability of the core magnetic material,

l_c the length of the mean magnetic line of force, cm, and

S_c is the cross section of the core, cm^2 (Fig. 1).

Considering that the voltage across a high-Q coil is practically sinusoidal, it is possible to assume that $\mu_\sim$ provides quite a satisfactory characteristic of the coil reactance.

At a certain value of flux density in the core, $\mu_\sim$ attains a maximum (see the curves of $\mu_\sim$ plotted against B_m, the amplitude of flux density, for steels type KhVP and EChAA in Fig. 2).

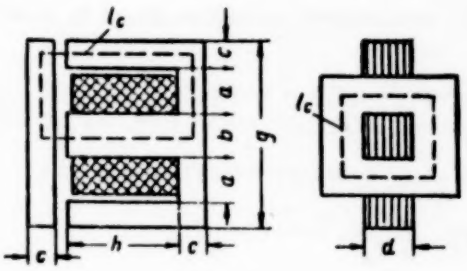

Fig. 1.

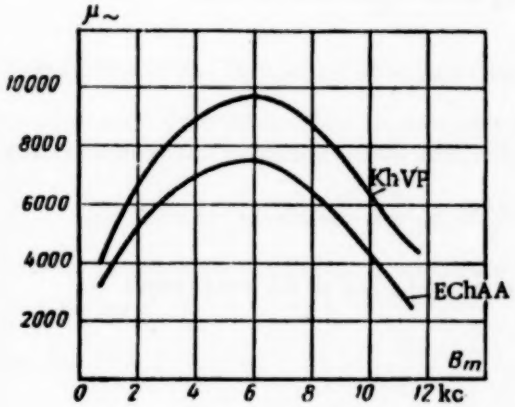

Fig. 2.

The operation of the coil at $\mu_\sim = \mu_{\sim max}$ will not only provide a maximum induction but will also ensure a stable x_L with variations of supply voltage (variations of B_m are proportional to those of the supply voltage and the $\mu_\sim$ characteristic with respect to B_m is flat at $\mu_{\sim max}$). Hence the choice of this operating condition is completely justified.

The stabilizing action of the airgap rises with an increase in the ratio $\frac{\delta\mu_\sim}{l_c}$. In fact from (1) it is easy to obtain that

$$\frac{\Delta L}{L} = \frac{\Delta x_L}{x_L} \simeq \frac{\Delta \mu_\sim}{\mu_\sim} \cdot \frac{1}{1+\frac{\delta\mu_\sim}{l_c}}. \qquad (2)$$

Let us denote $K_c = 1 + \frac{\delta\mu_\sim}{l_c}$ as the magnetic circuit stabilization coefficient.

Then (1) will acquire the form

$$x_L = \frac{0.4\,\pi\,W^2\omega\cdot 10^{-8}}{K_c} \cdot \frac{\mu_\sim S_c}{l_c}.$$

In order to determine the design value of K_c, required to stabilize the inductance for changes in the supply voltage U by a given amount ΔU, it is first necessary to calculate the

corresponding variation of flux density $\Delta B_m \simeq \frac{\Delta U}{U} B_m$.

For any shape of the curve $\mu_\sim = f(B_m)$ it is easy to find from the graph values of $\Delta\mu_\sim$, corresponding to ΔB_m and calculate K_c from (2):

$$|K_c| = \frac{1}{2} \cdot \frac{\Delta\mu_\sim}{\mu_\sim} \cdot \frac{1}{\frac{\Delta\omega_0}{\omega_0}}. \tag{3}$$

Numerical values for K_c can also be obtained experimentally for a given material in accordance with the permissible value of $\frac{\Delta\omega_0}{\omega_0}$ (i.e., $\frac{\Delta L}{L}$).

The reactive power of the coil at resonance $P_L = I_0^2 x_L$ (I_0 is the current in the coil at resonance) can be expressed by using (1a) as:

$$P_L = (I_{0\max} W)^2 \frac{0.4\pi\mu_\sim S_c \omega}{2 K_c l_c \cdot 10^8},$$

where $I_{0\max}$ is the amplitude of I_0.

Substituting for the ampere-turns $I_{0\max} W$, their value obtained from $\frac{\frac{0.4\pi I_{0\max} W}{K_c l_c}}{\mu_\sim} = B_m$, we finally have

$$P_L = \frac{B_m^2 K_c \omega V_c \cdot 10^{-8}}{0.8\pi\mu_\sim}, \tag{4}$$

where $V_c = l_c S_c$ is the volume of the core, cm^3.

The losses in the coil consist of the losses in the core P_c and those in the winding P_M. Since B_m is determined by the choice of the core material, power $P_{c\,sp}$ dissipated per unit volume can be calculated by usual formulae, and the total loss in the core from formula

$$P_c = P_{c\,sp} V_c. \tag{5}$$

The power losses in the winding are:

$$P_M = I_a^2 \rho \frac{l_{av} W}{q} = (I_{0m} W)^2 \frac{\rho l_{av}}{2 S_M},$$

where l_{av} is the length of a mean winding turn, cm,

$S_M = qW$ the copper cross section in the winding port, cm^2 (q is the copper cross section of the conductor), and

ρ is the resistivity of copper, ohms cm^2/cm.

Similarly to (4) we obtain:

$$P_M = \frac{B_m^2 K_c^2 V_c^2 V_M \rho}{0.32\pi^2 S_M^2 S_c^2 \mu_\sim^2} \tag{6}$$

($V_M = l_{av} S_M$ the volume of copper in the winding).

The Q of the coil is equal to the ratio of the reactive power P_L to the sum of the power losses

$$Q = \frac{P_L}{P_M + P_c}, \tag{7}$$

Introducing notation $Q_c = \frac{P_L}{P_c}$ and $Q_M = \frac{P_L}{P_M}$ it is possible to write (7) in the form

$$Q = \frac{1}{\frac{1}{Q_c} + \frac{1}{Q_M}}.$$

Obviously Q increases with either Q_c or Q_M.

According to (4), (5) and (6)

$$Q_M = \frac{0.4\ \pi\ \omega\ \mu_\sim S_M^2\ \ S_c^2 \cdot 10^{-8}}{K_c\ V_c\ V_M\ \rho}. \tag{8}$$

$$Q_c = \frac{B_m^2\ K_c\ \omega \cdot 10^{-8}}{0.8\pi\mu_\sim P_{c\cdot sp}}. \tag{9}$$

Q_c does not depend on the volume of the core V_c or that of the winding V_M, but only depends on the properties of the ferromagnetic material (B_m, $\mu_\sim$, $P_{c\ sp}$) and the choice of K_c.

Q_M depends on the size of the coil, being proportional to the square of the linear dimensions. If the dimensions increase proportionately and $C_1 = \frac{l_{av}^2}{S_M}$ and $C_2 = \frac{l_c^2}{S_c}$ remain constant, it becomes possible to write that

$$S_M = \left(\frac{V_M^2}{C_1}\right)^{1/3} \& \ S_c = \left(\frac{V_c^2}{C_2}\right)^{1/3}.$$

Taking this into consideration we obtain

$$Q_M = \frac{0.4\ \pi\omega \cdot 10^{-8}\ \mu_\sim}{K_c\ \rho} \cdot \frac{(V_M\ V_c)^{1/3}}{(C_1\ C_2)^{2/3}}. \tag{8a}$$

From the comparison of (7a), (9) and (8a) it is clear that an increase in the size of the coil above the value when Q_M becomes greater than Q_c is not expedient, since any further increase in Q_M will hardly affect Q.

Having obtained an expression for P_L and Q in terms of the coil parameters, it easy to find QP_L:

$$QP_L = \frac{\frac{1}{2\rho} B_m^2 \omega^2 V_c^2 \cdot 10^{-16}}{\frac{3{,}15\ P_{c\cdot sp}}{\rho\ B_m^2}\left(\frac{\mu_\sim}{K_c}\right)^2 + \frac{(C_1\ C_2)^{2/3}}{(V_M\ V_c)^{1/3}}}. \tag{10}$$

This expression can be used for a rational choice of the coil parameters.

In practice it is necessary to remember the limitations imposed by the heating of the winding, and the use of a certain type of capacitor in the tuned circuit.

By introducing in expression $B_m = \frac{0.4\ \pi\ I_{0\ max} W}{K_c l_c / \mu_\sim}$ the permissible winding current density j, a/cm^2, it is possible to check the feasibility of using core laminations of a given size and shape for a value of B_m at which $\mu_\sim = \mu_{\sim\ max}$:

$$B_m = \frac{0.4\ \pi \sqrt{2}\ \mu_\sim\ j\ S_M}{K_c\ l_c}. \tag{11}$$

Since capacity instability is as undesirable as inductance instability, the most stable capacitors are used in the frequency meter despite their relatively high cost and large size. The capacity of the condensers must be such that their reactive power is equal to $\frac{CU_{co}^2}{2} = P_L$ at resonance. In order to be able to decrease the capacity of the condenser, the voltage across it at resonance must be made sufficiently large. The choice of a nominal voltage across the condenser (not larger than half the breakdown voltage) will also determine the voltage across the coil. Since the voltage across the coil is usually substantial, its insulation and the method of winding require special consideration.

In designing the coil it is important to choose the core of a shape which would facilitate a constant airgap. In this respect the construction shown in Fig. 1 has certain disadvantages.

It should be noted that the formulae given above hold (or can be easily corrected to hold) for other normally used core shapes.

Recommended method of calculations. Above considerations lead to a certain technique in calculating the parameters for the tuned circuit components and in choosing design dimensions of the coil.

1. Determining QP_L on the basis of power relationships in the instrument [1, 2].

2. Determining from the graph $\mu_{\sim} = f(B_m)$ the values of $\mu_{\sim}\,\text{max}$ and $B_{m\,opt}$ (corresponding to $\mu_{\sim}\,\text{max}$ for a given core material) and calculating $P_{c\,sp}$.

3. Calculating on the basis of the required meter accuracy the permissible value for $\frac{\Delta\omega_0}{\omega_0}$ and the value of coefficient K_c for the condition $\frac{\Delta U}{U} = \pm 10\%$ (GOST 1845-52) (State Standard 1845-52).

4. Determining from (10) the value of QP_L on the basis of tentative dimensions of the core and windings. If the value thus obtained is smaller than the one required by para 1, the design size of the coil is increased and a new QP_L calculated. The QP_L finally obtained should not exceed by a large amount the required value, since this would involve an unnecessarily large size and cost of the coil and the condenser.

5. Checking by means of (11) the current density and if required the heating conditions of the coil.

6. Calculating the reactive power P_L by means of (4).

7. Selecting a type of condenser and a value of U_{co} (about 0.5-0.4 of the breakdown voltage) and determining the required capacity C, inductance and the number of turns of the winding by the formulae:

$$C \simeq \frac{P_L}{\omega_0 U_{c0}^2}, \quad L \simeq \frac{U_{cn}^2}{\omega_0 P_L},$$

$$W = 0{,}9 \cdot 10^4 \sqrt{\frac{LK_c l_c}{\mu_{\sim}\,\text{max} S_c}}.$$

8. Design calculation of the winding on the basis of the value obtained for W.

9. Calculation of the airgap

$$\delta = (K_c - 1)\frac{l_c}{\mu_{\sim}\,\text{max}}$$

Example of calculations. Calculation of a tuned dircuit for a frequency meter class 0.1 with a frequency range of 50 ±1 cps $QP_L = 100$.

For core material EChAA steel was used. According to graph of Fig. 2 $\mu_{\sim}\,\text{max} = 7600$ with $B_{m\,opt} = 5300$ gauss and $P_{c\,sp} \simeq 1$ w/kg.

Having chosen a value for $\frac{\Delta\omega_0}{\omega_0} = 3 \cdot 10^{-4}$ corresponding to an error of 0.015 cps (basic error 0.05 cps) we obtain from (3):

$$K_c = \frac{1}{2} \cdot \frac{200}{7600} \frac{1}{3 \cdot 10^{-4}} \simeq 44.$$

Having selected laminations Sh-18 with core dimensions a = b = d = 1.8 cm, c = 1.1 cm, h = 2.7 cm, g = 7.6 cm, we obtain $S_M \simeq 2$ cm^2 (taking the stacking factor into consideration), $l_{av} = 14.4$ cm, $V_M = 28.8$ cm^3, $l_c = 14.1$ cm, $S_c = bd = 3.24$ cm^2, $V_c = 45.7$ cm^3, $C_1 = 104$, $C_2 = 61.5$.

Assuming that PEL wire ($\rho = 1.75 \cdot 10^{-6}$ $\frac{\text{ohms} \cdot \text{cm}^2}{\text{cm}}$) was used for winding the coil we obtain from (10) $QP_L \simeq$ $\simeq 78$. This is considerably smaller than the required value and therefore the size of the coil must be increased. If Sh-19 laminations are used with core dimensions a = 1.7 cm, b = 1.9 cm, d = 1.2 cm, h = 4.6 cm, g = 7.7 cm, the constructional parameters of the coil will be: $S_M \simeq 3.9$ cm^2, $l_{av} = 14.6$ cm, $V_M = 57$ cm^3, $l_c = 18.1$ cm, $S_c = 3.8$ cm^2, $V_c = 69$ cm^3, $C_1 = 54.5$, $C_2 = 86$. Then QP_L attains 165 which is considerably larger than the required value.

It is expedient to return to the first sample, only increasing, for instance, d up to 2 cm. Then the values of some of the parameters will change to $l_{av} = 15.2$ cm, $V_M = 30.4$ cm, $S_c = 3.6$ cm^3, $V_c = 51$ cm^3, $C_1 = 115.5$, $C_2 =$ $= 55$. From (10) we find again that $QP_L \simeq 92$.

These coil dimensions can be considered satisfactory.

From (11) we obtain that $j = 1.2$ a/mm^2 which is quite permissible.

From (4) we obtain $P_L = 10.3$ w.

KSG type capacitors were used in the circuit. Assuming the voltage to be 400 v we obtain:

$$C = \frac{10.3 \cdot 10^6}{314 \cdot 400^2} \simeq 0.22 \ \mu f$$

Assuming C = 0.3 μf, we find:

$$L = \frac{1}{\omega_0^2 C} = \frac{10^6}{314^2 \cdot 0.3} = 34 \text{ henry},$$

$$W = 0.9 \cdot 10^4 \sqrt{\frac{34 \cdot 43.8 \cdot 14.1}{7600 \cdot 3.6}} \simeq 7900,$$

$$\delta = (43.8 - 1) \frac{14.1 \cdot 10}{7600} = 0.8 \text{ mm}.$$

A check of the above method of calculations has completely confirmed its ease of operation and sufficient accuracy for practical purposes.

It should be noted that the considerations outlines in this article and the formulae quoted do not apply only to supply-frequency frequency-meters. The proposed technique is valid for calculating and designing steel-cored induction coils for various tuned circuits since they are based on the aim of obtaining minimum dimensions, weight and cost for these components.

LITERATURE CITED

[1] M. L. Fish, Izmeritel'naia Tekhnika, No. 6, 1955.

[2] V. N. Mil'shtein and M. L. Fish, Works of the Penza Industrial Institute [in Russian] (ed. 2, 1954).

[3] V. N. Mil'shtein and L. M. Zaks, Izmeritel'naia Tekhnika, No. 1, 1955.

[4] L. M. Zaks, Elektrichestvo, No. 10, 1953.

[5] V. O. Arutiunov, Zh. Tekh. Fiz . No. 1, 1953.

SENSITIVITY OF BRIDGE CIRCUITS

G. K. Nechaev

Bridge circuits with a nonlinear variable arm are widely used in various measuring and automations devices. Existing methods of calculating bridge circuits do not take into account the nonlinearity of the variable arm resistance.

In this connection the article provides an analysis of the bridge sensitivity, taking into consideration the nonlinearity of the variable arm, and gives the prerequisites required for designing a bridge with optimum values for its arms from the point of view of maximum sensitivity and the best utilization of the power dissipated by the source.

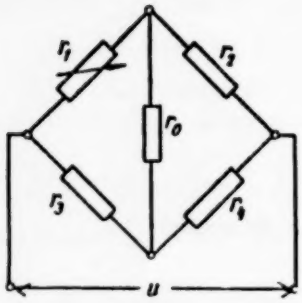

Fig. 1.

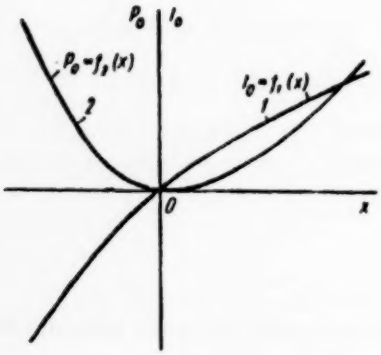

Fig. 2.

An unbalanced bridge is the most general case of a bridge circuit. Usually the relation between its output values of I_0, U_0 and P_0 and the measured quantity $\underline{x}$ is nonlinear. ($\underline{x}$ is the independent variable determining the resistance of the variable bridge arm). One of the parameters of such a circuit is its sensitivity.

As distinct from [1], in this bridge circuit two kinds of sensitivities should be considered: the differential and the mean [2].

The differential sensitivity is determined from the expression

$$S_x^I = \frac{\partial I_0}{\partial x};\quad S_x^U = \frac{\partial U_0}{\partial x};\quad S_x^P = \frac{\partial P_0}{\partial x}, \tag{1}$$

where

$$I_0 = I_0(x),\ U_0 = U_0(x) \text{ и } P_0 = P_0(x).$$

The mean sensitivity of an unbalanced bridge is related to finite variations in $\underline{x}$ and is expressed by

$$S_{x\,\mathrm{av}}^I = \frac{\Delta I_0}{\Delta x};\quad S_{x\,\mathrm{av}}^U = \frac{\Delta U_0}{\Delta x};\quad S_{x\,\mathrm{av}}^P = \frac{\Delta P_0}{\Delta x}. \tag{2}$$

Let us now find an expression for the differential sensitivity in one of the most common bridge circuits with one variable arm $r_1(x)$ (Fig. 1). The current in the measuring circuit of the bridge is represented by the relationship [3]:

$$I_0 = U\,\frac{a - r_1}{br_1 + c}, \tag{3}$$

where $a = \frac{r_2 r_3}{r_4} = r_{10}$ is the resistance of the first arm when the bridge is balanced:

$$b = \frac{(r_3 + r_4)(r_0 + r_2) + r_3 r_4}{r_4};$$

$$c = \frac{[(r_3 + r_4) r_0 + r_3 r_4] r_2}{r_4}.$$

Then the differential sensitivity with respect to current and voltage will be

$$S_x^I = \frac{\partial I_0}{\partial x} = -U\frac{ab+c}{(br_1+c)^2}r_1'; \tag{4}$$

$$S_x^U = \frac{\partial U_0}{\partial x} = -U\frac{ab+c}{(br_1+c)^2}r_0 r_1'; \tag{5}$$

$$\text{at } r_0 = \infty \; S_x^U = -U\frac{r_2 r_1'}{(r_1+r_2)^2}. \tag{6}$$

The power at the bridge output:

$$P_0 = I_0^2 r_0 = U^2\left(\frac{a-r_1}{br_1+c}\right)^2 r_0. \tag{7}$$

Sensitivity with respect to power:

$$S_x^P = \frac{\partial P_0}{\partial x} = 2I_0\frac{\partial I_0}{\partial x}r_0 = 2S_x^I I_0 r_0 = 2S_x^U I_0, \tag{8}$$

or from (3) and (5)

$$S_x^P = -2U^2\frac{(a-r_1)(ab+c)r_0 r_1'}{(br_1+c)^3}. \tag{9}$$

Here

$$r_1 = r_1(x) \;\&\; r_1' = \frac{dr_1}{dx}.$$

Let us note that the sensitivity is proportional to r_1'. Hence, from the point of view of increased sensitivity it is advantageous to use a resistance with a high value of r_1'. Thus in temperature measurements semiconductor thermosensitive resistances give a sensitivity higher by more than one order as compared with metal resistances.

The sign of the current I_0 changes as the bridge passes through the balance point (curve 1, Fig. 2) and $(S_x^I)_{I=0} \neq 0$. The power curve (curve 2) can only have positive values on either side of the balance. At $I_0 = 0$ function $P_0 = P_0(x)$ has a minimum $(P_0)_{I_0=0} = 0$ and $(S_x^P)_{I_0=0} = 0$. Let us note that curve $P_0 = P_0(x)$ is asymmetrical with respect to the vertical axis. Since at balance $r_1 = a$, the initial sensitivity (differential sensitivity at balance) with respect to current will be

$$S_{x\cdot\text{init}}^I = -\frac{U}{br_{10}+c}r_{10}', \tag{10}$$

where r_{10}' is the derivative of resistance r_1 with respect to x at bridge balance.

In a general case curve $S_x^I(x)$ can have a maximum both in the measuring range and outside it. The equation for a maximum is

$$\frac{\partial S_x^I}{\partial x} = -U(ab+c)\frac{(br_1+c)r_1'' - 2(r_1')^2 b}{(br_1+c)^3} = 0, \tag{11}$$

hence

$$br_1 + c = 2b\frac{(r_1')^2}{r_1''}. \tag{12}$$

Curve $S_x^I(x)$ has no maximum when $r_1(x)$ is linear, since in this case $r_1'' = 0$ and equation (12) does not hold.

When $r_1(x)$ is nonlinear it is possible in principle to have a maximum S_X^I within the measuring range. This may be required when it is desirable to have maximum sensitivity near the point corresponding to the nominal value of the measured quantity. [It is, however, possible that the limitations imposed by the bridge circuit will prevent the utilization of the required part of the r(x) characteristic and the achievement of the design conditions.] Such a bridge characteristic may be required both for measuring devices and in automatic control. Let us note that fulfilment of condition (11), i.e., $\frac{\partial S_X^I}{\partial x} = \frac{\partial^2 I_0}{\partial x^2} = 0$ means that the curve has a point of inflection and will, therefore, in the majority of cases cut the straight line drawn through the initial and final points of the curve, corresponding to x_1 and x_2. This is one of the condition for the function to approach a linear relationship [3].

It is very convenient to use relative units when calculating bridge circuits. In this case the bridge arm resistances should be expressed in relative units with respect to the variable arm $a = r_{10}$ at bridge balance. Then the conditions of bridge balance will be $r_{.2}\, r_{.3} = r_{.4}$ (here subscripts with points denote relative units).

By means of simple transformations and denoting $\psi = 2\frac{(r_1')^2}{r_1''} - r_1$ we obtain:

$$r_{.0} = \frac{\psi_.(r_{.2} + r_{.4}) + (\psi_. r_{.2} - r_{.4})\, r_{.2}}{(1 + r_{.2})(r_{.2} - \psi_.)}. \tag{13}$$

The values of $r_{.2}$ and $r_{.4}$ should be selected on the basis of the analysis given below, which confirms the recommendations in [4] and [5], and ensures the best power relationship in the circuit, i.e., a maximum P_0/P_1.

Thus the condition corresponding to the maximum S_X^P can be found:

$$\frac{\partial S_x^P}{\partial x} = 2 r_0 \left(\frac{\partial S_x^I}{\partial x} I_0 + \frac{\partial I_0}{\partial x} S_x^I \right) = 0 \tag{14}$$

or

$$\frac{\partial S_x^I}{\partial x} I_0 + (S_x^I)^2 = 0. \tag{15}$$

By substituting in (15) values of $I_0 S_X^I$ and $\frac{\partial S_X^I}{\partial x}$ we obtain

$$(ab + c)(r_1')^2 = (a - r_1)[(br_1 + c) r_1'' - 2b(r_1')^2] \tag{16}$$

From function $r_1(x)$ in (16) we obtain X_M and hence the required value of r_{1M}. Thus if $r(x) = r_0 + kx$ the resistance r_1 corresponding to the maximum value of S_X^P will be

$$r_{1M} = \frac{3ab + c}{2b}. \tag{17}$$

A more complicated case will be presented by a nonlinear function of r(x) as, for instance, in a thermo-sensitive resistance [3]:

$$r = Ae^{\frac{B}{T}}, \tag{18}$$

where A and B are constants of the thermo-sensitive resistance, and

T is the temperature (in degrees Kelvin).

Then (16) becomes:

$$A^2 e^{2\frac{B}{T}} - 2\left[\frac{B+T}{B-T}\frac{c}{b} + \frac{B-T}{B-2T}a\right] A e^{\frac{B}{T}} + \\ + \frac{B+2T}{B-2T}\frac{ac}{b} = 0, \tag{19}$$

whence T_M can be found for which the power sensitivity will be maximum.

Let us note that the power sensitivity can also be determined with respect to r_1 and $S_r^P = \frac{\partial P_0}{\partial r_1}$. In this case the type of functional relationship of $r_1(x)$ does not affect S_r^P.

With a linear $r_1(x)$ the value of r_{1M} (x_M) for determining $S_{x\,max}^P$ and $S_{r\,max}^P$ is the same. With a nonlinear relationship the values of r_1 M for $S_{x\,max}^P$ and $S_{r\,max}^P$ are different.

For determining r_0 which provides the values of $S_{x\,max}^P$ in the point required let us make use of (16) expressed in relative units. After transformations we obtain:

$$\frac{c_*}{b_*} = \frac{\left[1 - \Delta r_{*1}\left(r_{*1}\frac{r_1^*}{(r_1')^2} - 2\right)\right]}{\Delta r_{*1}\frac{r_{*1}^*}{(r_{*1}')^2} - 1} = \varphi_*, \tag{20}$$

where $\Delta r_{*1} = 1 - r_{*1}$.

The values of a, b and c in relative units are determined from

$$a_* = 1; \\ b_* = [(r_{*2}+1)(r_{*0}+r_{*2}) + r_{*4}]\frac{1}{r_{*2}}; \\ c_* = (r_{*2}+1)\,r_{*0} + r_{*4}. \tag{21}$$

After simple transformations we obtain

$$r_{*0} = \frac{\varphi_*(r_{*2}+r_{*4}) + (\varphi_* r_{*2} - r_{*4})r_{*2}}{(1+r_{*2})(r_{*2}-\varphi_*)}. \tag{22}$$

The values of r_{*2} and r_{*4} are selected on the basis of power considerations, i.e., in the same manner as in the preceding case.

Let us now examine the question of mean sensitivity.

The increment of current in the range of x changing from x_1 to x_2 will be:

$$\Delta I_0 = I_{02} - I_{01} = -U\frac{(ab+c)(r_{12}-r_{11})}{(br_{11}+c)(br_{12}+c)}, \tag{23}$$

and the mean sensitivity with respect to current in this region will be:

$$S_{x\,av}^I = \frac{\Delta I_0}{\Delta x} = -\frac{U(ab+c)}{(br_{11}+c)(br_{12}+c)}\frac{\Delta r_1}{\Delta x}, \tag{24}$$

where $\Delta r_1 = r_{12} - r_{11}$, $\Delta x = x_2 - x_1$.

The power increment ΔP_0 in the same range of Δx is determined by $P_0 = (I_{02}^2 - I_{01}^2)\,r_0$, and on this basis the mean power sensitivity is:

$$S^P_{x\,av} = \frac{(I_{02} - I_{01})(I_{02} + I_{01}) r_0}{\Delta x} = S^I_{x\,cp}(2I_{01} + \Delta I_0) r_0, \tag{25}$$

where $\Delta I_0 = I_{02} - I_{01}$.

At the limit when $\Delta x \to 0$, expression (25) is reduced to (8).

If the lower limit of the range corresponds to bridge balance, i.e., if $r_1 = r_{10}$ the expression for $S^I_{x\,av}$ and $S^P_{x\,av}$ assumes the form

$$S^I_{x\,av} = -\frac{U}{(br_{12} + c)} \frac{\Delta r_1}{\Delta x}, \tag{26}$$

$$S^P_{x\,av} = \frac{I^2_{02} r_0}{\Delta x} = S^I_{x\,av} I_{02} r_0. \tag{27}$$

In designing bridge circuits a high mean sensitivity over a certain range is often aimed at, in order to be able to use a less sensitive instrument. Sometimes it is required to obtain a maximum sensitivity in some given part of the measuring range. This can arise when a relay or a winding of a magnetic amplifier is connected to the output of the bridge.

In order to obtain maximum power sensitivity, it is necessary to match the resistance of the load to the bridge output and select optimum values for the resistances of the other bridge arms. The power ratio $\frac{P_0}{P_1}$ is determined by expression [4]:

$$k_P = \frac{P_0}{P_1} = \frac{r_0}{r_1} \frac{(r_2 r_3 - r_1 r_4)^2}{[r_3(r_2 + r_4) + r_0(r_3 + r_4)]^2} = \frac{\Delta r_1^2}{(r_{10} + \Delta r_1)} \frac{r_0 r_4^2}{[r_3(r_2 + r_4) + r_0(r_3 + r_4)]^2}, \tag{28}$$

or in relative units:

$$k_P = \frac{\Delta r_{\cdot 1}^2}{1 + \Delta r_{\cdot 1}} \frac{r_{\cdot 0} r_{\cdot 2}^2}{[(r_{\cdot 2} + r_{\cdot 4}) + r_{\cdot 0}(1 + r_{\cdot 2})]^2} = \frac{\Delta r_{\cdot 1}^2}{1 + \Delta r_{\cdot 1}} D. \tag{29}$$

The best k_p ratio will be obtained when D is at a maximum, and the value of r_0 corresponding to this condition is:

$$r_{\cdot 00} = \frac{r_{\cdot 2} + r_{\cdot 4}}{r_{\cdot 2} + 1}. \tag{30}$$

Then on the basis of (29) and (30) we have:

$$k_{P_0} = \frac{\Delta r_{\cdot 1}^2}{1 + \Delta r_{\cdot 1}} \frac{\left(\frac{r_{\cdot 2}}{2}\right)^2}{(1 + r_{\cdot 2})(r_{\cdot 2} + r_{\cdot 4})}. \tag{31}$$

Obviously when $r_{\cdot 2} \to \infty$, $D \to 1/4$, which corresponds to the results obtained by V. N. Mil'man and L. M. Zaks [5].

Figure 3 gives a family of curves $D = f(r_{\cdot 2})$ with r_{00} taken according to (30). These curves help to choose values for $r_{\cdot 2}$ and $r_{\cdot 4}$ and show how far from the ideal is the calculated circuit. An analysis of the curves also shows that in order to obtain as large a D as possible, $r_{\cdot 2}$ should be increased and $r_{\cdot 4}$ decreased. In designing the bridge, values for these resistances should be assumed in relative units without forgetting, however, to check the value of $r_{\cdot 3}$ and the power consumed by the circuit. In practice one should assume $r_{\cdot 2} = 2$ to 5 and $r_{\cdot 4} = 0.2$

to 0.5. Having selected these values we obtain $r_{.0}$ from (30). Since the resistance of the load in ohms is usually known, it is not difficult to determine the resistance of the variable arm at balance, i.e., to find $r_{10} = r_0/r_{.0}$. A maximum value for the mean power sensitivity in a certain range of parameter $\underline{x}$ (from x_1 to x_2) is obtained by selecting a corresponding bridge balance point.

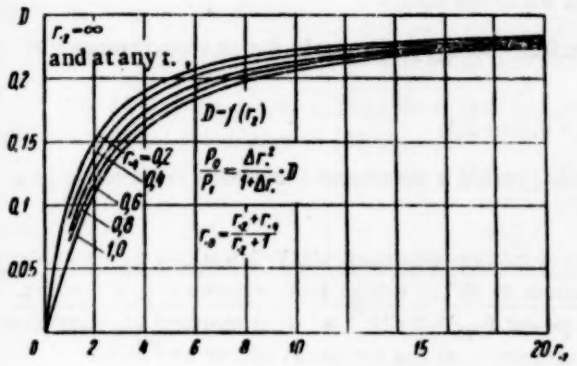

Fig. 3.

According to (3) and (25) the increment of P_0 is determined from

$$\Delta P_0 = U^2 r_0 \left[\left(\frac{a - r_{12}}{br_{12} + c} \right)^2 - \left(\frac{a - r_{11}}{br_{11} + c} \right)^2 \right]. \quad (32)$$

On the basis of the best possible utilization of the power dissipated in the variable arm r_1, it can be assumed that the maximum permissible value of current I_1 corresponds to the upper limit of $\underline{x}$.

The variable arm current is determined by

$$I_1 = U \frac{d}{br_1 + c}, \quad (33)$$

where $d = [(r_3 + r_4) r_0 + (r_2 + r_4) r_3] \frac{1}{r_4}$.

Then after transformations:

$$\Delta P_0 = I_{1M}^2 r_0 \left(\frac{a - r_{11}}{d} \right)^2 \left[\left(\frac{a - r_{12}}{a - r_{11}} \right)^2 - \left(\frac{br_{12} + c}{br_{11} + c} \right)^2 \right]. \quad (34)$$

The value of $\underline{a}$ must now be found at which ΔP_0 reaches its maximum. The values of r_2 and r_4 and sometimes those of r_0 remain unknown; they can be assumed from curves of Fig. 3 in relative units with respect to $\underline{a}$. Then equation (34) will take the form

$$\Delta P_0 = I_{1M}^2 \frac{(a - r_{11})^2}{f^2 d^2} \left[\left(\frac{a - r_{12}}{a - r_{11}} \right)^2 - \left(\frac{ka + r_{12}}{ka + r_{11}} \right)^2 \right], \quad (35)$$

where

$$f = (r_{.0} + r_{.2} + r_{.4}) \frac{1}{r_{.2}} + r_{.0};$$

$$k = \frac{r_{.0} + r_{.4} + r_{.0} r_{.2}}{\left[\left(r_{.0} + r_{.4} \right) \frac{1}{r_{.2}} + 1 + r_{.0} + r_{.2} \right]}.$$

The maximum value of $\underline{a}$ can be determined from $\frac{d(\Delta P_0)}{da} = 0$.

After transformation we shall obtain the equation:

$$a_0 a^4 + a_1 a^3 + a_2 a^2 + a_3 a + a_4 = 0, \quad (36)$$

where

$$a_0 = k^2,$$
$$a_1 = k[(1 - k) r_{12} - 2k r_{11}],$$
$$a_2 = k[(r_{11} + r_{12}) k - 4 r_{12}] r_{11},$$
$$a_3 = (3k - 1) r_{11}^2 r_{12},$$
$$a_4 = r_{11}^3 r_{12}.$$

The required positive value of $\underline{a}$ can be obtained by an approximate method by splitting (36) into two equations. By assuming several values for $\underline{a}$ it is possible to plot two curves, whose crossing point will correspond to the required value of $\underline{a}$. Calculations given below show that by this method the power increment at the output of the bridge can be increased as compared with the case when r_{11} corresponds to the balance of the bridge.

Conclusions. 1. The proposed relationships provide a method of designing a bridge curcuit with a nonlinear variable arm which has a maximum $S_{\underline{x}}^{I}$ or $S_{\underline{x}}^{P}$ at a point within the range of $\underline{x}$.

2. With a maximum of $S_{\underline{x}}^{I}$ in the middle of the $\underline{x}$ range, function $I_0(x)$ will attain the nearest approach to linearity.

3. In designing one should choose $r_{.2} = 2$ to 5 and $r_{.4} = 0.2$ to 0.5.

4. It is possible to calculate the value of r_{10} which would provide a maximum increment of power P_0 in a given range of $\underline{x}$.

Example 1. Designing of a bridge circuit with a thermo-sensitive resistance MMT-1 working as a transducer in the range of 30-50°C under condition that S_{θ}^{I} attains maximum at 40°C. Bridge load resistance is 450 ohms. Thermo-sensitive resistance has a maximum dissipated power $P_{1M} = 2 \cdot 10^{-3}$ w. It is required to determine the resistances of the bridge arms, the supply voltage and the sensitivity of the circuit at 30, 40 and 50°C.

Let us assume values for r_2 and r_4 in relative units $r_{.2} = 4$ and $r_{.4} = 0.4$.

Let us assume that the value of the thermo-sensitive resistance R_{20} at 20°C lies between 1000 and 2000 ohms. For such values $B \simeq 2000$°K.

According to (18)

$$r_1' = -\frac{B}{T^2} r_1$$

and

$$r_1^{\cdot} = \frac{B}{T^2}\left(\frac{B}{T} + 2\right) r_1,$$

Then

$$\psi = 2\frac{(r_1')^2}{r_1^{\cdot}} - r_1 = \frac{B - 2T}{B + 2T} r_1$$

or

$$\psi_{\cdot} = \frac{B - 2T}{B + 2T} r_{.1}.$$

Since T = 273 + 40 = 313°K,

then $$\psi_{\cdot} = \frac{2000 - 626}{2000 + 626} e^{\frac{2000}{313} - \frac{2000}{303}} = 0{,}436.$$

Then according to (13):

$$r_{.0} = \frac{0{,}436(4 + 0{,}4) + (0{,}436 \cdot 4 - 0{,}4) \cdot 4}{(1 + 4)(4 - 0{,}436)} = 0{,}409.$$

The resistance of the variable arm at balance will be:

$$r_{10} = \frac{r_0}{r_{\cdot 0}} = \frac{450}{0.409} = 1100 \text{ ohm}.$$

Among normally produced thermistors the nearest to this value is the one with R_{20} = 1200 ohms, R_{30} = 960 ohms, R_{40} = 790 ohms, R_{50} = 670 ohms, which we shall take for further calculations (instead of r_{10} = 1100 ohms we now have $r_{10} = R_{30}$ = 960 ohms).

The bridge arm resistances will be in ohms r_2 = 3840 ohms, r_4 = 384 ohms and r_3 = 96 ohms.

We obtain the supply voltage from the conditions that at 50°C there will be maximum power dissipation in the thermistor. According to (33):

$$U = \sqrt{\frac{P_{1M}\, r_{10}}{r_{\cdot 12}}} \cdot \frac{b.r_{\cdot 12} + c.}{d.}.$$

Here $r_{\cdot 12} = R_{50}$.

On the basis of the above formula

$$b. = 5.75;\ c. = 3.05;\ d. = 1.76;\ r_{\cdot 12} = \frac{670}{960} = 0.7.$$

Then

$$U = \sqrt{\frac{2 \cdot 10^{-3} \cdot 960}{0,7}} \cdot \frac{5.75 \cdot 0.7 + 3.05}{1.76} = 6,7 \text{ v}.$$

The sensitivity of the circuit at 30, 40 and 50°C is determined from (4):

$$S^I_{30} = \frac{U}{r_{10}} \frac{b. + c.}{(br_{\cdot 10} + c.)^2} \frac{B}{T^2_{10}} r_{\cdot 10} =$$

$$= \frac{6,7}{960} \cdot \frac{5.75 + 3.05}{(5,75 + 3,05)^2} \cdot \frac{2000}{303^2} = 17.1 \cdot 10^{-6}\ a/°C;$$

$$S^I_{40} = 17.5 \cdot 10^{-6}\ a/°C;\ S^I_{50} = 16.5 \cdot 10^{-6}\ a/°C.$$

It will be seen that S^I_{40} is the maximum, but it differs very little from the boundary values and, hence, the function $I_0(\theta)$ is approaching linearity.

Example 2. Designing a bridge circuit with a thermo-sensitive resistance as a transducer, under condition of maximum increment of load power in the range of 40 to 50°C, by means of calculating r_{10} which would correspond to the said maximum. The parameters of the thermistor are: R_{40} = 790 ohms, R_{50} = 670 ohms and at θ = 50°C, $I_{1M} = 1.22 \cdot 10^{-3}$ amp. The load resistance is r_0 = 500 ohms.

Let us assume values for bridge arms $r_{\cdot 2} = 2$ and $r_{\cdot 4} = 0.2$. Let us tentatively take the relative value of resistance r_0 as $r_{\cdot 0} = 0.2$. If the value of r_0 obtained by calculation differs considerably from the one assumed, the process must be repeated.

Let us determine the value of coefficient k

$$k = \frac{r_{\cdot 0} + r_{\cdot 4} + r_{\cdot 0}\, r_{\cdot 2}}{(r_{\cdot 0} + r_{\cdot 4}) \frac{1}{r_{\cdot 2}} + r_{\cdot 0} + r_{\cdot 2} + 1} =$$

$$= \frac{0.2 + 0.2 + 0.2 \cdot 2}{(0.2 + 0.2) \frac{1}{2} + 0.2 + 2 + 1} = 0,235.$$

The values of coefficients α will be

$$\alpha_0 = k^2 = 0.235^2 = 0.0552,$$
$$\alpha_1 = k\,[(1-k)\,r_{12} - 2\,kr_{11}] =$$
$$= 0.235\,[0.765 \cdot 0.67 - 2 \cdot 0.235 \cdot 0.79] = 0.0332,$$
$$\alpha_2 = k\,[(r_{11} + r_{12})\,k - 4\,r_{12}]\,r_{11} =$$
$$= 0.235\,[(0.79 + 0.67)\,0.235 - 4 \cdot 0.67]\,0.79 = -0.434,$$
$$\alpha_3 = (3\,k - 1)\,r_{11}^2\,r_{12} =$$
$$= (3 \cdot 0.235 - 1)\,0.79^2 \cdot 0.67 = -0.123,$$
$$\alpha_4 = r_{11}^3\,r_{12} = 0.79^3 \cdot 0.67 = 0.33.$$

The values of r_{11} and r_{12} are taken in kilohms.

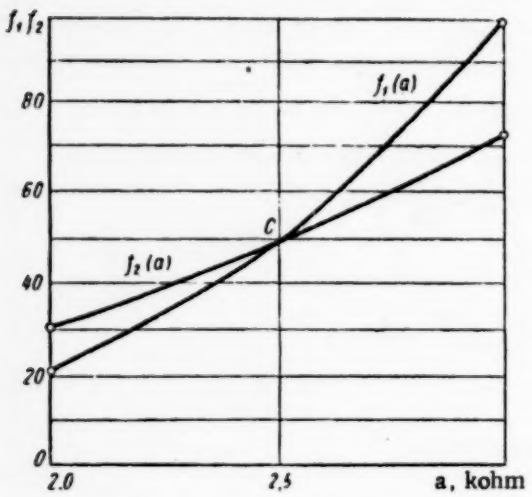

Fig. 4.

As a result of it we obtain the equation:

$$a^4 + 0{,}605\ a^3 - 7{,}85\ a^2 - 2{,}23\ a + 6 = 0.$$

This equation can be split in two

$$f_1(a) = a^4 + 0.605\ a^3,$$
$$f_2(a) = 7.85\ a^2 + 2.23\ a - 6.$$

By giving a several values, we obtain $f_1(a)$ and $f_2(a)$. The intersection of the curves (Fig. 4) gives the required value of a.

Thus $a = r_{10} = 2.5$ k ohms. Then $r_2 = 5$, $r_3 = 0.1\,a = 0.25$ kohms and $r_4 = 0.05$. The assumed value of r_0 agrees with the results obtained. For checking purposes let us calculate values of ΔP_0 by assuming according to (34) values for a. The results are given in the Table in relative units $k\Delta P_{01}$ corresponding to $a = r_{11}$.

a, kohm	0.79	1.0	2.0	2.5	3.0	4.0	5.0	6.0	7.0
$\Delta P_0/\Delta P_{01}$	1.0	3.22	6.22	6.3	6.24	5.73	5.5	5.03	4.62

The maximum of ΔP_0 corresponds to the calculated value of a. Thus, by choosing an optimum value for a, the increment of the power in the load is considerably increased.

LITERATURE CITED

[1] M. A. Kaganov, Izmerital'naia Tekhnika, No. 2, 1956

[2] A. D. Nesterenko, Foundations of the Design of Balanced Electrical Measuring Circuits [in Russian] (Kiev, 1953).

[3] G. K. Nechaev, Doklady Akad. Nauk SSSR, v. 96, No. 1, 1954.

[4] G. K. Nechaev, Collection of Works of the Electrotechnical Institute of the Acad. Sci. UkSSR [in Russian] (ed. 12, 1955).

[5] V. N. Mil'shtein and L. M. Zaks, Izmerital'naia Tekhnika , No. 1, 1955.

HIGH AND ULTRAHIGH FREQUENCY MEASUREMENTS

REFERENCE DIODE COMPENSATION VOLTMETER

B. E. Rabinovich and A. M. Fedorov

The VNIIM (All-Union Scientific Research Institute of Measurements) developed a reference diode compensation voltmeter OKV-2 for measuring voltages from 25 mv to 100 v in the range of 30 cps to 300 Mc based on a balancing method of measuring voltages [1, 2] which does not require calibration against reference ac instruments. The accuracy of the instrument is determined by that of the standard cell emf, incorporated in the set, and the accuracy of resistances in the dc circuit.

The theory of the measuring method and the schematic of the voltmeter are given below.

The diode voltampere characteristic in the region of small currents obeys the exponential law:

$$i = Ge^{KU}, \tag{1}$$

where i is the diode current at voltage U,
G the diode current at voltage U = O, and
K is a diode parameter related to the cathode temperature and determined experimentally.

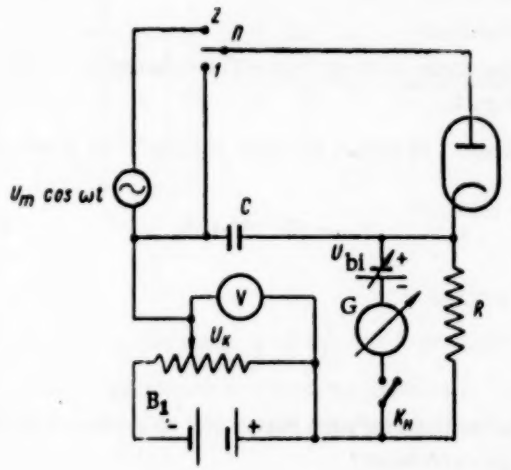

Fig. 1.

If the sum of a sinusoidal voltage of amplitude U_m and a dc bias voltage U are fed to the diode, the instantaneous current value will be expressed by:

$$i = Ge^{(KU_m \cos \omega t - KU)}. \tag{2}$$

The mean value of this current is:

$$i_0 = \frac{1}{2\pi}\int_0^{2\pi} Ge^{-KU} e^{KU_m \cos \omega t}\, d\omega t = Ge^{-KU} I_0(KU_m), \tag{3}$$

where $I_0(KU_m)$ is the Bessel function of order zero of an imaginary variable.

Two methods of measurement are used in voltmeter OKV-2 based on relationships (1) and (3): the method of a constant mean diode current used at large voltages and the method of a constant bias used at small voltages.

Constant mean diode current method. The schematic of this method is given in Fig. 1.

Position 1 of switch S is used for "zero setting." At first the bias voltage U_K is set to zero and the diode takes current:

$$i_{a1} = Ge^{-Ki_{a1}R}. \tag{4}$$

Next such an initial bias is chosen

$$U_{bi} = i_{a1}R, \tag{5}$$

that on pressing push button K_H no current will flow through the galvanometer. Then switch S is thrown to position 2 for measuring. The current through the diode rises. By applying an additional bias U'_K it is possible to obtain the same mean current i_{a2} through the diode as in the first operation. Then there will be no current flowing through the galvanometer. The mean value of the current through the diode will be:

$$i_{a2} = Ge^{-K\left(U_{bi}+U'_K\right)} I_0(KU_m) \tag{6}$$

and

$$i_{a1} = i_{a2}. \tag{7}$$

It is possible to obtain from (4), (5) and (6), and taking into consideration (7), the relation between the amplitude of the measured voltage and the increase in bias U'_K:

$$\frac{U'_K}{U_m} = \frac{\ln I_0(KU_m)}{KU_m}. \tag{8}$$*

The correction $\Delta U' = U_m - U'_K$, which should be added to U'_K in order to obtain U_m, can be found from expression

$$K\Delta U' = K\left(U_m - U'_K\right) = KU_m - \ln I_0(KU_m). \tag{9}$$

Relationship (9) can be represented graphically [2] or in the form of a Table (the latter is adopted in voltmeter OKV-2) as a function of variable KU'_K.

In fact

$$KU'_K = \ln I_0(KU_m). \tag{10}$$

Hence the correction, which is a function of KU_m (9), can be represented as a function of KU'_K.

Thus by determining experimentally U'_K and K the corresponding value of $\Delta U'$ is found, by means of which U_m is easily obtainable.

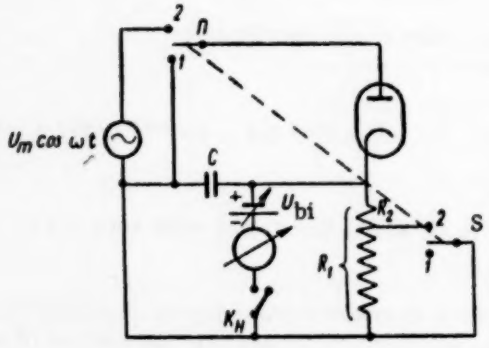

Fig. 2.

Constant diode bias method. The schematic of this method is shown in Fig. 2.

In position 1 of switch S ("zero setting") the diode takes current:

$$i_{a1} = Ge^{-KI_{a1}R_1}. \tag{11}$$

Such a bias voltage

$$U_{bi} = i_{a1}R_1, \tag{12}$$

is chosen that on pressing push button K_H no current will flow through the galvanometer.

Next switch S is thrown to position 2 for measurement. The diode current decreases. The resistance in the cathode circuit is decreased to value R_2, when there is no current flowing in the galvanometer:

$$i_{a2}R_2 = U_{bi} \tag{13}$$

The mean value of the current is then equal to

* $\ln = \log_e$.

$$i_{a2} = Ge^{-KU_{bi}} I_0(KU_m). \tag{14}$$

It follows from (11), (12), (13) and (14) that

$$\frac{i_{a2}}{i_{a1}} = I_0(KU_m) = \frac{R_1}{R_2}, \tag{15}$$

whence

$$I_0(KU_m) = \frac{R_1}{R_2}. \tag{16}$$

It will be seen from (16) that at a certain value of the diode parameter K the amplitude of the measured voltage U_m is determined entirely by a ratio of resistances in the cathode circuit. Hence, with a definite K (in set OKV-2, K = 10) and R_1, the value of the voltage is determined by the value of the single resistance R_2.

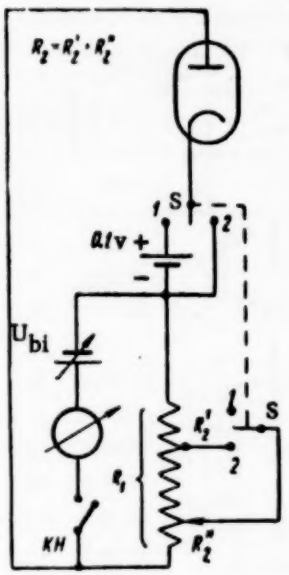

Fig. 3.

Determining diode parameter K. This parameter can be determined experimentally from two points on the voltampere characteristic. For this purpose the ratio of two diode currents corresponding to two values of the bias voltage are measured

$$\frac{i_{a1}}{i_{a2}} = e^{-K(U_1 - U_2)}. \tag{17}$$

Whence

$$K = \frac{\ln \frac{i_{a1}}{i_{a2}}}{U_2 - U_1} = \frac{2{,}3 \lg \frac{i_{a1}}{i_{a2}}}{U_2 - U_1}. \tag{18}$$

The schematic used for determining parameter K is shown in Fig. 3.

In position 1 of switch S the diode current is:

$$i_{a1} = Ge^{-K(i_{a1}R_1 + 0{,}1)} = Ge^{-KU_1}. \tag{19}$$

The bias voltage

$$U_{bi} = i_{a1}R_1, \tag{20}$$

is adjusted so that there is no current flowing through the galvanometer.

Next the switch is thrown to position 2. Resistance R_2 is adjusted to such a value that on pressing push button K_H there is no current flowing in the galvanometer, which corresponds to condition:

$$i_{a2}R_2 = U_{bi} \tag{21}$$

The current flowing through the diode will then equal to

$$i_{a2} = Ge^{-Ki_{a2}R_2} = Ge^{-KU_2} \tag{22}$$

It will be seen from (19), (20), (21) and (22) that

$$U_2 - U_1 = 0{,}1 \text{ v} \tag{23}$$

and

$$\frac{I_{a1}}{I_{a2}} = \frac{R_2}{R_1}. \tag{24}$$

Then

$$K = \frac{2{,}3 \lg \frac{R_2}{R_1}}{0{,}1}. \tag{25}$$

It will be seen from (25) that with the help of the circuit shown in Fig. 3 the parameter of the diode is determined in terms of the ratio R_2/R_1 of resistances. Since R_1 = const, the variable part R_2'' of resistance R_2 can be calibrated in terms of the diode parameter K.

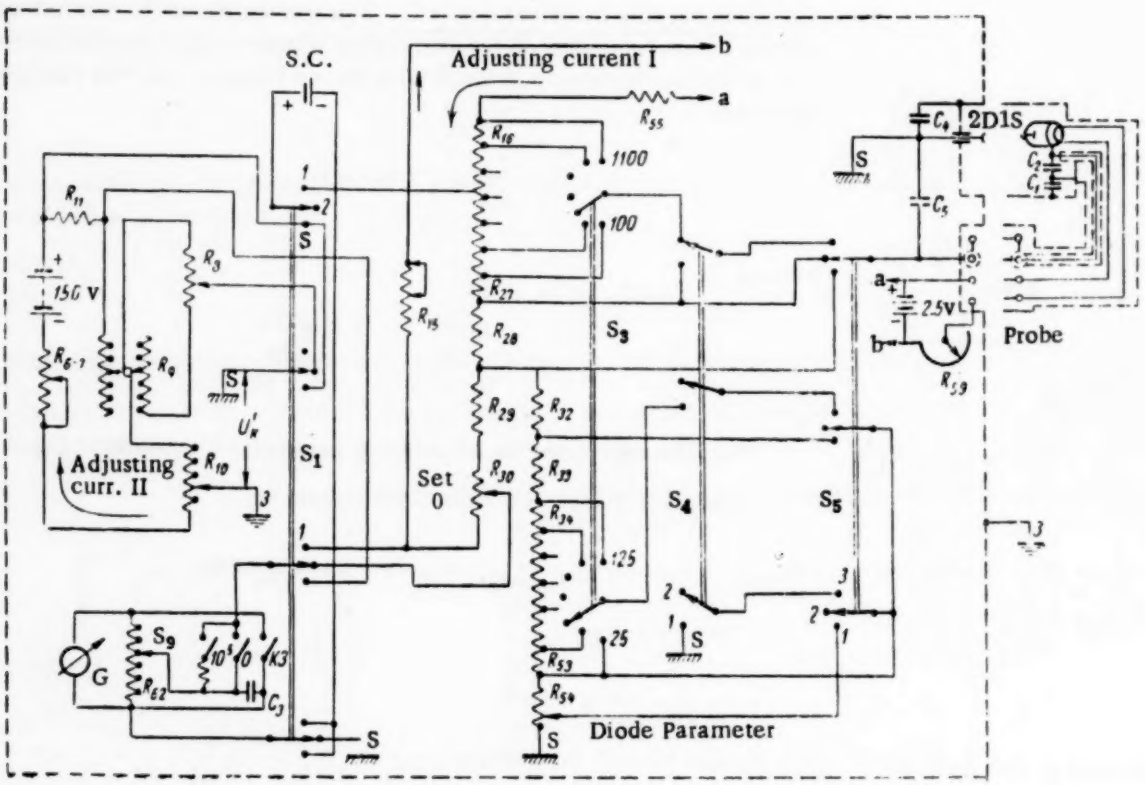

Fig. 4.

Voltmeter schematic. In the actual voltmeter circuit (Fig. 4) the bias voltage U_{bi} and the compensation voltage U_K are obtained from potential drops across standard resistances with the current through them adjusted by means of a standard cell in a manner similar to the one used in dc potentiometers. Variations in the bias and compensation voltages are made by means of changes in the standard resistances.

The bias voltage is obtained from the voltage drop produced by 1 ma flowing through resistances R_{16} to R_{30} and is taken off resistor R_{29} and the upper end of variable resistor R_{30}. The same current produces a drop of 0.1 v across R_{28}. Cathode resistors R_{32} to R_{54} serve to balance the bias voltage. In the position "diode parameter" the operation selecting switch establishes appropriate connection, leaving in the cathode circuit only resistor R_{32} and part of the variable resistor R_{54} corresponding to R_2' and R_2'' of Fig. 3. The dial of R_{54} is calibrated in diode parameter values.

For convenience of operation it is recommended to set the value of this parameter at 0.1 K = 1.000 ±0.001. This is done by adjusting the diode heater current.

It has been pointed out that the voltmeter uses two methods of measurement, those of the constant mean diode current and constant bias. By the first method effective sinusoidal voltages in the range of 0.1 to 100 v are measured. In this case the balancing voltage is taken off calibrated resistances R_8, R_9 and R_{10} carrying a current of 14.14 ma adjusted by means of the standard cell. The "multiply" switch reduces this current to 0.1 or 0.01 of its initial value thus reducing the compensating voltage in the same ratio.

The readings of R_8, R_9 and R_{10} are calibrated in effective voltage values so that the voltage U'_K actually produced by them is $\sqrt{2}$ times greater than the voltage U_K indicated on their dials. The measurement results are calculated by the formula

$$U_x = U_K + \Delta U, \tag{26}$$

where U_X is the effective value of the measured voltage,
ΔU the correction obtained from the table, and
U_K is the indication of the dials of R_8, R_9 and R_{10}.

Column A of the Table shows the values of product U_K (0.1K), column B the corresponding values of the correction and column C the correction differences per volt.

Correction Table

A, V	B, V	C, V	A, V	B, V	C, V	A, V	B, V	C, V	A, V	B, V	C, V
0.02	0.05787		0.15	0,10771		0.90	0.1602		7.0	0.229	
		0,909			0.156			0.035			0,004
0.03	0.06696		0.20	0,11552		1,00	0.1637		8.0	0.233	
		0,690			0.125			0.026			0.003
0.04	0 07386		0.25	0,12178		1.5	0.1767		9,0	0.236	
		0.549			0.105			0.019			0.003
0.05	0.07935		0.30	0.12701		2.0	0.1861		10	0,239	
		0.457			0,089			0.015			0,0026
0.06	0.08392		0.35	0.13147		2.5	0,1938		20	0,265	
		0,393			0.079			0,012			0.0012
0.07	0,08785		0.40	0.1354		3,0	0,1999		30	0.277	
		0.343			0.070			0.009			0,0010
0.08	0.09128		0,45	0.1389		3.5	0.2046		40	0.287	
		0,302			0.062			0,009			0.0010
0.09	0,09430		0.50	0.1420		4.0	0.2093		50	0.297	
		0.276			0.054			0.008			0.0005
0.10	0.09706		0.60	0.1474		4,5	0,2132		100	0.32	
		0.249			0.049			0.008			0.0002
0 11	0.09955		0,70	0,1523		5 0	0,217		200	0 34	
		0.230			0.042			0.006			
0.12	0.10185		0.80	0.1565		6.0	0,223				
		0.195			0.037			0.006			

The method of obtaining the correction is as follows.

1. It is determined from measurement that

$$A' = U_K\,(0.1K).$$

2. The value of A nearest to A' on the low side and corresponding values of B and C are found from the table. The error is calculated from

$$\Delta U = \frac{B + (A' - A)C}{0,1K}.$$

It will be seen that with 0.1 K = 1 the calculation is greatly simplified.

The voltmeter can also measure set value voltages in multiples of 100 mv in the range of 100 mv to 1100 mv. This method is convenient for calibrating instruments at fixed points and it is also based on the constant mean diode current method.

The set values of the compensating voltage are produced across the calibrated resistors R_{16} to R_{26} carrying a current of 1 ma.

Set voltages in multiples of 5 mv in the range of 25 to 125 mv are measured by means of the second method.

When the second method of measurement is used cathode resistors R_{34} to R_{54} are shorted and the cathode circuit resistance decreased [see (16)].

When measuring voltages which are not multiples of 5 mv the galvanometer is not brought back to zero; in this instance a linear interpolation of the galvanometer scale is used.

The second method is used for measuring small voltages, in particular for checking the reference output voltages of standard signal generators.

In order to provide a path for the ac component of the detected current capacitors C_3, C_4 and C_5 and constructional capacitances C_1 and C_2 in the diode probe are provided.

Construction and basic characteristics of the instrument. The voltmeter (Fig. 5) is mounted in a metal container 650 × 450 × 400 mm, whose front panel carries the control of the instrument.

The voltmeter is fed by one storage battery 2NKN-45 and two dry anode batteries BAS − G-80 − L-2,1, mounted in the set and easily accessible.

The voltmeter will measure sinusoidal voltages from 25 mv to 100 v in the range of 30 cps to 300 Mc. The basic error of measurement at low frequencies does not exceed $\pm(0.2 + \frac{0.08}{U_x})$ % where U_x is the measured voltage in volts.

The error is referred to a percentage of the measured value and not the full scale deflection, which is especially valuable for a reference voltmeter.

The variation of readings with frequency is determined by the type of diode chosen (2D1S) and the construction of the probe, which hardly reduces the natural resonance frequency of the diode.

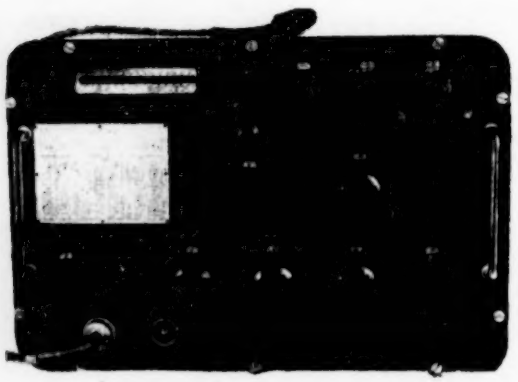

Fig. 5.

The natural resonance frequency of the input circuit at the "section" of the diode cap is equal to f_p = 2100 Mc.

The resonance error is determined by the usual formula

$$\Delta_0 = \frac{1 - \cos\frac{\pi}{2}\frac{f}{f_p}}{\cos\frac{\pi}{2}\frac{f}{f_p}} 100\% \qquad (27)$$

and amounts to +0.2% at 100 Mc and to +2% at 300 Mc.

Tests have shown that the transit error, which has a negative sign, is proportional to frequency, depends on the diode used and the value of the voltage measured; on an average it is 1.5% per 100 Mc.

The voltmeter has a good frequency characteristic at lower frequencies and measures with the accuracy indicated from 30 cps.

The effect of the wave form on the measurements has been dealt with in [3, 4].

The voltmeter will measure correctly only if the output circuit of the measured source has a dc path and no dc emf's, which is easily ensured when measuring standard signal generators or tube voltmeters.

Voltmeter OKV-2 can also be used for measuring power in a 75 ohm resistance in a range of 5 μw to 130 w (mean power) and attenuation down to 20 db with an error of $< \pm 0.05$ db.

It can also measure dc voltages up to 140 v by the compensation method with an error ±(0.1% + 0.2 mv). It then uses a measuring current of 0.3 μa.

LITERATURE CITED

[1] Aiken and Berdsell, Trans. AIEE, 57, 173, April (1938).

[2] B. E. Rabinovich, "Analysis of the basic systematic errors in ac voltage measurements by means of detected current compensation" [in Russian] (Trudy VNIIM, ed. 13/73, 1953).

[3] B. E. Rabinovich, Izmerital'naia Tekhnika, No. 4, 1956.

[4] A. M. Fedorov, Izmerital'naia Tekhnika , No. 3, 1958.

REFERENCE INSTRUMENT FOR MEASURING THE DEPTH OF AMPLITUDE MODULATION COEFFICIENT IN UHF STANDARD SIGNAL GENERATORS

P. A. Shpan'on

The application of the normal method of measuring the depth of modulation to small standard generator signals involves large errors, the most important of them being due to the nonlinearity of the detector characteristic and to the inertia of electrons, which cannot as yet be calculated for small signals.

Although it is possible to neglect electron inertia for frequencies up to 300 Mc, an increased GSS signal up to a value when detection becomes linear can introduce distortion of the modulated wave due to the nonlinearity of the amplifier amplitude characteristic.

We describe below a method of measuring the depth of modulation in small UHF amplitude-modulated voltages, a method in which the nonlinearity of theIF amplifier amplitude characteristic does not affect in theory the error of measurement. A schematic of the instrument constructed on the basis of this principle is appended and the ability of this instrument to measure the depth of modulation in UHF standard signal generators is explained (with a modulating frequency of 1000 or 400 cps).

The modulated UHF signal with a carrier frequency amplitude of several millivolts whose depth of modulation is to be measured is transformed by a linear frequency converter in such a way that the intermediate frequency amplitude is modulated at the same depth as the initial signal. The intermediate frequency amplitude is fed to a high-frequency potential divider which is adjusted in such a way that the maximum value of the envelope at the output of the divider is equal to the minimum value of the envelope at its input. According to the definition of the depth of modulation coefficient this equality can be represented as:

$$\frac{U_{\text{mod}}}{k}(1+m)=U'_{\text{mod}}(1-m), \tag{1}$$

where $\frac{k}{U_{\text{mod}}}$ is the division ratio, and
U_{mod} is the carrier amplitude.

The voltages from the divider are fed alternately to the input of the intermediate frequency amplifier. Equation (1) means that the two instantaneous voltages at the amplifier input are equal. If the amplifier amplitude characteristic is monotonic and the bandwidth is such that the sidebands are not suppressed, these amplitudes will be also equal at the amplifier output, independently of the shape of the amplitude characteristic, although the waveform, in a general case, can be somewhat distorted. This equality at the output of the intermediate frequency amplifier is checked by means of an oscilloscope and the required depth of modulation is determined from the relationship

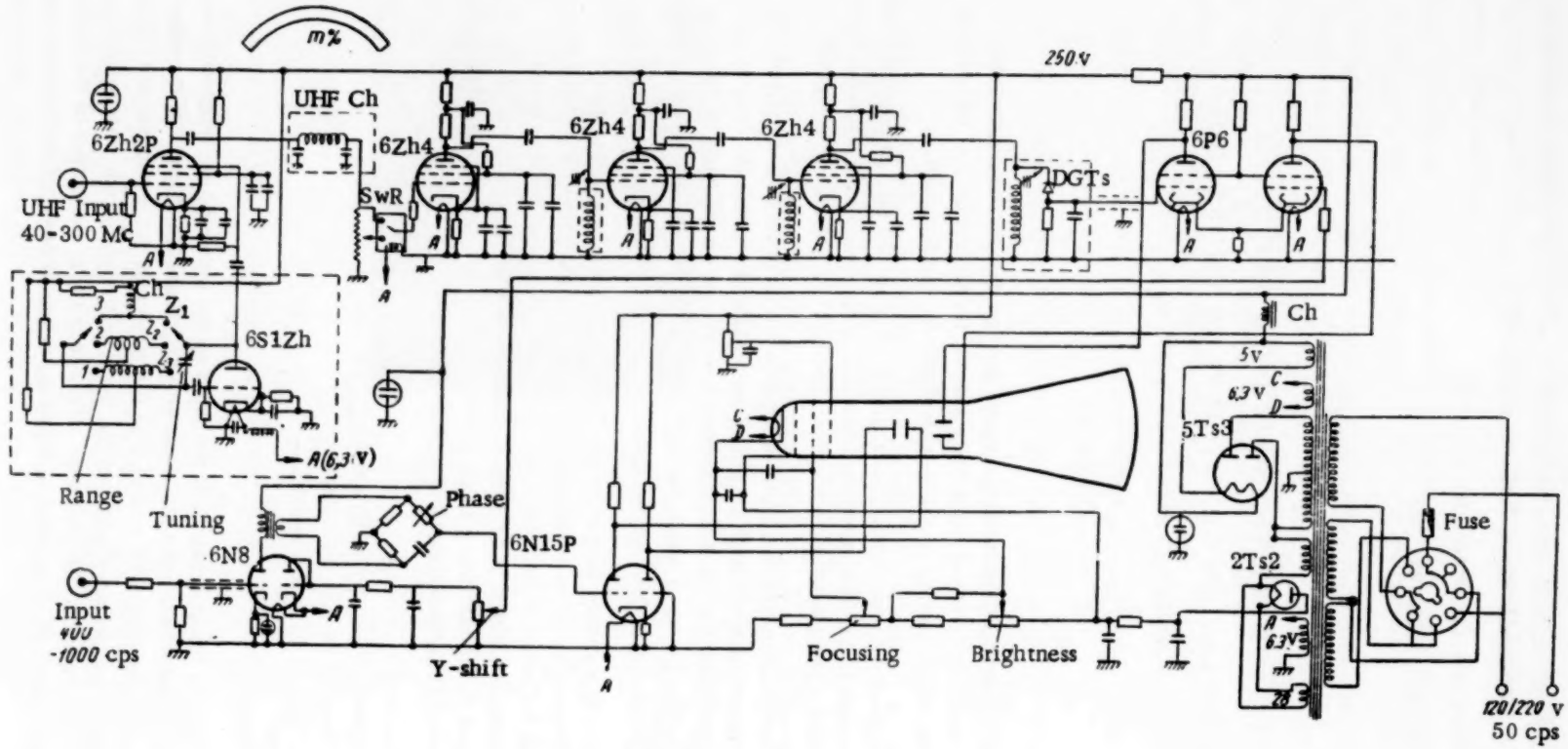
m%
250 v
UHF Ch
6Zh2P
6Zh4
6Zh4
6Zh4
6P6
DGTs
UHF Input
40-300 Mc
SwR
Ch
Z1
6S1Zh
A(6,3 v)
Range
Tuning
Phase
6N15P
6N8
Input
400
-1000 cps
Y-shift
Focusing
Brightness
Ch
5v
6,3 v
5Ts3
2Ts2
6,3v
Fuse
120/220 v
50 cps

Fig. 1.

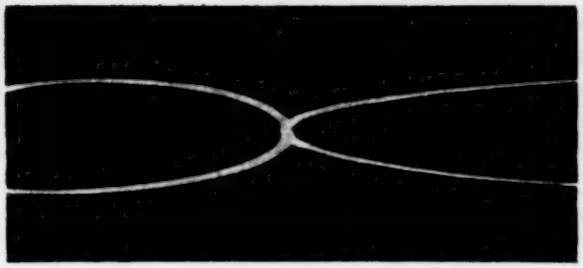

Fig. 2.

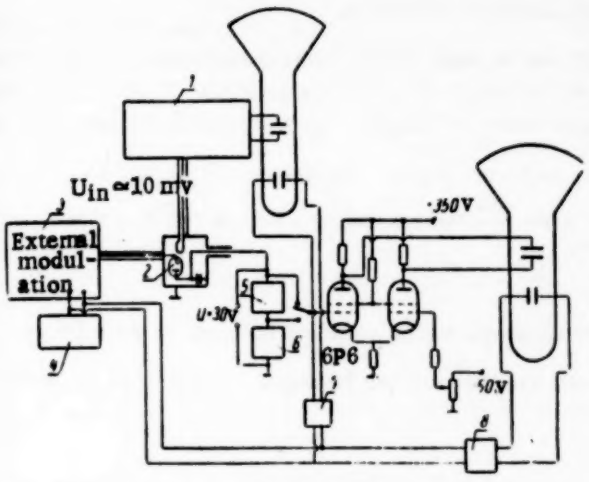

Fig. 3. 1) Instrument MKh-5; 2) linear diode 6D4Zh; 3) standard signal generator type GSS-12; 4) audio-frequency generator type 3G2A; 5 and 6) resistance boxes type R58; 7 and 8) phase shifting devices.

$$m = \frac{k-1}{k+1}. \qquad (2)$$

The schematic of the instrument MKh-5, based on the method described, is given in Fig. 1.

The modulated UHF signal is fed to the linear converter tube 6Zh2P. The intermediate frequency voltage (1 Mc) is fed to the continuously adjustable potential divider R and from the whole of the divider and a part of it to the mechanical switch. The signal passes next through the intermediate frequency amplifier, is detected, amplified in a paraphase amplifier and fed to a cathode-ray tube. If the horizontal plates of the tube are fed by a modulating voltage with a correctly selected phase and the initial UHF voltage conforms to (1), an image like the one shown in Fig. 2 will appear on the screen. The continuously variable divider is calibrated in percentage of the depth of modulation.

The error in this method of measuring the depth of modulation comprises the following errors:

1) error due to the nonlinearity of conversion,

2) error due to parasitic frequency modulation of the generator produced by the amplitude-modulated UHF oscillations,

3) error due to the division ratio of the continuously variable divider R,

4) error in obtaining equality (1) on the cathode-ray tube,

5) error due to the detector and the paraphase amplifier.

Let us evaluate each of the component errors.

It has been established experimentally that with low carrier voltages in the range of 100 kc to 25 Mc, the error due to possible nonlinearity of the converter can be neglected. This statement also hold for UHF working. It is known [1, 2] that the statistical mutual conductance S_0 of tubes becomes complex with rising frequency:

$$S = S_1 + jS_2 = S_0 \frac{\sin \varphi_a}{\varphi_{a/2}} \cos \frac{\varphi_a + \varphi_g}{2} - jS_0 \frac{\sin \varphi_{a/2}}{\varphi_{a/2}} \sin \frac{\varphi_a + \varphi_g}{2} \qquad (3)$$

i.e., S_1 and S_2 acquire transition angles in the cathode-grid φ_g and grid-anode φ_a spaces, depending on ac voltages only. The mutual conductance of a UHF converter should behave in the same manner. Hence, one should expect a decrease in the modulus of the mutual conductance with rising frequency which, however, should not affect the linearity of the converter. In the circuit in question, this fact can be easily checked in the following manner: at a certain carrier voltage the depth of modulation and the ratio of the divider are chosen so as to produce the image shown in Fig. 2 on the oscillograph screen. By changing the amplitude within wide limits (1 to 40 mv) it is possible to ascertain that the upper and lower curves will continue to touch each other. This indicates the linearity of the converter. It should be noted, by the way, that such checking is a proof of the smallness of the parasitic cross-modulated signals, since their effect on the measurement of m must depend on the amplitude of the fundamental signal [3].

Parasitic frequency modulation in some UHF generators (GSS-7 and SG-1) producing amplitude-modulated oscillations causes the intermediate frequency also to become frequency modulated. With a sufficiently narrow bandwidth of the amplifier, this frequency modulation is converted into amplitude modulation and superimposed on the initial amplitude modulation which is to be measured. In order to avoid errors the flat part of the amplifier frequency characteristic must be greater than twice the frequency deviation of the generator. A simple calculation shows that by shunting the tuned circuits of the intermediate frequency amplifier with resistances of the order of 1500 ohms a portion of the frequency characteristic is obtained which is flat over 200 kc, with a frequency deviation not exceeding 0.5%. Such a flat portion is sufficient to pass a signal with a parasitic frequency modulation deviation Δf of 50 kc without producing an additional parasitic amplitude modulation. Experimentally this is confirmed (with the accuracy of observation on a cathode-ray tube) by the preservation of the contact between the upper and lower half of Fig. 2 when a signal of 150 Mc, m = 80%, Δf = 50 kc is received with a certain mistuning of the heterodyne frequency with respect to the frequency at which the oscilloscope image is the largest, i.e., with a certain displacement of the mean intermediate frequency.

Thus when measuring the depth of modulation, the error due to parasitic frequency-modulation at the highest working frequency of generator GSS-7, where the frequency deviation at m = 80% is approximately 50 kc, does not exceed 0.5%. For frequencies below 80 Mc, where the greatest accuracy for GSS-7 is guaranteed, this error can be neglected.

The potential divider ratio is adjusted at 1 Mc with an error $\frac{dk}{k}$ not exceeding 1% at m = 20% and not exceeding 3% at m = 80%.

The error $\frac{d\alpha}{\alpha}$ of estimating when the curves on the oscilloscope screen coincide does not exceed 1% at m = 30% and rises to about 3% at m = 80%. Both these errors are random and can be added according to the mean square law.

Then the total error will be

$$\left(\frac{dm}{m}\right)=\frac{1-m^2}{2m}\sqrt{\left(\frac{dk}{k}\right)^2+\left(\frac{d\alpha}{\alpha}\right)^2}. \qquad (4)$$

The numerical values of $\frac{dm}{m}$, calculated on the assumption that $\frac{dk}{k}$ and $\frac{d\alpha}{\alpha}$ increase linearly with m, are given in Table 1.

The error due to the detector and the paraphase amplifier is negligibly small, since the nonlinearity of these two circuit elements does not affect in theory the measurement of m, and the irregularity of their frequency characteristics in the frequency range extending over several harmonics of the maximum modulation frequency of 1000 cps, with the load resistances shown in Fig. 1, is negligible.

TABLE 1

m%	$\frac{1-m^2}{2m}$	$\left(\frac{dk}{k}\right)$%	$\left(\frac{d\alpha}{\alpha}\right)$%	$\left(\frac{dm}{m}\right)$%
20	2.4	1.0	1.0	3.4
30	1.5	1.1	1.1	2.3
40	1.0	1.2	1.2	1.7
50	0.7	1.4	1.4	1.5
60	0.5	1.7	1.7	1.3
70	0.3	2.2	2.2	1.1
80	0.2	3.2	3.2	1.0

It can be assumed, therefore, that in the absence of frequency modulation of the signal, the error of measuring the depth of modulation is determined by (4). With a parasitic frequency deviation < 50 kc the measurement errors can be 0.5% higher than those shown in Table 1.

In order to check the accuracy of these calculations the error values thus obtained were compared with those obtained by other methods. For checking purposes, in a manner similar to [3], a diode method of measuring the depth of modulation was adopted with a circuit similar to IM-8, but with the peak diodes replaced by a mechanical switch, a paraphase amplifier and a cathode-ray oscillograph, and the potentiometer replaced by two

resistance boxes type R-58 (Fig. 3). The error of measurement by this method due to the nonlinearity of the diode dynamic characteristic at a rectified dc voltage of the order of 30 v, and due to inaccuracy of reading the oscillograph indications, amounts to not more than 1.5%.

Additional errors in measuring the depth of modulation by the checking method, due to raising the carrier frequency up to 200 Mc are very small. In fact the resonance effects due to their linearity do not in theory affect the measurements of the depth of modulation. An additional error can only be introduced by the effect of the electron inertia.

The absolute error in measuring the peak voltage U due to the electron inertia at UHF is represented by the formula [5]:

$$\Delta U = \alpha \sqrt{U}, \tag{5}$$

where $\alpha = df \cdot 5.04 \cdot 10^{-2}$, and

d is the distance between the anode and the cathode (in cm) and f is the frequency (in Mc).

On the basis of equation $m = \frac{U_{max} - U_{min}}{U_{max} + U_{min}}$ and taking into consideration that $\Delta U_{max} = \alpha \sqrt{U_{max}}$ and $\Delta U_{min} = \alpha \sqrt{U_{min}}$ we obtain after simple transformations equation

$$\frac{\Delta m}{m} = \frac{\sqrt{U_{max}\, U_{min}}}{\sqrt{U_{max}} + \sqrt{U_{min}}} \cdot \frac{\alpha}{U_{mod}}, \tag{6}$$

if $U_{mod} = \frac{U_{max} + U_{min}}{2}$ (which is correct for sinusoidal modulation). The last equation can be written in the form:

$$\frac{\Delta m}{m} = \left\{ \frac{\sqrt{1+m}}{\sqrt{1+m} + \sqrt{1-m}} \cdot \frac{\sqrt{U_{min}}}{\sqrt{U_{mod}}} \right\} \cdot \frac{\alpha}{\sqrt{U_{mod}}}. \tag{7}$$

This equation shows that in measuring the depth of modulation, the relative error due to the electron inertia at a carrier voltage of 1 v is always smaller than the relative error in measuring that voltage.

TABLE 2

Readings of the diode modulation meter, %	Readings of the modulation meter described above, %	Discrepancy in readings, %
60.0	60.0	0
55.0	54.9	0.2
50.0	49.5	1.0
45.0	45.0	0
40.5	40.0	1.2
30.6	30.2	1.2

In the case under consideration ($d = 120\,\mu$, $f = 200$ Mc and $U_{mod} \approx 30$ v at $m \leq 80\%$).

$$\frac{\Delta m}{m} < 1\%. \tag{8}$$

The depth of modulation of a UHF oscillation of the order of 160 Mc was measured simultaneously by the modulation meter described above and by the diode method. The measurement results are given in Table 2.

The values given are an average of 10 measurements. Comparisons were not possible at $m > 60\%$, since generator GSS-12 cannot produce modulations deeper than 60%.

Conclusions. An analysis of the errors and a comparison with the check method of measurement show that the modulation meter described above can be used as a reference instrument for checking generators of the type of GSS-7, GSS-17 and GS-1 (at 40 mc) with respect to their depth of modulation.

LITERATURE CITED

[1] Khol'man, Generation and Amplification of Decimeter and Centimeter Wavelengths [in Russian] (Soviet Radio Press, 1948).

[2] Zuhrt, "Die Leistungsverstärkung bei ultrahohen Frequenzen und die Grenze der Rückkopplungsschwingungen" Zeitschrift fur Hohfrequentechnik, March, 1937.

[3] Siforov, Radio-Receiving Devices [in Russian] (Voenizdat, 1954).

[4] P. A. Shpan'on, Izmerital'naia Tekhmika, No. 6, 1955.

[5] R. Valitov and V. Sretenskii, Radio Measurements at Ultrahigh Frequencies [in Russian] (Voenizdat, 1951).

ADDITIONAL FREQUENCY ERRORS DUE TO THE TRANSMISSION OF ELECTRICAL OSCILLATIONS

E. V. Artem'eva and V. F. Lubentsov

Oscillations with a highly stable frequency obtained from standard crystal generators are often transformed in their practical application to lower frequencies (division) of higher ones (multiplication) and transmitted to their users over wire lines or by radio.

The phase characteristics of the frequency converters and the transmitting media, do not remain constant with time, due to the variations in their parameters and the presence of fluctuations, which in turn lead to frequency changes in the generated and transmitted oscillations, i.e., to additional errors.

The value of these errors is of the same order as that of the errors and instability of the standard frequencies; hence, in order to be able to utilize to the full the stable standard frequencies, it is necessary to study the sources of these errors.

If the phase characteristic of a circuit for a given frequency f changes in t sec by $\Delta\Phi$ radians, the frequency of the oscillations being propagated along this circuit will acquire an additional error γ, which can be calculated from the formula:

$$\gamma = \frac{\Delta\varphi}{2\pi t}. \tag{1}$$

Hence the value of the relative error will be:

$$\gamma_0 = \frac{\Delta\varphi}{2\pi t f}. \tag{2}$$

A partial investigation of errors due to frequency division was carried out in 1951 by the Central Scientific Research Bureau of the Unified Time Service (TsNIB). The present article examines the sources of additional frequency errors due to the transmission of electrical oscillations over wire communication lines and radio channels and gives the measurement results.

The basic elements of the transmitting media consist of wire communication lines, repeaters, radio transmitters and receivers and the medium of propagation between the transmitting and receiving antennae. The propagation circuit contains various elements depending on the type of transmission. Let us first examine the effect of the instability of each element on the frequency of the transmitted signal, and finally give the data obtained for various circuits as a whole.

1. Wire communication line. It is known [1] that when a current is propagated along a line with distributed constants, its changes in amplitude and phase can be expressed by means of the propagation constant ν.

$$\nu = \beta + j\alpha,$$

where β is the attenuation constant, and
α is the phase shift constant.

Constants α and β depend on the line parameters and the propagation frequency. The attenuation in various lines is not the same; for instance, in a cable it is much higher than in an oper wire circuit. For transmission over large distances, therefore, repeaters are inserted in the line. If α remains constant, the transmitted oscillations will acquire a phase shift, but their frequency will remain constant. If, however, α varies with time the frequency of oscillations will change by the amount:

$$\frac{\alpha_2-\alpha_1}{t_2-t_1} = \frac{\Delta\alpha}{\Delta t} = 2\pi\Delta f. \qquad (3)$$

Cable lines are less subject to metereological effects than open wire lines; therefore, they produce smaller variations in α; special lines with interpair screening of the type ShV produce smaller variations than lines of type TZB.

On interurban lines, in addition to the continuous phase shift, sudden irreversible phase changes occur due to jumps in the parameters of the transmission circuit.

As long ago as 1952, the TsNIB started experimental investigations of additional errors with the view of evaluating the quality of communication lines used for transmitting standard frequency signals. The investigations were carried out according to the following method: for this purpose two similar communication lines in the same route such as Moscow-Khar'kov-Moscow, Moscow-Leningrad-Moscow and other routes were used; a standard 1000 cps signal was sent along one line, looped back at the far end along the other line and returned to the sending end. The phase difference between the sending and receiving voltages was measured by means of a electronic phase meter [2] at equal time intervals. For this test the following four types of interurban lines were chosen:

a) a synchronized carrier circuit without a hybrid termination;

b) a special carrier circuit;

c) a voice-frequency telephone circuit with a hybrid termination, and

d) a voice-frequency telephone circuit without a hybrid termination.

The synchronized carrier and the special carrier circuits have the smallest phase stability. The largest phase variations in oscillations propagated along these circuits are of the order of 3°. The largest phase variations in voice-frequency circuits do not exceed 1°. Such phase variations orrurring during intervals of 20 minutes produce relative frequency variations of $7\cdot10^{-9}$ and $2\cdot10^{-9}$ respectively.

In 1956 a type ShV cable line was investigated. Its relative phase instability was of the same order, that is 2 to $3\cdot10^{-9}$.

Many years' experience in comparing standard frequency generators of VNIIFTRI (Moscow), VNIIM (Leningrad) and KhGIMIP (Khar'kov) has shown that with simultaneous comparison, i.e., by using simultaneously two circuits with their own repeaters and other equipment, the value of the error amounts on the average to $\pm5\cdot10^{-9}$.

2. Radio Transmitter. The phase shift in the transmitter is due, in the main, to mistuning of tuned circuits. Phase shift measurements in transmitters produced the following results. At a carrier frequency of 10 Mc, a phase change of 10° over an interval of one minute produces an additional relative frequency error of $\gamma_0 = 5 \cdot 10^{-11}$.

At a carrier frequency of 200 kc, a phase change of 10° per minute produced an additional relative error of the order of $\gamma_0 = 2 \cdot 10^{-9}$ and at a carrier of 20 kc, about $\gamma_0 = 2 \cdot 10^{-8}$.

Under normal working conditions, such a large spontaneous mistuning of the transmitter tuned circuits is hardly likely to occur, with rising requirement for accuracy in transmitting standard frequencies; however, it becomes necessary to take into account the possibility of such errors arising. This particularly applies to the range of long and extra-long waves. Measurements at 10 Mc, during the heating up of a transmitter, showed that the error was of the order of the error of measurement (of the order of $1 \cdot 10^{-9}$).

3. Medium between the transmitting and receiving antennae. The propagation process between the transmitting and receiving antennae is very complex, but it can be represented approximately in the following way. The radio waves propagated along the earth's surface from the transmitting vertical dipole antennae leave the earth at a tangent for the ionosphere, where the short waves are reflected from the upper ionized layers (if their frequency is below the critical); medium waves are to a certain extent bent round the earth's surface before being reflected from the lower layers of the ionosphere, and the long and extra-long waves are bent a considerable distance round the earth's surface before being reflected, to a certain extent, from almost the lower boundary of the ionized space.

The propagation of the last type of waves can be represented as the passage of waves along a space waveguide formed by the surface of the earth and the lower boundary of the ionosphere.

The periodic variations of the sources of ionization (the main one being the sun) leads to a periodic displacement of the ionized layers in space, to their formation and disappearance. The greatest change in the height of the ionized layers takes place during the rising and setting of the sun, when the speed of their displacement reaches 15-20 m/sec. In the remaining part of the day the displacement is insignificant. In addition to the daily variations in the ionosphere there also exist smaller variations of an annual and an 11-year period due to solar activity.

The propagation of the electromagnetic waves during the displacement of the ionized layers is accompanied by changes in their frequency, due to the changes in the length of the propagation paths between the transmitting and receiving antennae (Doppler effect).

The change in frequency is determined by the difference between the sending and receiving frequency and is calculated from the formula

$$\gamma = \frac{f}{c} \sum_{1}^{n} 2V_i \cos \theta_i, \tag{4}$$

where f is the frequency of the transmitted oscillations,
V the speed of displacement of the reflecting region,
c the radio-wave speed
n the number of reflections, and
θ is the angle at which the waves enter the ionized layer.

The VNIIFTRI carries out systematic measurements of the frequencies transmitted by the radio station MSF in London and WWV in Washington.

Figure 1 shows the characteristic curve of the periodic change in the difference between the frequency received from London and the VNIIFTRI standard. It will be seen that the largest changes take place during the rising and the setting of the sun, their relative values attaining $1 \cdot 10^{-7}$ and changing in sign. During daylight at the transmitting and receiving ends the changes in the relative difference amount to some $1 \cdot 10^{-8}$.

The 10 Mc signal transmitted by MSF was measured during the eclipse of the sun on June 30, 1954. Figure 2 shows the results obtained. Instants t_1 and t_2 correspond to the beginning and the end of the eclipse in the 10 Mc region of reflection. The relative change in frequency amounted to $1 \cdot 10^{-7}$.

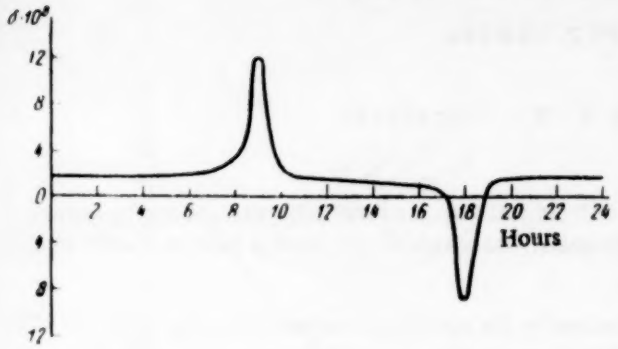

Fig. 1.

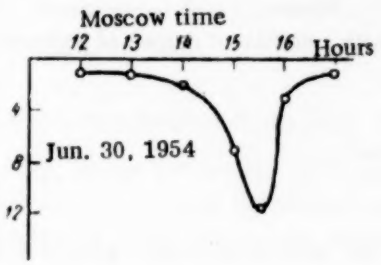

Fig. 2.

The propagation of longer waves takes place in the region with the least density of ionization, which is displaced relatively little during the day. It has been established experimentally that oscillations of 200 kc transmitted over a distance of 800 km acquire during 24 hours an additional relative frequency error of the order of $5 \cdot 10^{-9}$.

Preliminary results of investigations of the propagation of a frequency of 16 kc over a distance of 5000 km [3] give reasons to believe that the additional relative frequency error was of the order of $1 \cdot 10^{-9}$.

4. Radio Receiver. If a low standard frequency of 1000 cps is adopted, the receiver changes the phase of the received signals. The reason for this effect is the same as the one in transmitters, i.e., the mistuning of the tuned circuits.

Investigation of the errors due to the receivers have shown that the errors lie beyond the limits of the relative error of measurement of $2 \cdot 10^{-10}$.

If the standard frequency is received by the heterodyne method the error due to the receiver is completely eliminated [4].

Conclusions. Existing data shows that all the elements of the circuit, whether propagating or transforming oscillations, introduce frequency errors in the transmitted signals. The relative errors due to the frequency divider is 10^{-8} to 10^{-10} and frequency multipliers 10^{-12} to 10^{-13} [5]. Wire lines introduce an error of $1 \cdot 10^{-8}$ to $1 \cdot 10^{-9}$, depending on their type and the frequency transmitted.

Radio transmitted signals acquire additional frequency errors depending on the frequency transmitted and the distance of propagation. Thus low frequency transmissions are accompanied by relative errors of the order of 1 to $5 \cdot 10^{-9}$ and high frequency ones by errors varying from $1 \cdot 10^{-8}$ (if the transmitting and receiving ends are not separated by the rising or setting sun) to $10 \cdot 10^{-8}$ (if the transmitting and receiving ends are separated by the rising or setting sun).

The existing accuracy of the standard frequency oscillations and the prospects of its further improvement by using resonance absorption frequencies of various atoms and molecules make it imperative to investigate on a wide scale the circuits and propagation media used in conveying the signals to their users.

LITERATURE CITED

[1] B. P. Aseev, Oscillatory Circuits [in Russian] (Moscow, 1955).

[2] V. F. Lubentsov and S. Ia. Rombro, Izmerital'naia Tekhnika , No. 2, 1955.

[3] J. A. Pierce, Proc. IRE, No. 5, pp. 584-588, 1955.

[4] Instruction No. 215-54 of the Committee of Standards, Measures and Measuring Instruments [in Russian].

[5] M. Z. Klyumel', Izmerital'naia Tekhnika, No. 4, 1957.

FREQUENCY TEMPERATURE COEFFICIENTS OF AT-CUT QUARTZ LENSES

E. D. Novgorodov and N. Kh. Neparidze

Quartz AT-cut lenses, with a Q factor of the order of 5-10 million , considerably increase the frequency stability of crystal oscillators and can be used in master frequency standards,if they have a zero or a sufficiently low frequency temperature coefficient (f.t.c.)

Existing quartz lenses [1] do not possess such f.t.c. values in the operating temperature range of 20 to 60°C, and can only be used in underground quartz generators, whose temperature instability is extremely small.

We give below the results of investigations carried out by the Khar'kov State Institute of Measures and Measuring Instruments (KhGIMIP) of the f.t.c. of 32 high-Q AT-cut quartz lenses.

It appears that at normal temperatures, the relative change in frequency with temperature of quartz lenses, similarly to round AT-cut quartz plates [2, 3], can be expressed with a sufficient degree of precision by the equation:

$$\frac{\Delta f}{f_0} = a\Delta T + b\Delta T^2 + c\Delta T^3, \qquad (1)$$

where coefficients a, b and c are functions of the angle of cut θ , the ratio of the lense diameter d to its thickness h, the number of the lens' operating overtone and the initial temperature. The curve which represents this relation is a cubic parabola and depending on the values of coefficients a, b and c has the shape of I, II or III (Fig. 1). In the first and second case the lens' f.t.c. has at certain temperatures a zero value.

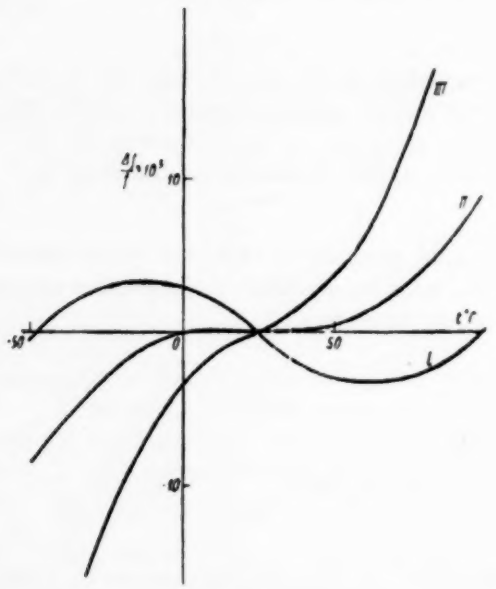

Fig. 1.

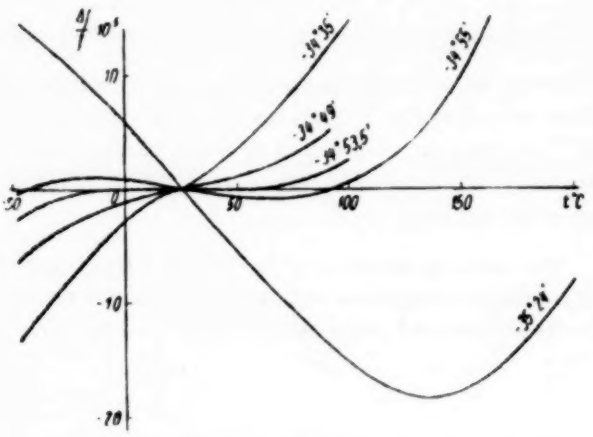

Fig. 2.

Figure 2 shows the relation for various angles of cut between the frequency and temperature of quartz lenses working at the basic frequency of 500 kc (d/h = 10.4) and Fig. 3 that of lenses working at 1 Mc (d/h = 8.6).

Each of these curves was obtained by taking the mean of experimentally obtained curves of 4-5 quartz lenses made out of plates of the same cut and working with the same gap.

Lenses with an angle of cut of −34°47' for 1 Mc and −34°53' for 500 kc have a zero value of f.t.c. in the range of 20-50°C. At larger angles two zero values of f.t.c. appear at temperatures increasingly further away from that region with increasing angles of cut. At angles of cut smaller than those given above the zero f.t.c. is lacking.

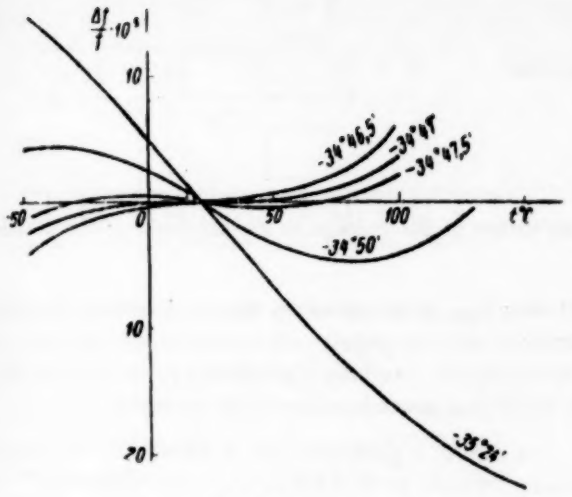

Fig. 3.

The optimum angles of cut for lenses are smaller than those for round flat plates [4] of the same d/h ratio. This difference increases with increasing convexity of the lenses [5].

In the tested lenses, whose graphs are given in Fig. 2 and 3, the ratio d/R was made equal to 0.43, since such a lense configuration with other conditions being equal provided, according to the authors of this article, the highest Q. At this ratio the optimum angles of cut for lenses differed from those for round plates of 4-5'. In lenses with a d/R = 0.21 the difference in the angle of cut is smaller and equal to about 2' (d/h = 18.0).

The variations of the f.t.c. with the angle of cut are very large, especially in the range of 20 to 50°C, a change of the angle of cut by 1' changes the mean f.t.c. in that range by $1.5 \cdot 10^{-7}$ per degree. This makes the series manufacture of lenses with a f.t.c. smaller than $1 \cdot 10^{-7}$ very difficult for a given temperature, since the production of lenses from plates with an error in the angle of cut smaller than 1' was found to be impossible in practice.

Among other factors influencing the f.t.c. one should point out the value of the airgap between the quartz and the electrodes, which presents the possibility of correcting small deviations of the f.t.c. from the required value due to deviations in the angle of cut produced during the manufacture of lenses.

The method of fixing the lenses does not have any appreciable effect on the f.t.c.; thus in the process of investigations no observable changes in the f.t.c. appeared when the lenses were fixed by means of threads, springs or rods.

Conclusions. A method of producing small, including zero values of the f.t.c. for quartz lenses was found and thus the possibility of their application was extended from standard oscillators with an underground thermostatic control to normal thermostatically controlled standard oscillators.

LITERATURE CITED

[1] A. W. Warner, Proc. IRE, vol. 42, No. 9, (1954).

[2] R. Bechmann, Arch. Electr. Ubertragung, XI, 9, No. 11, (1955).

[3] R. Bechmann, Proc. IRE, vol. 44, No. 11, (1956).

[4] E. A. Gerber, Proc. IRE, vol. 43, No. 10, (1955).

[5] R. Bechmann, J. Scient. Instr., vol. 29, No. 3, (1952).

MEASUREMENT OF A GENERATOR VOLTAGE STANDING-WAVE RATIO BY MEANS OF A PHASE SHIFTER

L. N. Brianskii

When accurate measurements of waveguide circuits are made, it is necessary to know the voltage standing-wave ratio of the generator and often to match the generator for a v.s.w.r. close to unity. The measurement of the v.s.w.r. of a generator with a decoupling attenuator is usually made by means of a measuring line (Fig. 1).

based on the phenomenon that with a mismatched generator, the voltage at the antinode changes with the electrical length of the circuit, due to the changing of phase relations between the primary reflected wave and reflected waves of a higher order.

The v.s.w.r. of the generator is determined from the formula:

$$\text{v.s.w.r.} = \frac{U_{\text{ant max}}}{U_{\text{ant min}}} \qquad (1)$$

where $U_{\text{ant max}}$ and $U_{\text{ant min}}$ are the maximum and minimum values of the voltage at the antinode of the standing wave.

In practice the v.s.w.r. of a generator is measured as follows: U_{ant} is measured for several positions (8-10) of the short circuit, then the $U_{\text{ant max}}$ and $U_{\text{ant min}}$ are determined and the generator v.s.w.r. calculated. It will be seen that these measurements are very cumbersome, especially for matching a generator, when after each change of the matching transformer tuning elements, the whole measuring procedure has to be repeated.

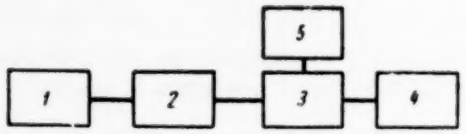

Fig. 1. Block schematic of the measurement of a generator v.s.w.r. by means of a measuring line. 1) Generator; 2) decoupling attenuator; 3) measuring line; 4) moving short-circuiting plunger (short circuit); 5) indicator.

In case of a generator with a waveguide output, the measurement of its v.s.w.r. can be considerably simplified and speeded up by using, instead of the measuring line a phase shifter and a probe head. Two equally suitable schematics used for this purpose are shown in Fig. 2. The antinode is made to coincide with the stationary probe of the head by means of the short-circuit or the phase-shifter No. 2 and then the measuring itself is made with phase-shifter No. 1.

Thus the theory on which the measurement is based remains unaffected, since (1) holds with any method of changing the electrical length of the circuit.

By turning the knob of phase shifter No. 1, the voltage at the probe detector will change from U_{max} to U_{min}. Since normally v.s.w.r. close to unity are measured, (1.2 to 1.3), the amplitude of the wave reflected from the generator is small and the position of the antinode is almost independent of the phase relations among the reflected waves; in any case, the probe does not go out of the limits of the practically flat-topped standing wave envelope.

Hence

$$U_{\text{max}} \simeq U_{\text{ant max}} \qquad (2)$$

$$U_{\text{min}} \simeq U_{\text{ant min}} \qquad (3)$$

and the generator v.s.w.r. $= \sqrt{\frac{U_{\text{max}}}{U_{\text{min}}}}$ (4)

(when the probe detector is working on the square-law part of its characteristic).

The measurement of the generator v.s.w.r. by this method is very simple and only takes a few seconds. The simplification of the measuring method consists in keeping, contrary to the normal procedure, the distance between the short circuit and the probe constant, when the electrical length of the circuit is changed.

The advantages of above method become especially noticeable when matching a generator.

The total price of the probe head and phase shifter does not exceed on the average 50-60% of the measuring line price.

The accuracy of measurement is, in any case, no lower than with a measuring line, since, although the combined additional probe-head and phase-shifter error equals 1 to 2%, due to reflections from the phase-shifter plates, the errors due to the uneven movement of the probe, the effect of the cavity, etc. whose value in the best measuring lines amounts to no less than 2-3% are eliminated.

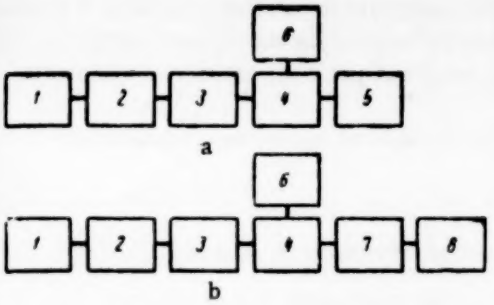

Fig. 2. Block schematic of the measurement of a generator v.s.w.r. by means of a phase shifter. 1) Generator; 2) decoupling attenuator; 3) basic phase shifter No. 1; 4) probe head; 5) moving short-circuiting plunger (short-circuit); 6) indicator; 7) auxiliary phase shifter No. 2; 8) fixed short circuit (end cap).

Of the apparatus used the least known is the phase shifter. It consisted of a waveguide section with a sharp-edged polystyrene plate moving from the walls to the center of the waveguide. Thus the phase shifter is similar in construction to attenuator type 671 and 521, with the difference that the plate has no absorbing layer and is suspended on two threads, instead of a relatively thick rod, in order to reduce the v.s.w.r. of the phase shifter itself.

Above method was checked over a wide range of 3 to 0.7 cm wavelengths, producing good results.

It is also possible to measure larger values of v.s.w.r., but it becomes necessary then to correct for the relative position of the probe and the antinode by means of the phase shifter No. 2 or the short circuit.

LITERATURE CITED

[1] "Measuring technique on centimeter wavelengths," Soviet Radio, vol. 1 and 2, 1949.

[2] M. E. Gertsenshtein and L. N. Brianskii, Izmerital'naia Tekhnika, No. 1, 1956.

[3] M. E. Gertsenshtein and L. N. Brianskii, Izmerital'naia Tekhnika, No. 6, 1956.

[4] Barlow and Cullen, Measurements at Ultrahigh Frequencies, [in Russian] (Translation edited by Shteinshleiger) (IL, M., 1952).

EXTENSION OF THE LIMITS OF APPLICATION OF A HETERODYNE WAVEMETER

E. N. Garmash

Heterodyne wavemeters type 526, 527, 528 and VS-221, with an error of measurement not exceeding 0.01% are used in the range of 125 kc to 20 Mc. They have two ranges, that of 125 to 250 kc and 2000 to 4000 kc.

The range of 125 kc to 20 Mc is covered by means of harmonics of the first and second ranges, with higher order harmonics being used only for checking and not for measuring the frequency.

Normally heterodyne wavemeters are used when the approximate value of the measured frequency is known [1, 2, 3].

Below we describe a method which extends the frequency range of measurement by using heterodyne wavemeter harmonics of a higher order.

When an unknown frequency is measured it is first of all necessary to find its ordinal of the heterodyne wavemeter harmonic by means of two zero beat points. The ordinal of the harmonic and the fundamental frequency provide the value of the measured frequency.

Let us denote f_x as the unknown measured frequency, f_1 as the fundamental (first harmonic) of the heterodyne wavemeter at the first zero beat tuning, f_2 as the same, but for the second tuning, f_3 as the same, but for the third tuning, n as the ordinal of the heterodyne wavemeter fundamental frequency at the first zero beat tuning.

When the heterodyne wavemeter frequency is changed from its maximum to its minimum value a number of zero beat points are obtained between the measured frequency and the heterodyne wavemeter harmonics. As the heterodyne wavemeter frequency is decreased each consecutive zero beat point corresponds to a harmonic whose ordinal is higher by unity than the previous one.

We can write for the first zero beat point:

$$f_x = f_1 n; \tag{1}$$

and for the second:

$$f_x = f_2(n+1);$$

the third:

$$f_x = f_3(n+2)$$

etc.

From (1) and (2) we have:

$$n = \frac{f_2}{f_1 - f_2}. \tag{4}$$

From (1) and (3):

$$n = \frac{2f_3}{f_1 - f_3}. \tag{5}$$

From (4) the ordinal of the heterodyne wavemeter harmonic is obtained and from (5) it is checked. From (1) the unknown frequency is determined. The sequence of measurement can be as follows:

1. By reducing the heterodyne wavemeter fundamental frequency from its maximum value, the first zero beat point between the heterodyne wavemeter harmonic and the measured frequency is obtained.

2. The scale of the heterodyne wavemeter is calibrated from the nearest crystal oscillator check point.

3. The wavemeter is tuned back to the zero beat and the frequency f_1 of the first zero beat point is read off the wavemeter scale.

4. The fundamental frequency is then reduced until the second zero beat point is obtained and its frequency f_2 determined from the heterodyne wavemeter scale.

5. The frequency is further decreased to the third beat point whose frequency f_3 is read off the scale.

6. From the readings thus obtained the actual frequencies f_1, f_2 and f_3 are read off the calibration chart.

7. The ordinal of the harmonic is obtained from (4) and its accuracy checked from (5). Since the calibration is made only once frequencies f_2 and f_3 will be measured inaccurately and the harmonic number will be fractional. The nearest whole number should be taken.

8. The unknown generator frequency is obtained from (1).

The checking of this method at various frequencies showed its applicability not only within the measuring range of the wavemeter but also far beyond the limits of its second range, where measurements were carried out by means of higher order harmonics.

At high frequencies (of the order of 100 Mc) above method can only be used to measure frequencies of powerful generators, since at higher harmonics the heterodyne-wavemeter oscillator harmonics considerably decrease in amplitude leading to a lower sensitivity. The table shows the input voltage of heterodyne wavemeter type 526 which provides an output voltage of 0.5 v. This voltage is sufficiency large to be able to detect the zero beats by means of headphones.

TABLE

f_{meas}, Mc	20	40	60	80	100
U_{in}, mv	4	25	220	1000	4200

The sensitivity of various models can differ considerably from above table.

LITERATURE CITED

[1] S. F. Korndorf, A. S. Bernshtein and M. I. Iuroslavskii , Radio Measurement, [in Russian], (GEI, 1953).

[2] Description and Instructions for a Crystal Heterodyne Wavemeter, pub., Zavoda-Izgotovitelia [in Russian] (1953).

[3] A. K. Balikhin, Radio Measurements, [in Russian] (Voenizdat, 1949).

UTILIZATION OF AN OSCILLOGRAPH SCANNING GENERATOR FOR FREQUENCY DIVISION

P. T. Smirnov

Normally for frequency division, often required in testing and development work, multivibrators of various frequencies synchronized with the voltage whose frequency it is required to divide are used; sometimes amplification of the measured frequency is required.

When frequency dividers are lacking it is possible to employ for this purpose a cathode-ray oscillograph using its Y-axis amplifier for the measured signal amplification and its relaxation generator for frequency division.

The voltage whose frequency is to be divided is fed to the oscillograph input and the scanning generator is adjusted to obtain on the oscillograph screen the same number of waveforms as the number by which the frequency has to be divided. The frequency and synchronization of the generator should be adjusted and the interference filtered out so as to obtain a clear, stationary image on the screen; when the image is blurred there is no frequency division. The saw-tooth voltage of divided frequency is obtained from the X-plate terminals and fed to the input of radio receivers, oscillographs, etc.

Synchronization should be periodically checked during operation.

This method provides frequency division by a factor up to 10-20 for frequencies up to 20 to 30 kc and by a factor up to 5-10 for frequencies up to 1 Mc.

INFORMATION

IN THE TECHNICAL COMMITTEE NO. 12 OF THE INTERNATIONAL ORGANIZATION ON STANDARDIZATION

G. D. Burdun

From November 12-16, 1957 , there took place in Copenhagen the IV session of Technical Committee No. 12 of the International Organization on Standardization (ISO/TC 12), which carried out work in the field of: "Quantities, units, denotations, conversion factors and conversion tables." The secretarial duties of the committee are taken care of by the Danish organization on standardization.

It is the object of the committee to work out proposals for international recommendations on units of measurement, symbols for quantities and units and establishment of conversion factors and conversion tables.

Active members of the ISO/TC 12 committee are: Austria, England, Belgium, Brazil, Hungary, Germany, Holland, Denmark, India, Italy, Norway, Poland, Portugal, Rumania, USSR, U.S.A., France, Czechoslovakia, Sweden and Switzerland.

In its activities the committee cooperates with a number of other organizations such as: the International Committee on Measures and Weights, the International Committee on Legislative Metrology, the International Union of Pure and Applied Physics, the International Union of Pure and Applied Chemistry, the International Electrotechnical Commission and the International Commission of Illumination.

In the first order agenda plan of the ISO/TC 12 committee there is specified the composition of a paper which would include the following tables of quantities and units: 0. Basic quantities and units of the M.K.S.A. system; 1. Quantities and units of space and time; 2. Periodical and related phenomena; 3. Mechanics; 4. Heat; 5. Electricity and magnetism ; 6. Light; 7. Sound; 8. Chemistry and atomic physics. In the future other fields of science and technology may be included. The paper to be worked out should contain not only recommendations for standardization but also information as, for example, the conversion of units, used but not always recommended, into recommended ones.

During the years of 1952 to 1955 three sessions of the ISO/TC 12 committee took place, in which the first four divisions of the specified plan of operation were discussed. The committee approved the final version of the first two divisions: "Basic quantities and units of the MKSA system " and "Quantities and units of space and time." These were in 1956 accepted by the council of ISO as International Recommendation ISOR 31, part 1.

In 1956-1957, by means of correspondence between the committee members, a project of recommendations in the Division of Periodical and Related Phenomena was accepted and substituted for approval to the ISO council.

Recommendation ISOR 31, Part I.

This recommendation is the first international recommendation on units of measurement accepted by the ISO council. It consists of an introduction, Table 0, "Quantities and units of the MKSA system" and Table 1, "Quantities and units of space and time."

In the introduction are stated the basic principles used in construction of the tables of quantities and units, and the problems of notations and abbreviations. In the introduction, also, a list of other systems of units is given, including the nonmetrical systems used in England and the USA, and it is stated that the metric units are especially recommended.

Table 0 contains a list of basic quantities and units of the MKSA system and the corresponding international abbreviations. The name of "MKSA system" is applied to a system in which the basic units are: meter – kilogram – second – degree Kelvin – ampere – candle power; these were established by the Xth General Conference on Measures and Weights as the basic units of the international system of units. The resolution of October 6, 1956 of the International Committee on Measures and Weights that this system be named "International System of Units," was not reflected in the ISO recommendation.

Table 1, which comprises the quantities and units of space and time is divided into two separate parts – left and right. On the left-hand side are contained the most important quantities of space and time, together with notations for them and, in some cases, definitions. For quantities, identical with elementary concepts of everyday life (such as length, time, etc.) definitions are not given. In all there are 11 quantities: angle, solid angle, length, area, volume, time, speed of rotation, angular velocity, angular acceleration, velocity and acceleration.

The right-hand side contains the units of these quantities, their international abbreviated notations and definitions, and, in some cases, abbreviated names for the units.

When there are several units given for a quantity, then they are arranged in the following sequence: (1) MKSA units; (2) CGS units; (3) MTS* units; (4) metric technical units of the MK(force) S system; (5) other units belonging to the metric system; (6) units of the foot-pound-second system; (7) British technical units; (8) other units.

The names of the MKSA units are given in bold face and large letters, all others in smaller print.

Some units listed under the headline "others" are included only for the sake of information and are not recommended.

Decimal, fractional and multiple units are not given, with the exception of cases when they have special names (as for instance: are, ton, micron etc).

For all units of measurement abbreviations are given. International abbreviations are given in a special column; in their absence, the abbreviated name is given in the same column as the full name.

An important part of recommendation R31 are the "conversion factors" for units of measurement. In the column headlined "conversion factors," two kinds of figures are given: "basic coefficients," and "ordinary coefficients."

The figures of the first kind are assemblies of coefficients, which are necessary for computation of all the other coefficients. They are printed in bold face type. Basic coefficients derived from exact determinations normally are given up to and including the 7th decimal figure; if they are complete within 7 decimals or less, the word "exact" is added, and if they are known to more than 7 decimal points, they are given in full. Basic coefficients derived from experiments are given with an accuracy supported by the present accuracy of the experiments. Usually that means that only the last given figure is doubtful. However, if the experiment justifies more than 7 significant figures, the coefficient in the tables is usually rounded off to the 7th digit.

The following are a few examples of basic conversion factors or coefficients – right angle: 1 L = 1.570796 rad.; inch: 1 inch = 25.4 mm (exact); liter: 1 liter = 1.000028 dm^3.

Ordinary conversion factors are printed in ordinary type and are stated with not more than 6 significant figures. They are given with an accuracy supported by the corresponding basic coefficient. When they consist of 6 figures or less, the word "exact" is added. As an example the conversion factor $1\frac{\text{mile}}{\text{hour}} = 0.44704\frac{\text{m}}{\text{sec}}$ (exact) may serve.

In an appendix to the tables of recommendation R31, definitions are given for the basic units: meter, kilogram, second, ampere, degree Kelvin and candlepower, as established by the General Conference on Measures and Weights. In the same place in smaller print are given the definitions of the basic units of the British Empire system: the yard and the pound.

The IVth Session of ISO/TC 12

At the 4th session of TK12 there were present representatives of 16 countries, which are active members of the committee. Representatives of Brazil, India and of the USA were absent. Representatives of Finland and Yugoslavia were present as observers.

*Meter-ton-second system.

Representatives of all 6 above mentioned international organizations* who cooperate with ISO/TC also took part in the work of this session.

The basic items on the program of the IV session of the committee were as follows:

1. Discussion of the second draft of the project of ISO recommendations on "Quantities and units in mechanics."

2. Discussion of the project of ISO recommendations in "Quantities and units in heat."

3. Discussion of the second edition of the Secretariat's project: "Some principles of printing symbols and numbers."

4. Discussion of the Secretariat's project: "Rounding off of numbers."

5. Discussion of the project "Mathematical signs and symbols" reworked by the Secretariat.

6. Information of the Secretariat regarding the examination of the ISO recommendations projects on "Quantities and Units in Acoustics" by the ISO's Technical Committee No. 43 (on acoustics).

In this session comments and remarks received from various countries regarding the second edition of the proposed ISO recommendations on "Quantities and Units in Mechanics," together with the conclusions of a consulting committee on these matters are discussed in detail. As a result of these discussions, about 20 changes were introduced in the proposed text of the document. A resolution was adopted at the session which, after the changes were made, approved the proposed text for ISO recommendations on quantities and units in mechanics. On this basis the Secretariat shall compose a third edition of proposed ISO recommendations on mechanical quantities and units for distribution among and final examination by the members of ISO/TC 12.

There was a matter of principle involved in a question which was raised by the members of the International Committee on Measures and Weights (ICMW) attending this session; the question concerned the introduction into the general part of the document on mechanical quantities and units of a reference to the decision of ICMW to give to the MKSA system of units the name of "International System of Units." After a lengthy discussion, the question was decided positively, and it was decided to place in the aforesaid document a corresponding footnote, and in an appendix, an excerpt of the resolution of the International Committee on Measures and Weights of October 6, 1956, in which the name of "International System of Units" was attached to a system based on the six fundamental units: meter, kilogram, second, degree Kelvin, ampere and candlepower.

The discussion of proposed international recommendations for heat quantities and units proceeded on the basis of a resumé of comments and suggestions by a committee of consultants, copies of which were distributed among the delegates. As a result of the discussions, numerous changes and improvements were introduced in various points of the proposed recommendations. The Secretariat was commissioned to compose a revised edition of the document on the basis of the discussions, and to send it out to the participating countries.

In addition to the discussion of the problems connected with the tables of quantities and units in mechanics and heat, during this session three documents submitted by the Secretariat were discussed: "Some principles concerning the printing of symbols and numbers," "Rounding off of numbers" and "Mathematical signs and symbols." The discussion that took place will make it possible for the Secretariat to compose new versions of recommendations on these items.

Proposed recommendations on "Quantities and units in acoustics " which were composed by the Secretariat of ISO/TC 12, the first edition of which was sent out to the members of the Committee, are at present under examination by ISO/TC 43 (Committee on Acoustics).

---

*See page 236.

CONFERENCE OF THE GROUP FOR FORMULATING INTERNATIONAL RECOMMENDATIONS FOR TABLES OF QUANTITIES AND UNITS IN THE DIVISION OF SOUND

I. G. Rusakov

The conference took place in London in January of 1958. It was called by the secretariat of working group No. 6 of Technical Committee No. 43 of the International Organization for Standardation ISO/TC43 on Acoustics; this group was created in accordance with a resolution approved at the plenary meeting of ISO/TC43 in Paris in January of 1957. The group comprised representatives of the USSR, England, USA, Denmark, Italy, Germany, and France. The Danish Standards Organization provided the secretariat for the group.

Calling of this meeting of the working group was necessary because of the substantial differences which appeared during attempts to reach agreement by correspondence. A draft of "Tables of Quantities and Units" in the "Sound" section was proposed by committee ISO/TC12 (International Standards Organization Committee on Quantities, Units, Denotations, and Conversion Factors). Comments were received from 9 countries, from the USSR among others. Some of these countries have national standards on acoustical quantities and denotations of their own. In addition there are in existence coordinated recommendations of the International Electrotechnical Commission (IEC) on some of these quantities incorporated into tables. This explains the differences in opinions and comments which were expressed regarding the proposed draft.

In the work of the present conference representatives of USSR, England, Germany, and Denmark took part. The representatives of the USA, France, and Italy were not present at the sessions of the conference, but sent detailed comments on all questions connected with the proposed "Tables of Quantities and Units."

At the conference the main subject of discussion was the formulation of definitions for acoustical quantities and units, on which there was the most disagreement between the comments of the national committees. As a result of these discussions, the working group succeeded in achieving agreement on most of the controversial issues. A small group of not yet resolved problems was included in the report of the working group which will be presented by the Secretariat for consideration by the plenary meeting of ISO/TC43 ("Acoustics"), which is to take place at Stockholm in July of 1958.

As was noted in the course of the conference, the main difficulty in defining acoustical quantities consists in the great variety and complexity of conditions under which these quantities appear. Acoustical quantities are continuously varying in time and in space, and therefore their exact logical definition is complicated and lengthy. Therefore, it was decided not to seek exactness and completeness of definition in these tables, but to be restricted to simplified, abbreviated formulations, with the object of merely giving explanations and clear outlines of the items subject to definition.

Upon a proposal by the Soviet delegation, in the introduction to the tables was included an indication that the definitions of acoustical quantities in these tables refer to linear acoustics, and that second order effects are not considered. Also upon our proposal, a footnote was included in the section on acoustical energy (or intensity) to the effect that in cases when the energy varies with time, it is necessary to take the average value over a period of time during which the sound energy can be regarded as stationary in a statistical sense. The USSR definition for sound energy flux was taken as a basis and included in the tables after a small amendment as to English style. The definition for mechanical impedance was accepted in the formulation of the English standard. Considerable changes were introduced in the tables in the section on levels.

Definitions of levels of loudness and of background are given in the tables in conformity with the complete definitions prepared by other groups of ISO/TC43 ("Acoustics").

As the most important unit of sound pressure for acoustics, the newton (N) per square meter was chosen, which is the unit of the MKSA system. This unit is recommended by the tables in the first place. Alongside with this, the tables contain also the "bar" unit which is equal to $10^5 N \cdot /m^2$. A note was added which reads: "the microbar (1 μbar = 1 dyne/cm^2) is sometimes also called a barye."

In addition to these important changes, there also were some others accepted in the proposed tables. Specifically, the subject "frequency interval" with the octave as a unit for it was added; at the same time, however, the group came to the conclusion that the dimensions of musical intervals should not be included in the tables on "sound."

As a result of this conference, the proposed tables of acoustical quantities and units were materially improved; they will be submitted in their present form together with a report of the Secretariat for consideration by the plenary meeting of ISO/TC43 ("Acoustics"), after which they will be subject to approval and acceptance in ISO/TC12.

CONFERENCE ON MECHANOTRONS*

L. A. Goncharskii

In December of 1957 there took place in Moscow a scientific-technical conference on problems of mechanotron techniques, which was called by the Moscow regional administration of the society of scientific-technical workers in the instrument manufacturing industry.

At that conference there were present more than 220 representatives from some 100 organizations in Moscow, Leningrad, Gorki, Kiev and other cities of the Soviet Union. Nineteen reports and communications were presented.

The mechanotronic technique is one of the new promising sections of modern applied electronics. It permits realization of apparatus of high sensitivity and high efficiency for study and control of mechanical parameters of machines, mechanisms, engineering structures, and transportation vehicle, and also offers a new approach to the solution of a number of difficult problems of modern measuring technique. In addition to the various technical applications, the uses of mechanotrons (that is of mechanically controlled electron and ionic tubes) in medical and physiological instrumentation are also of interest.

The conference showed, that in a number of laboratories at universities, research institutes, engineering bureaus and industrial plants, there was and is going on development of various types of mechanotrons and of measuring and control devices using mechanotrons; in many of these organizations the number of scientists and engineers engaged in the development of new designs and systems with mechanotrons has increased. Simultaneously, also the scientific level of this work has been raised. Among the most promising developments in our country in the field of mechanotrons tested under laboratory conditions, that were reported at this conference, are the following: twinned diodes with longitudinal external control by electron currents, which are to be used in a number of devices for direct counting or registration (without amplification of the transducer signal); triodes with longitudinal external control by electron currents, which are distinguished by high voltage sensitivity and which are to be used with high internal resistance loads, such as for instance electronic amplifiers and converters; triodes with external probe control by electronic currents, which are distinguished by high voltage sensitivity; twinned diodes of external longitudinal control by impeded glow discharge, which have high voltage sensitivity; twinned diodes of internal longitudinal control by electron currents and glow discharges, which are to be used for measurements and recording of static and dynamic accelerations.

At the conference the expeditiousness of the use of mechanotrons for the following control and measurement instruments was confirmed:

1) Micrometers for visual and automatic control of linear dimensions of parts and products and for active control of dimensions during machining operations, and also high precision micrometers for the control of deformations of bodies during various experiments (for instance for recording of thermal deformations in dilatometers).

2) Manometers for measurement and recording of pressures in various ranges and in various media (of a dynamic as well as of a static nature).

3) Hardness testers and profile measuring instruments.

* Mechano-electronic transducers.

4) Dynamometers for control of the operation of machines and mechanisms, and for testing of materials, and also sensitive dynamometers for various scientific investigations.

5) Electronic balances.

6) Tensometers for the control of mechanical stresses in research as well as in investigations of machines, mechanisms, engineering constructions, geological rock specimens etc.

7) Seismic transducers for control and recording of vibrations during operation of machines, mechanisms and instruments, in seismographic oil prospecting and in other operations.

8) Transducers of accelerations for determination of inertia forces that are active in various parts of machines, mechanisms, instruments, engineering structures and transportation devices.

9) Transducers of velocity of liquid and gas flows.

10) Telemetering geophysical measuring and recording apparatus.

Mechanotrons can also be used to advantage in medical instrumentation for studying of the blood circulation system, of the respiratory systems, of motor functions, of activities of the nervous system and of other functions of the human body.

The conference pointed out the necessity of creation in the radio industry of experimental engineering groups for development, on the basis of the experience gained in laboratory work in our country and abroad, of prototype models of mechanotrons and preparation of their quantity production, and also for the organization of through tests on small production lots of mechanotrons.

The conference applied to the Committee on Radioelectronics for cooperation in the organization of production of mechanotrons in experimental and small production lots, in order to have them tested, in the shortest possible time, in various sections of the national economy and in order to obtain, in the shortest possible time, information on the most necessary types of such tubes for apparatus used in various sections of research and industry.

Electronic and ionic acceleration transducers of high sensitivity will be advantageously manufactured on the basis of existing experimental, small lot and mass production models of electron and ionic tubes, by making small design changes in the electrode systems of receiver-amplifier tubes, and keeping intact the basic technological process of tube construction. This makes it expedient to study the various types of electronic and ionic tubes in existence with a view of determining which of them are most suitable for creation of electronic and ionic acceleration transducers with interior control.

During discussions on perspectives and best directions for further development of mechanotrons, it was pointed out, that it will be advantageous to concentrate on developments of mechanotron systems which are the most simple and the most dependable in operation. In particular, the advantages of developing in the first place the mechanotrons with longitudinal electronic or ionic control action was stressed. It was pointed out in connection with this, that the presently developed types of such mechanotrons do not yet possess the limits of current or voltage sensitivity possible for this type of device. As to other systems of mechanical steering of electron and ion currents, again in the first place those should be further developed, which are the simplest. In this connection, specifically, the use of mechanotrons based on beam systems is entirely justified only when the specific operational requirements compensate for the great complexity in construction of such a tube.

In connection with the necessity of orienting the electronic vacuum tube industry as to selection of the most needed types of mechanotrons and to the approximate demand for them, the conference commissioned the MONTO committee on electronic instruments to draw conclusions from the materials on these questions, which this committee recommended to address to the MONTO committee (Moscow, Volchonka 5, Moscow Division of MONTO of Priborprom).

In conclusion the wish was expressed to have the Moscow Division of NTO Priborprom (Scientific Technical Organization of the Instrument Manufacturing Industry) organize the next conference on the same subject in 1958.

REVIEWS AND ABSTRACTS

ATOMIC BATTERIES

V. S. Merkulov

The conversion of the energy of radioactive emissions into electrical energy has become of great interest now that artificial radioactive elements with high specific activities are being produced in large quantities, and the application of these elements has revealed practical methods of producing sources of electrical power – atomic batteries. Characteristic features of such batteries are their very constant voltage and their long life. Their operation is not affected by various external factors, such as temperature. They are durable and have small dimensions, and the cost of certain types may be comparatively low as further progress is made in isotope production. It is true that present atomic sources of voltage and low current possess little power, since the efficiency of conversion of the energy of radioactive emissions into electrical energy is usually only a few per cent and in the best case (direct charging sources) the efficiency reaches 20-30%. Hence atomic batteries can be employed in systems and devices which require low-power supply sources. They will certainly find wide application in measurement technique and instrument construction. For example, these batteries may be widely used as reference voltage and current sources in all kinds of measuring equipment, in dosimeters, clock mechanisms, program equipment, triggers of signal devices and in many other instruments and appliances requiring low-power, constant-voltage, long-life sources, the operation of which is not affected by external factors.

A description is given below, from information in the literature, of some experimental models of different kinds of atomic batteries using strontium-90 (Sr^{90}), tritium (H^3) or promethium-147 (Pm^{147}), and an account of their basic characteristics is given.

Of the radioactive emissions β-radiation is the type mainly used in atomic batteries; α-radiation causes great damage to the substance and, besides, there is no pure α-emitter with a suitable half-life T. The most suitable α-emitter would appear to be radioactive Po^{210}, the half-life of which is 138 days.* γ-Radiation produces low specific ionization and, in addition, the employment of γ-sources in batteries requires the application of appropriate protection measures. An opportunity of using γ-emission is presented by the method of semiconductor junctions, and a suitable γ-emitter in this case might be the radioactive isotope Am^{241}, which emits a very soft γ-radiation and which possesses a long life (E_γ = 60 kev, T = 470 years).

Of the available β-emitters which find wide application in instrument construction, the following radioactive isotopes can be used in atomic batteries:**

Sr^{90} (E_β = 0.61 Mev, T = 19.9 years); H_3 (E_β = 17.95 kev, T = 12.4 years); Pm^{147} (E_β = 0.223 Mev, T = 2.6 years). A promising β-emitter is the radioactive Ni_{63} (E_β = 0.067 Mev, T = 85 years) which possess the fortunate combination of low-energy emission and a long half-life. In the selection of a β-emitter we also have to ensure that the radioactive element is easily obtained, that it is cheap and possesses high specific activity.

In the development of atomic sources of electric power, the following methods may be employed to convert the energy of radioactive elements into electrical energy: the direct charging method (with and without dielectric), the contact potential method, and the methods using semiconductor junctions, phosphors and thermocouples.

* Po^{210} preparations with activities 57 and 146 curies have been employed in an electric power source, using the thermocouple method. In this case the energy of radioactive decay is directly transformed into heat, which is transmitted to thermocouples which convert the heat energy into electrical energy. The maximum power of the sources were 1.8 and 9.4 mw respectively [1].

** The daughter product of the isotope Sr^{90} is the short-lived isotope Y^{90}, which emits β-particles with a peak energy of 2.18 Mev (for β-sources, the maximal energies of the particles are always given).

The direct charging method can only be used with charged particles. High-voltage batteries, the basic design of which is shown in Fig. 1a, have been devised using this method. A battery of this type is a self-charging condenser, the radioactive layer 2 being deposited onthe inner, well-insulated electrode 1. The electrode with the radioactive substance is contained in a vacuum. The outer electrode 3, usually in the form of a cylinder or sphere, is the collecting electrode (collector). Beta-particles emitted by the radioactive element reach the collector and charge it negatively with respect to the inner electrode.

In the design of high-voltage direct charging sources the main difficulty is the problem ofinsulation between the electrodes. The quality of the insulation determines the value of the maximal voltage attainable with a source of this type using a particular isotope. With good insulation the voltage of an atomic battery working on this principle may reach several hundred kilovolts. The electric current obtainable from a direct charging battery is extremely low, and hence their power is also low.

An atomic electric power source with a power of 0.2 mw [1, 2] has been designed on the principle of the direct charging method. The maximal voltage of the device was 365 kv (with a very low current); the internal resistance was 10^{14} ohm. 250 mc of the radioactive isotope Sr^{90} was employed in the device. The life of atomic sources using Sr^{90} is 20 years or more.

A valuable quality of the direct charging battery is the high efficiency of conversion of the radioactive energy. In the laboratory device of this design,the efficiency was 20%. Nevertheless, high-voltage atomic batteries have a limited application, and are used mainly in dosimeters. The reason, as already mentioned, lies in the fact that they give very weak currents and possess excessively high internal resistance. By using much larger amounts of radioactive materials the characteristics of the batteries of this type may be improved to some extent.

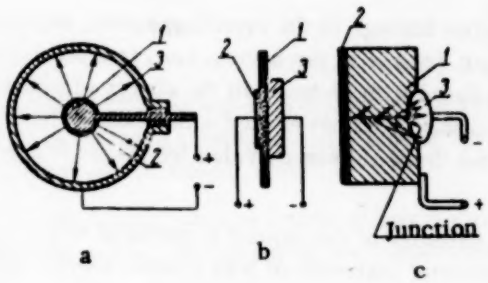

Fig. 1.

A high-voltage direct charging source of simpler design (the vacuum is not necessary) may be obtained, if a dielectric is employed (Fig. 1b) [3, 4]. As a dielectric we can use plates of mica, polystyrene, or other thin material, since the dielectric must be "transparent" to β-radiation. In the presence of dielectric 1,high-energy β-particles, emitted by the radioactive preparation, reach the collecting electrode after passing through the dielectric layer. Charged particles created by ionization, however, do not pass through the dielectric.

Figure 2 shows one of the best known modifications of the direct charging atomic battery employing a dielectric. The radioactive substance 1 is enclosed in a polystyrene capsule 2, which together with the insulator 3 is inserted in the aluminum collector 4. The collector is shielded by a lead screen 5 enclosed in a copper tube 6. This whole assembly is contained in the case 7. Contact with the isotope is effected by means of a contact lead of monel. The first source of this design employed an Sr^{90} isotope preparation; the peak output voltage of the device was 7 kv. The efficiency of energy conversion was 33%.

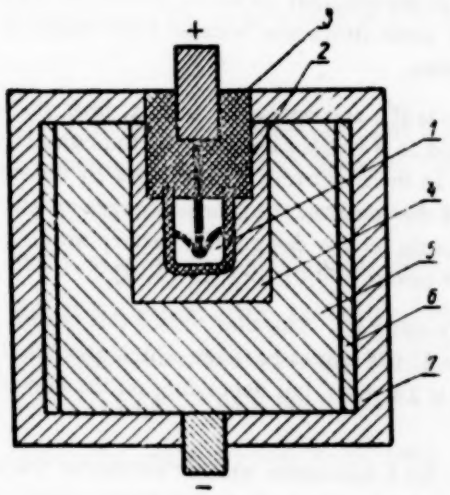

Fig. 2.

Improved models of this battery [5, 6] are of larger size and give a voltage of 20 kv and a current of 10^{-11} a with 2 mc, and $5 \cdot 10^{-11}$ a with 10 mc of Sr^{90}.

The employment of a dielectric, however, still does not rid the battery of the above-mentioned faults, which are inherent to direct charging voltage sources.

Much greater practical interest attaches to atomic batteries in which the operation is based on the use of semiconductor junctions. In these devices there is also a direct conversion of radioactive energy into electrical energy, and in this case,it is possible to use uncharged particles (including visible light), as well as charged particles, i.e., this method is the basic principle of both atomic and solar batteries.

The basic design of this battery is shown in Fig. 1c. On one side of a semiconducting plate 1 of silicon or germanium, a fine layer of radioactive substance 2 is deposited. On the other side of the strip the collecting electrode 3 is fastened. The β-emission, penetrating the semiconductor, tears from its atoms a considerable number of additional electrons and thus forms pairs of free carriers, the movement of which gives rise to the electric current. The semiconductor in this case is the source of a large number of secondary electrons, i.e., it acts as an amplifying device. Thus, in a silicon semiconductor, for instance, each bombarding β-particle emitted by the radioactive isotope Sr^{90} gives rise, on the average, to 200,000 secondary electrons. With such high amplification the faults inherent to the direct-charging batteries are to a large extent eliminated. Hence, atomic batteries using a semiconductor can be employed, for instance, for the supply of simple transistor circuits.

This was the principle for the design of an experimental atomic battery of extremely small size [7]. A thin layer of 50 mc of the radioactive isotope Sr^{90} was deposited on the surface of a miniature semiconducting plate of 0.32 cm^2 area. The output voltage of the element of the Sr^{90} battery was 0.2 v, the current was 5 μa. The efficiency of converting the radioactive energy into electrical energy for this device was 1% but it can apparently be increased to 10%. For demonstration purposes the Sr^{90} battery was used to supply an audio oscillator fitted with semiconducting triodes.

There are several methods of raising the efficiency of energy conversion in batteries based on the method of semiconductor junctions. The efficiency increases:

with increase in intensity of the radioactive emission;

with increase in the fraction of radioactive emission penetrating the semiconductor;

with increase in the number of charge carriers reaching the junction region.

The Sr^{90} atomic battery with a semiconductor element has also certain faults.

Firstly, high-energy β-particles produce considerable radiation damage in the crystal structure, which in time leads to a loss of efficiency, and hence to a drop in the output voltage of the device, i.e., to a reduction in its life. True, the destructive action of the emission is greatly reduced with decrease in the energy of emission and the radiation damage is practically absent if the energy of emission does not exceed a threshold value characteristic for each semiconducting material. For instance, the threshold energy value for silicon is approximately 0.3 Mev, for germanium it is 0.5 Mev.

Hence, to avoid radiation damage in the semiconductor in batteries of this type, it is essential to employ either radioactive emitters of low-energy β-particles, or semiconductor materials of high atomic weight, which are characterized by a higher threshold energy value.

Secondly, when very large amounts of the radioactive isotope Sr^{90} are used in small-size batteries which have no shielding, it is extremely difficult to keep the intensity of the external radiation below the permissible level. The question of protection from external radiation is still more important because high-energy β-particles generate in the substance more penetrating bremsstrahlung radiation.

An easily available source of exceptionally soft β-emission is H^3, and operating with it, from the viewpoint of external radiation, is practically without risk. H^3 was employed in a battery operated by the contact potential method. When pairs of charge carriers are created by ionization in the electric field produced by the contact potential difference of the surfaces of bimetallic electrodes, then the movement of these charges creates a current which can be used in an external circuit. This was the principle for the design of a battery which gave an output voltage up to 400 v with a very low current, and an output power of 0.01 to 1 μw [8, 9].

Figure 3 shows the principle of the construction of a battery using H^3. The element of this battery is a small cylinder, inside which are placed pairs of bimetallic plates 1, the spaces between which are filled with the radioactive substance 2 (H^3). The optimal life of the H^3 battery is 18 years, but depending on the construction, the life may vary between 10 and 30 years.

The use of phosphors formed the basis of an original design for a miniature atomic battery of the same size as the head of a cabinet screw, and in which the energy was derived from the radioactive disintegration of the isotope Pm^{147} [10, 11, 12, 13]. The principle of operation of the Pm^{147} atomic battery (Fig. 4), as distinct from the operating principle of the batteries discussed earlier, was based on a two-stage conversion process. The

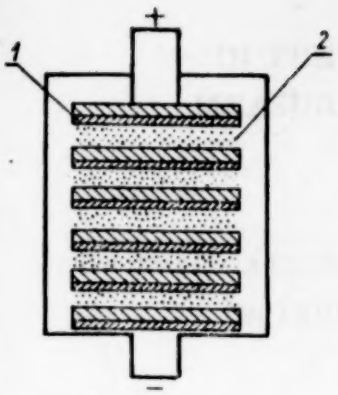

Fig. 3.

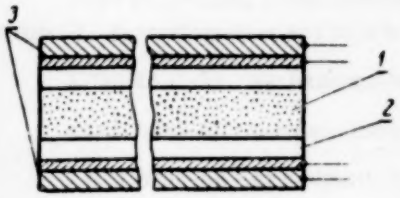

Fig. 4.

energy of the radioactive emission of isotope Pm^{147} was transformed directly directly into light, which in turn was converted into electrical energy by the photoelectric effect.

The light source 1 of the battery was a mixture of a powdered phosphor with an oxide of the radioactive isotope ($Pm_2^{147}O_3$). The phosphor employed was cadmium sulfide, or a mixture of cadmium sulfide and zinc sulfide, with particle sizes 10 to 50 μ. For the preparation of the light source, 50 mg of the phosphor and 5 mg of the oxide of the radioactive isotope Pm^{147} of activity 4.5 curies were used. The area of the active surface of the light source was 1 cm^2. The light source was placed in a very small container 2 of transparent plastic which was resistant to the action of the radioactive emission. The phosphor used also possessed good resistance to radiation. Beta-particles emitted by the radioactive isotope Pm^{147} were absorbed by the phosphor which, under the action of the bombarding particles, emitted quanta of electromagnetic radiation in the red and infrared regions of the spectrum.

The red and infrared radiation emitted by the phosphor was received by one or two special silicon photocells 3, which had peak sensitivity in the radiation range 6900-8200 A.

A Pm^{147} atomic battery working on this principle possesses the advantage that the sensitive (semiconducting) layer of the photocell is protected from the direct action of the β-emission and thus suffers no radiation damage. This is easily ensured even in batteries of very small size, since the Pm^{147} emits pure low-energy β-radiation which is completely absorbed by the phosphor in amount 50 mg/cm^2, which corresponds to a layer only 0.13 mm thick. The remaining β-emission, not absorbed by the phosphor, is stopped by the wall of the plastic container and does not reach the photocell.

An atomic voltage source of this design had a nominal power of 20 μw, which would be reduced by half only after 2.5 years. Dependent on the connection of the photocells, the voltage of the device varied between 0.25 and 1 v.

The Pm^{147} battery is safe to handle, since the β-emission is completely absorbed within it. For protection from possible x-rays, excited by β-particles in the substance, the voltage source element is contained in a small tantalum capsule. The battery with protective tantalum shield is 15 mm in diameter and 5 mm thick.

LITERATURE CITED

[1] E. G. Linder, P. Rappaport, and J. J. Loferski, Report No. 169 to the International Conference on the Peaceful Uses of Atomic Energy (Geneva, 1955).

[2] E. G. Linder and S. M. Christian, Journal of Applied Physics, 1952, 23, 1213.

[3] J. H. Coleman, Nucleonics, 1953, 11, No. 12, 42.

[4] P. Rappaport and E. G. Linder, Journal of Applied Physics, 1953, 24, 1110.

[5] Nucleonics, 1956, 14, No. 12, 71.

[6] A. Thomas, Nucleonics, 1955, 13, No. 11, 129.

[7] Radio and Television News, 1954, 51, 42.

[8] Electronics, 1954, 27, 212.

[9] Chemical and Engineering News, 1954, 32, 1622.

[10] Electrical Engineering, 1957, No. 4, 361.

[11] Newsweek, 1957, 49, 39.

[12] Machinery L., 1957, 19, No. 19a, 76.

[13] Nucleonics, 1957, 15, No. 3, 99.

[14] Atomic Energy Newsletter, 1957, 16, 5.

IN THE COMMITTEE OF STANDARDS FOR MEASURES AND MEASURING INSTRUMENTS

NEW PUBLICATIONS ON STANDARDS FOR MEASURES AND MEASURING INSTRUMENTS, APPROVED BY THE COMMITTEE

(Recorded in January-February, 1958)

New Standards

AUSS (All-Union State Standard)* 6019-58 Cold water meters, vane type. Replacing AUSS 6019-51. AUSS 7164-58. Potentiometers and balanced bridges, automatic, electronic. Replacing AUSS 7164-54.

AUSS 8667-58. Sacharimeters, glass. Replacing Standards Division's* 40012.

AUSS 8668-58 Lactodensitometer, glass. Replacing Standards Division's 40011.

AUSS 8700-58 Gas counters, rotating. Technical requirements. Introduced for the first time.

AUSS 8711-58 Ampermeters and Voltmeters. Technical requirements. Replacing the parts of AUSS 1845-52 and AUSS 3043-53 dealing with ampermeters and voltmeters.

New Instructions for Checking of Measures and Measuring Instruments

Instructions 93-58 for checking of gages for road control. Replacing instruction 93-51 of the former committee on measures and instruments.

Instruction 97-58 for checking of hourly output rating devices.

Instruction 132-58 for checking of indicating thickness meters.

Instruction 273-58 for checking of sensitometers.

Instruction 276-58 for checking of portable selenium photometers.

Methodical Directions on Checking of Measures and Measuring Instruments Approved by the Technical Board of the Committee

Methodical directions No. 164 on checking of gasmeters by means of exchangeable nozzles.

Methodical directions No. 165 on checking of prototype weights of the 1st category. Replacing the parts of instructions 73-47 pertaining to checking of 1st category prototype weights.

Methodical directions No. 166 on checking of dead weight piston type manometers of the 1st category up to 2500 kg-wt/cm^2. Replacing methodical directions No. 94 b, of the former Measures and Instruments Committee.

Methodical directions No. 167 on checking of permeameters.

---

* All-Union State Standard = GOST; Standards Division = OST.

CHANGES IN INSTRUCTIONS PRESENTLY IN FORCE ON CHECKING OF WEIGHT MEASURING INSTRUMENTS

I. M. Staroverov

The Committee on Standards, Measures and Measuring Instruments has introduced as of February 15, 1958, a number of changes and supplements in the latest instructions on checking of weight measuring instruments (instructions 40-56, 57-56, 66-56, and 69-56).

I. Instruction 40-56 for Checking of Master Balances

In checking of balances the number of times that equilibrium determinations with or without a load must be made is dependent upon the category into which the balance belongs, namely:

in checking of balances of the 1st category 10 times
in checking of balances of the 2nd category 5 times
in checking of balances of the 3rd category 3 times

In accounts of observed results data on variations must be included of weight determinations at near zero loads and at maximum loads.

Determination of variations for balances of the 3rd category has been introduced and in connection therewith note 3 and point 12n have been replaced by the following note:

"3. In the absence of an arresting device in balances of the 3rd category, the determination of equilibrium according to points 12k and 12l is carried out after a deliberate deflection of one of the balance pans until it strikes."

The metrological requirements for weight shifting balances of the 3rd category have been changed, in consequence whereof the note to Table 1 in appendix 1 has now been amended to read as follows:

"Note. Weight shifting balances of the 3rd category will now be issued with three weight ranges: up to 20 kg., to 1 kg and to 20 g."

Weight shifting balances presently in use may have two weight ranges: of 20 kg, and 1 kg, or of 20 kg and 500 gm.

Metrological characteristics of weight shifting balances of the 3rd category must be as follows:

Loads		Maximum permissible value of a scale division, mg		Maximum permissible error due to the inequality and variation in the arms, mg	
Maximum	Minimum	at maximum load	without load	at maximum load	without load
20 kg	2 kg	1000	400	1000	400
1 kg	50 g	100	20	100	20
500 g	50 g	50	20	50	20
20 g	1 g	5	5	5	5

In addition, Table 1 of Appendix 1 was supplemented by a second note of the following content: "Checking of weight standards of 20 kg in the shape of parallelepipeds can be carried out on master balances of the 3rd category under the condition that the value of a division and the variation does not surpass 500 mg.

II. Instruction 57-56 for Checking of Equal Arm Balances

Requirements for uniformity in damping of balance oscillations have been changed; decrease of the span of oscillations determined from four observations shall not surpass one division on each side in the first and fourth quarter of the scale and one half of a division in the second and third quarters (middle part of scale).

In balances having a microscale, decay of the oscillations swing must not surpass five divisions for the first and fourth scale quarters and two divisions in the central parts of the scale.

Decay of oscillations in balances equipped with special damping devices must be smooth, without jerks, and the pointer, before coming to complete rest, must make not more than three oscillations.

The requirements for analytical balances with built-in weights have been changed.

Checking of two-pan balances with built in weights is carried out by the same methods as checking of ordinary analytical balances.

Checking of the built-in weights is made on the balances of which they are parts by means of comparison of the built in weights with 1st category standard weights, taking into account the indicated deviations of the standard.

The built in weights are placed one after another into their cradles, and the standard weights are put on the opposite balance pan.

Divergences between equilibrium positions of balances with and without load (inaccuracies) must not surpass:

a) with loads consisting of milligram weights, ±0.2 mg

b) with loads consisting of gram weights – half of the inaccuracy permissible for an analytical weight of the same mass (see appendix 2k to instruction 69-56).

The total inaccuracy of a two-pan balance of the analytical group, as a result of the use of built-in weights, must not surpass 1.2 mg in any combination of weights.

Check up of one-pan balances of the analytical group with built-in weights is carried out by successively placing the built-in weights into their cradles and balancing them with 1st category standard weights (in accuracies of the standard weights are taken into account).

Observed divergences in equilibrium positions of unloaded and loaded balances, when loaded with several weights together, as well as when loaded with single weights, must not surpass the limits established for two pan balances.

Permissible margins of inaccuracy for analytical balances and for 2nd class technical balances have been tightened. In connection therewith, Tables 1 and 3 of Appendix 4 have been replaced by the tables (p. 250).

III. Instruction 66-56 for Checking of Master Weights of the 2nd and 3rd Categories

The methods of checking of master weights of the 2nd category have been changed, namely:

Checking of master weights of the 2nd category against master weights of the 1st category made of copper alloys is carried out without taking into account aerostatic buoyancy forces. When using 1st category master weights made of steel for checking 2nd category master weights, 1st category milligram master weights are added to the 1st category master weights to eliminate the effects of aerostatic forces, according to the table on page 251.

IV. Instruction 69-56 for Checking Ordinary Weights

The requirements for application of the table of permissible inaccuracies in weights (Appendix 2k to the instruction) have been made more precise, namely:

When checking weights – analytical, technical of the 1st and 2nd classes, metallic technical weights of the 3rd class and conditional weights newly made, repaired and in service – permissible inaccuracies given in the table of Appendix 2 apply.

TABLE 1 (from Appendix 4)

Balances of the Analytical Group

Designation of balances	Highest permissible load in g	Balances with microscales			Balances without microscales		
		Variation in mg (not over)	At 10% and 100% of (highest) load in mg. (not over)		Variation in mg (not over)	At 10% and 100% of (highest) load in mg (not over	
			Value of scale division	Error from beam inequality		Value of scale division	Error from beam inequality
Assaying	0.5	–	–	–	0.03	0.03	0.03
Microbalance	20	0.01	0.01	0.03	0.05	0.1	0.1
Analytical, 1st Class	200	0.1	0.1	0.4	0.2	0.4	0.4
Analytical, 2nd Class	200	0.2	0.2	1.0	0.5	1.0	1.0

Notes:

1. Inaccuracies of balances with built in weights are indicated in points 29 and 30 of the present instruction.

2. When checking microbalances, which are coming out of repairs, or which are in continuous use, also during inspections, twice the here indicated variations are permissible.

3. When checking balances of the analytical group, which are in continuous use, and also during inspection, twice the inaccuracy from beam inequality is permissible.

TABLE 3 (from Appendix 4)

Technical Balances, 2nd Class

Highest load	Permissible deviation from zero without load in mg	Value of a scale division and permissible inaccuracy due to beam inequality in mg	
		at 10% of load	at 100% of load
1 g	2	3	5
5 g	2	4	10
10 g	3	5	10
20 g	3	6	20
50 g	5	10	40
100 g	5	10	50
200 g	10	25	50
500 g	15	40	80
1 kg	20	60	100
5 kg	50	150	300
10 kg	100	200	500
20 kg	200	500	1000
50 kg	400	600	3000

Note: In balances that do not have a scale, a weight corresponding to the permissible inaccuracy, when placed on one of the pans, must disturb the equilibrium to the extent that the pointer shall go out beyond the yoke carrying it by not less than half of its length.

When the above weights are checked in routine inspections or inspections by experts, their absolute errors must not surpass the values given in the table of Appendix 2, but may have positive as well as negative values.

In checking of ceramic weights, newly made, in circulation and also during routine or expert inspections, permissible errors given in the table of Appendix 2 should be applied.

In addition it is indicated, that it is permissible to check technical weights of the 1st, 2nd, and 3rd classes and also small weights and riders for oil testing balances at the places of their use on an analytical or technical

balance of the 1st class, provided the value of a division of said balance is not less than three times the permissible error of the weights being checked.

Also as in instruction 66-56, the margin requirements for divergence of results obtained in control checks and prior checks of 1st class analytical and technical weights have been changed: the total divergence must now not surpass one half of the sum of the maximal errors in determination of all weights being subjected to the control check.

The formula in p. 13 of this instruction has been amended: in this formula, erroneously, below index B there was written the mass of the master weight instead of the mass of the weight being checked, found by one of the methods outlined in par. 11.

In the table of permissible errors for weights, given in Appendix 2, a column is added entitled: Maximal errors in determination of technical weights of Class 1.

Nominal values of steel master weight of 1st category in kg	1000	500	200	100	50	20	10	5	2	1	0.5	0.2	0.1
Mass values of wgts. to be added on pan containing 1st category master wgts.	10 g	5 g	2 g	1 g	500 mg	200 mg	100 mg	50 mg	20 mg	10 mg	5 mg	2 mg	1 mg

Notes:

1. To steel master weights of the 1st category of nominal masses of 50 g and less, milligram weights are not added, and checking of master weights of the 2nd category is carried out without correction for effects of aerostatic force.

2. In tests involving comparison of 3rd category weights with 2nd category weights, corrections for effects of aerostatic force are not introduced.